Establishment of tools for genetic modification of the thermophilic methanogenic archaeon *Methanothermobacter thermautotrophicus* ΔH

Dissertation

der Mathematisch-Naturwissenschaftlichen Fakultät

der Eberhard Karls Universität Tübingen

zur Erlangung des Grades eines

Doktors der Naturwissenschaften

(Dr. rer. nat.)

vorgelegt von

Christian Fink

aus Fürth

Tübingen

2021

Gedruckt mit Genehmigung der Mathematisch-Naturwissenschaftlichen Fakultät der Eberhard Karls Universität Tübingen.

Tag der mündlichen Qualifikation:	20.10.2021
Dekan:	Prof. Dr. Thilo Stehle
1. Berichterstatter:	Prof. Dr. Largus T. Angenent
2. Berichterstatter:	Prof. Dr. Wolfgang Wohlleben

Table of contents

A. Abstract (German)

Das hydrogenotrophe methanogene Archaeon *Methanothermobacter thermautotrophicus* wurde als Modelmikrobe für Methanogenese und thermophile Lebensweise im Allgemeinen in Studien der Grundlagen- und angewandten Forschung innerhalb der letzten Jahrzehnte eingehend erforscht. Ihre schnelle Teilungsrate und das robuste Wachstumsverhalten im Vergleich zu anderen methanogenen Archaeen macht *M. thermautotrophicus* Spezies zu einer vergleichsweise zugänglichen methanogenen Mikrobe. In Verbindung mit hohen Methan Produktionsraten, kurzen *Lag*-Phasen nach einem Transfer und der thermophilen Charakteristik eignet sich *M. thermautotrophicus* sehr gut zur Implementierung in groß angelegten Biomethanisierungsverfahren zur Energiespeicherung und Kohlenstoffrecycling, wie dem Power-to-Gas Verfahren.

In dieser Studie veranschaulichen wir die Entwicklung von verlässlichen Methoden zur gentechnischen Veränderung von *M. thermautotrophicus* ΔH. Hierfür haben wir eine Methode etabliert, welche DNA Transfer zwischen *Escherichia coli* S17-1 und *M. thermautotrophicus* ΔH mittels Konjugation ermöglicht. Als Trägermaterial für den DNA Transfer haben wir zum einen das modulare Shuttle-Vector-System pMVS (plasmid *Methanothermobacter* Vector System) zur Expression von heterologen Genen erstellt, welches den Austausch von Selektionsmarkern und Replikons für *E. coli* und *M. thermautotrophicus* ΔH durch seltene Erkennungssequenzen für Restriktionsenzyme erleichtert. Ein thermostabiles Neomycin-Resistenzgen fungiert hierbei als Selektionsmarker und das kryptische Plasmid pME2001 aus *M. marburgensis* als Replikon in *M. thermautotrophicus* ΔH. Zum anderen erschufen wir eine Plattform, bei der, mittels Suizid-Vector-Konstrukten, heterologe DNA in das *M. thermautotrophicus* ΔH Genom integriert werden kann. Hierbei konnten wir Lokus-spezifische Integration mit zwei Selektionsmarkern beweisen, einerseits mit einem Formiat-Dehydrogenase Operon (fdh_{Z245}) aus *M. thermautotrophicus* Z-245, das *M. thermautotrophicus* ΔH zur Verwendung von Formiat als Energieträger befähigt. Andererseits wurde spezifische Integration mit dem Neomycin-Resistenzgen aus dem pMVS gezeigt. Doppelte homologe Rekombination, welche zur gezielten Deletion eines Genomabschnittes führte, konnte durch Substitution mit dem Neomycin-Resistenzgen nachgewiesen werden.

Der erfolgreiche DNA Transfer und Replikation des Shuttle-Vector-Konstrukts ermöglichten uns die heterologe Expression einer thermostabilen β-Galaktosidase (*bgaB*) aus *Geobacillus stearothermophilus* als Reportergen in *M. thermautotrophicus* ΔH. Die Analyse durch quantitative *in-vitro* Assays mit o-Nitrophenyl-β-D-galactopyranosid (ONPG) als chromogene Substanz ergab signifikante Unterschiede im Expressionsmuster von vier verschiedenen synthetischen und natürlichen Promotern von *M. thermautotrophicus* ΔH zueinander.

B. Importance

An annual surge in the emission of greenhouse gases at a global scale demonstrated a shift of the climatic conditions, especially in the northern hemisphere towards higher temperatures (Riahi *et al.* 2017). In particular, the emission of carbon dioxide contributes heavily to such drastic consequences of global warming. It causes acidification of the oceans (Doney *et al.* 2009) and creates a greenhouse effect in the atmosphere. Therefore, it is in our best interest to minimize carbon dioxide emissions. However, a rising economy generates a constant need for energy. To meet these requirements, Germany enacted the *Energiewende*. This act aimed for a 90-95% reduction in greenhouse gas emissions by the year 2050 in comparison to 1990 and a production of at least 80% of the electric power in Germany by power plants based on renewable energy production (Henning and Palzer 2014). At the same time, carbon emissions from fossil sources need to be circumvented to minimize harmful effects from climate change. The power-to-gas platform is utilized to store renewable electric power and decarbonize the natural gas grid. The microbe *Methanothermobacter thermautotrophicus* is already applied as an industrial biocatalyst for the biological methanation step in large-scale power-to-gas processes. To improve the biocatalyst in a targeted fashion, genetic engineering is required. With our shuttle- and suicide-vector system for heterologous gene expression and gene deletion in *M. thermautotrophicus* ΔH, we set the cornerstone to engineer the microbe for optimized methane production, but also for production of high-value platform chemicals in power-to-x processes.

C. Abstract

The hydrogenotrophic methanogenic archaeon *Methanothermobacter thermautotrophicus* has been studied as a model microbe for methanogenesis and thermophilic microbial lifestyle in basic- and applied science for decades. Its short doubling times and robust growth behavior compared to other methanogenic archaea make *M. thermautotrophicus* a relatively accessible methanogenic archaeon. Combined with its high methane production rates, short lag phase after transfer, and thermophilic characteristics, *M. thermautotrophicus* is highly suitable for industrial scale biomethanation processes for energy storage and carbon recycling such as power-to-gas.

In this study, we report the establishment of a reliable method for genetic modification of *M. thermautotrophicus* ΔH based on interdomain conjugation with *E. coli* S17-1 for DNA transfer. We developed the modular shuttle vector system pMVS (plasmid *Methanothermobacter* vector system) that facilitates transfer of genetic cargo into *M. thermautotrophicus* ΔH with exchangeable selectable markers and replicons for host and recipient microbe by the use of rare restriction enzyme recognition sites. In the first successful pMVS vector, a thermostable kanamycin resistance gene served as selectable marker against neomycin and the cryptic plasmid pME2001 from *M. marburgensis* as a replicon in *M. thermautotrophicus* ΔH.

Additionally, we provide a platform to integrate heterologous DNA in the genomic DNA of *M. thermautotrophicus* ΔH *via* suicide vector constructs. We demonstrated site-specific genome integration at the *mth58-mth61* (MTH_RS00275-290) fimbriae operons with a formate dehydrogenase operon ($fdh_{Z\text{-}245}$) from *M. thermautotrophicus* Z-245 that enable *M. thermautotrophicus* ΔH to grow on formate, which qualifies $fdh_{Z\text{-}245}$ as a prototrophy-based selectable marker. Furthermore, we integrated the thermostable neomycin resistance from the pMVS design. With that, we showed deletion of a target genomic sequence *via* double homologous recombination events by substitution with the neomycin resistance gene.

Furthermore, the successful DNA transfer into *M. thermautotrophicus* enabled us to transport genetic cargo from *E. coli* to *M. thermautotrophicus via* the pMVS. With that, we proved heterologous gene expression of a thermostable β-galactosidase (*bgaB*) from *Geobacillus stearothermophilus* as a functional reporter gene on a pMVS vector in *M. thermautotrophicus* ΔH. For that, we performed quantitative *in-vitro* enzyme activity assays with o-Nitrophenyl-β-D-galactopyranosid (ONPG) as chromogenic substance and tested four different synthetic and native promoters, which resulted in significantly different expression levels of *bgaB* among the respective promoters.

I. Background

With the reclassification by Carl Woese in the 1970s, methanogenic archaea have been added to the newly described third domain of life, which is the domain of archaea (Woese and Fox 1977, Woese *et al.* 1990). Methanogenic archaea form an early branching polyphyletic group in the domain of archaea (Fox *et al.* 1977). In the past, methanogenic archaea were divided in the five orders of Methanococcales, Methanomicrobiales, Methanosarcinales, Methanobacteriales, and Methanopyrales. These orders all belonged to the phylum of euryarchaea. Due to metagenomic data, additional orders of methanogenic archaea, such as Methanocellales, Methanomassilliicoccales, and Methanonatronarchaeia, were described. These discoveries and further findings of potential new archaeal phyla led to a reevaluation of the existing phylogenetic tree of methanogenic archaea. At the moment there are different opinions about the true phylogenetic tree, but it is already clear that methanogenic archaea are not limited to the phylum of euryarchaeota any longer (Adam *et al.* 2017, Spang *et al.* 2017). The fact that methanogenic archaea were found in different phyla makes them potential candidates as the closest descendent of the last universal common ancestor (LUCA) of Bacteria and Archaea. It has been postulated that the LUCA probably possessed a Wood-Ljungdahl-like fermentation pathway similar to that of acetogenic bacteria (Ragsdale and Pierce 2008) and methanogenesis pathways of methanogenic archaea. Additionally, it is assumed that the LUCA lived in thermophilic environments and metabolized carbon dioxide *via* carbon dioxide fixation pathways (Weiss *et al.* 2016).

However, methanogenic archaea are not only widespread in thermophilic environments such as hot springs, deep sea black smokers, and peat soil, but also across mesophilic or psychrophilic anaerobic environmental niches (Lyu *et al.* 2018). Besides rice paddies, perma-frost soil, cow rumen, termite-, or the human intestinal tract, methanogenic archaea are inhabiting anthropogenic artificial environments such as waste-water treatment plants, sewage sludge, biogas plants, or anaerobic digesters (Lyu and Whitman 2019). The wide-spread distribution of methanogenic archaea is accompanied by the ability to metabolize a vast variety of substrates such as acetate (acetoclastic methanogenesis), hydrogen and carbon dioxide (hydrogenotrophic methanogenesis), or methylated compounds (*e.g.*, methyl sulfides, methyl amines, methanol) (methylotrophic methanogenesis) (Thauer *et al.* 2008). This broad range of substrates requires a large diversity of metabolic pathways and evolutionary enzyme adaptions, which provide a great endeavor for explorations. Accompanied by the analysis of metabolic pathways, the analysis and adaption of individual enzymatic reactions show great potential for industrial applications. As an example, a ketoacid-elongation pathway was already

heterologously expressed in *E. coli* and yielded in 6-aminocaproic acid of up to 160 mg/L (Drevland *et al.* 2008, Turk *et al.* 2016). Another target is the isoprenoid production for fragrance, drug, or other valuable chemical synthesis, which methanogenic archaea natively synthesize as a lipid compound. With isoprenoids, it was already proven that *in-situ* production is possible in genetically modified *Methanococcus maripaludis* with geraniol production and recently with *Methanosarcina acetivorans* (Lyu *et al.* 2016) (Aldridge *et al.* 2021). Another approach could be decontamination of environmentally toxic sulfide compounds through methanogenic archaea, which use these compounds as a sulfur source (Malone Rubright *et al.* 2017, Perona *et al.* 2018, Lyu and Whitman 2019).

Hydrogenotrophic methanogenic archaea with their ability to fix carbon dioxide and produce methane are already used for a carbon recycling and energy storage system in the biomethanation step of the power-to-gas concept (Schiebahn *et al.* 2015, Götz *et al.* 2016, Enzmann *et al.* 2018). A combination of the carbon dioxide fixation step from the power-to-gas concept and genetic engineering of hydrogenotrophic methanogenic archaea on the product side leads to power-to-x processes with the production of high-value chemicals in a more sustainable fashion. Therefore, it is required to possess robust techniques for genetic modification of methanogenic archaea. So far, there are well-established genetic systems available for heterotrophic mesophilic *Methanosarcina* spp. and hydrogenotrophic mesophilic *Methanococcus* spp. as well as early-stage genetic systems for thermophilic methanogenic archaea such as *Methanocaldococcus jannaschii* and *Methanoculleus thermophilus*. However, for hydrogenotrophic thermophilic Methanobacteriales, such as *Methanothermobacter thermautotrophicus* and *Methanothermobacter marburgensis* approaches towards a robust genetic system remained still in a developmental stage, so far.

II. Literature review on genetic systems for methanogenic archaea and the microbe of interest *M. thermautotrophicus*

To provide detailed insight into established genetic systems of methanogenic archaea, I start this literature review with a collection of existing material, methods, and techniques for genetic modification of mesophilic hydrogenotrophic *Methanococcus* spp. and heterotrophic *Methanosarcina* spp., but also of thermophilic hydrogenotrophic *Methanocaldococcus jannaschii* and *Methanoculleus thermophilus* in the following sections. An emphasis is placed on the crucial parameters for genetic modification, such as methods for DNA transfer and optimization of heterologous DNA templates for genomic DNA integration (suicide vector constructs) or extrachromosomal replication (shuttle vector constructs), including selectable markers and establishment of tools for regulation of gene expression in methanogenic archaea. Furthermore, the microbe *M. thermautotrophicus* ΔH is described as well as previous studies on the genetic tractability of *Methanothermobacter* spp..

1. Methods for DNA transfer in genetic systems for methanogenic archaea

DNA transfer into the host microbe is the first hurdle to overcome for genetic cargo to enter the respective microbe. Several methods and techniques for DNA transfer have been established, because not all methods lead to successful DNA transfer with every microbe. DNA-transfer methods into *Methanococcus* spp. developed during the past years. In the beginning, successful DNA transfer was achieved with protocols based on natural competence *via* transformation of protoplasts and protoplast electroporation (Micheletti *et al.* 1991, Patel *et al.* 1994). However, the low transformation efficiencies of the aforementioned methods led to the establishment of chemical-based DNA-transfer methods (Micheletti *et al.* 1991, Patel *et al.* 1994, Sarmiento *et al.* 2011). A common chemical-based method is the PEG-mediated chemical transformation (Moore and Leigh 2005, Costa *et al.* 2013). This development and the improvement of the shuttle vector system rose the frequencies of DNA transfer into *Methanococcus* spp. from 8-9 transformants/µg DNA to $5.3 \cdot 10^6$ transformants/µg DNA (Walters *et al.* 2011). An additional method for DNA transfer in *Methanococcus* spp. is an interdomain conjugation approach from *E. coli* S17-1 to *M. maripaludis* with efficiencies of up to $2 \cdot 10^{-6}$ transformants per recipient cell (Dodsworth *et al.* 2010).

For *Methanosarcina* spp., electroporation of protoplasts, PEG-mediated chemical, and liposome-mediated transformation were shown to result in successful DNA transfer (de Macario *et al.* 1996, Metcalf *et al.* 1997). Because transformation frequencies of electroporation were lower (10^2 per microgram of DNA per $2 \cdot 10^8$ cells) compared to liposome-mediated DNA transfer (10^7 transformants per microgram of DNA per $1 \cdot 10^9$ cells) and PEG-mediated DNA transfer after optimization for *Methanosarcina acetivorans*, the latter two

methods became state of the art techniques for DNA transfer into *M. acetivorans* (Deobald *et al.* 2018, Enzmann *et al.* 2018, Farley and Metcalf 2019).

The DNA-transfer protocols for the thermophilic methanogenic archaea *M. jannaschii* and *M. thermophilus* are both based on DNA uptake *via* natural competence. DNA transfer into *M. jannaschii* was accomplished with a low-temperature cultivated *M. jannaschii* pre-culture that was concentrated by centrifugation, mixed with linearized heterologous DNA, and followed by a heat shock (Susanti *et al.* 2019). For DNA transfer into *M. thermophilus*, a concentrated cell culture was mixed with circular heterologous DNA and subsequently used as an inoculum of fresh mineral medium. During overnight incubation at optimal growth temperature, DNA transfer was observed (Fonseca *et al.* 2020).

2. Tools for genetic modification systems of methanogenic archaea

With DNA-transfer protocols for the respective methanogenic archaea, it is possible to transport genetic cargo into the microbial cell. Tools for genetic modification systems enable several useful applications such as deletion of native genes or expression of heterologous genes.

2.1. Genetic tools for *Methanococcus* spp.

The system for genetic modification in the order of Methanococcales is mainly targeted to two species; *Methanococcus voltae* and *M. maripaludis*. Gernhardt *et al.* (1990) described a first suicide vector system for *M. voltae*. The first functioning construct with a sufficient number of transformants was pMip2 (**Figure 1A**) (Gernhardt *et al.* 1990). The vector backbone of pMip2 was based on a pUC18 high-copy-number vector. Since it was shown that puromycin inhibits growth and *in-vitro* protein biosynthesis of *M. voltae* at low concentrations, a puromycin resistance cassette (*pac*) was chosen as a selectable marker for *M. voltae* (Lacalle *et al.* 1989, Sarmiento *et al.* 2011). This puromycin resistance cassette was found in *Streptomyces alboniger*. It was identified as a puromycin N-acetyltransferase enzyme that inactivates puromycin by acetylation and therefore could be used as a resistance towards puromycin in genetic systems (Lacalle *et al.* 1989). The enzyme is temperature stable up to 70°C for at least 12 min when extracted from *E. coli* (Paik *et al.* 1985). As a promoter for expression of the *pac* cassette in *M. voltae*, the promoter region of the methyl-coenzyme M reductase gene (*mcr*), $P_{mcrB(M.v.)}$ was selected. The methyl-coenzyme M reductase is conserved in all methanogenic archaea as it catalyzes the last step of methanogenesis (*i.e.*, the reduction of the methyl-group to methane and coenzyme M) (Ellermann *et al.* 1988, Thauer 2019). For this reason, the *mcr* gene is also applied as a genetic marker for calculation of phylogenetic trees of methanogenic archaea (Luton *et al.* 2002). Because the $P_{mcrB(M.v.)}$ promoter is similar across the polyphyletic group of methanogenic archaea, it has a broad host range and it is also used for genetic

modifications in *Methanosarcina* spp. and *Methanoculleus thermophilus* (Guss *et al.* 2008, Fonseca *et al.* 2020). Besides the $P_{mcrB(M.v.)}$ promoter region of the *mcr* gene, also the terminator region of *mcr* is conserved in methanogenic archaea and used as the $T_{mcr(M.v.)}$ terminator of the *pac* cassette (Luton *et al.* 2002, Guss *et al.* 2008).

Additional to pUC18 as the vector backbone and the *pac* cassette as the selectable marker for positive selection, the *hisA* gene from *M. voltae* has been implemented as a homologous region for homologous recombination with genomic DNA of *M. voltae*. *HisA* is an important gene for histidine biosynthesis. When the *hisA* gene was interrupted by a double homologous recombination event, *M. voltae* showed histidine auxotrophy accompanied with puromycin resistance through substitution of *hisA* with *pac* (Gernhardt *et al.* 1990). Furthermore, this led to a positive and negative selection ability for analysis of the integration mechanism (single- or double homologous recombination) of pMip2 in genomic DNA of *M. voltae*. Most of the follow-up constructs for genomic DNA integration in *Methanococcus* spp. were based on pMip2 (**Figure 1A**).

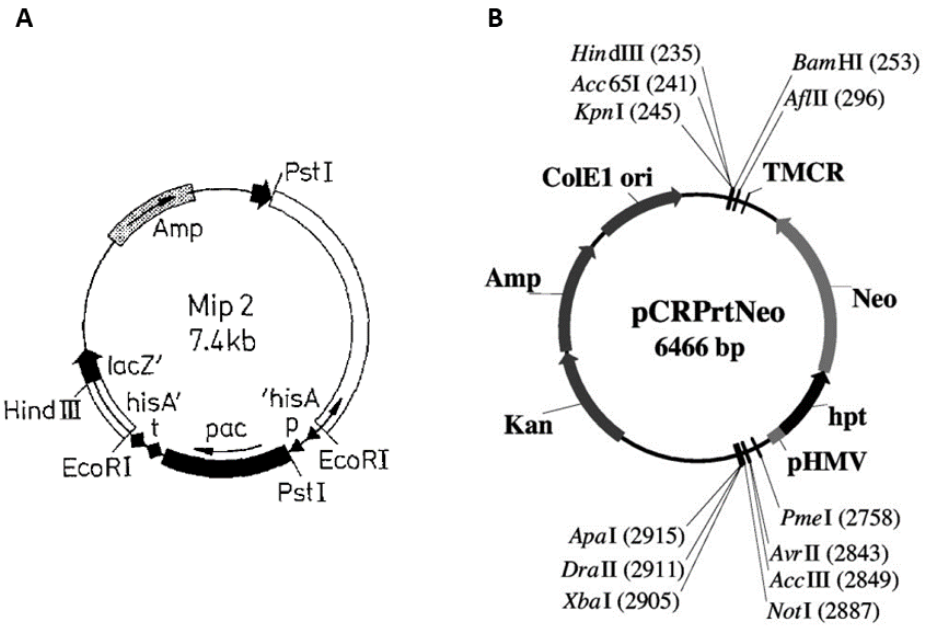

Figure 1. Suicide vector constructs for genome integration in *Methanococcus* spp. **A**) Vector map of pMip2. The 7.4-kb suicide-vector construct is assembled of a pUC18 high-copy number vector containing an ampicillin resistance as selectable marker and an origin of replication for *E. coli*. Additionally, *pac* as selectable marker for *M. voltae*, flanked by homologous regions of the *his*A gene of *M. voltae* fused into the multiple cloning site (MCS) of the pUC18 vector (Gernhardt *et al.* 1990). **B**) Vector map of pCRPrtNeo. The 6.5-kb vector is assembled from a pUC19 high-copy number vector containing an ampicillin and kanamycin resistance as selectable markers and an origin of replication for *E. coli*. Additionally, a neomycin resistance and the *hpt* gene as positive and negative selectable markers for *M. maripaludis,* respectively, flanked by two MCSs for implementation of homologous regions of the target gene (Moore and Leigh 2005).

The modification of genomic DNA with pMip2 and improved versions of this suicide vector leave the selectable marker and occasionally the entire *E. coli* vector backbone as a significant alteration (scar) in the genomic DNA compared to native genomic DNA before modification. To circumvent the scar, the technique of marker-less mutagenesis was established for *Methanococcus* spp.. Since this technique requires selectable markers for positive and negative selection, a marker for negative selection in *Methanococcus* spp. had to be found. Several purine analogs such as 8-Aza-2,4 diaminopurine (8-ADP), 6-Azauracil (6-AU), 2-methylpurine, and 8-Azahypoxanthine, were shown to have toxic effects on *Methanococcus* spp.. The enzyme hypoxanthine phosphoribosyl transferase (Hpt) is responsible for degradation of purines and purine analogs. Therefore, the deletion of the *hpt* gene in *Methanococcus* spp. resulted in a resistance towards toxic purine analogs 8-ADP or 8-aza-hypoxanthin. Thus, the *hpt* deletion mutant *M. maripaludis* strain Mm900 was adopted for marker-less mutagenesis protocols (Moore and Leigh 2005). Besides the *hpt* gene, uracil analogs, such as 8-AU, are degraded by the corresponding gene uracil-phosphoribosyl transferase (*upt*). A deletion of the *upt* gene results in a resistance towards 8-AU. However, an *hpt* deletion was easier to pursue than a *upt* deletion in *M. maripaludis* (Moore and Leigh 2005).

After generation of the *hpt* deletion strain *M. maripaludis* Mm900, the suicide vector system pCRPrtNeo for marker-less mutagenesis was established (**Figure 1B**). Other than in pMip2 with the puromycin resistance *pac*, a neomycin resistance was implemented for positive selection (Argyle *et al.* 1996, Moore and Leigh 2005). No replicon for *M. maripaludis* was included in the suicide vector. Therefore, the suicide vector was not replicated in the methanogenic archaeon. The vector pCRPrtNeo carried two multiple cloning sites (MCS) for implementing 500 bp up- and downstream homologous flanking regions of the desired target gene for deletion. In the first recombination event either one of the homologous flanking regions recombined, or both of the homologous flanking regions underwent homologous recombination, resulting in a deletion of the desired target gene, and therefore substitution of the gene of interest with the genes for antibiotic resistances (*hpt*, *pac*). After the first homologous recombination event, neomycin was used for positive selection while 8-ADP showed toxicity on the microbe through the *hpt* gene as a negative selectable marker. After several transfers under neomycin selective pressure to exclude residual non-resistant wild-type *M. maripaludis*, the mutant was cultivated in non-selective liquid media. This enabled for a loss of the selectable markers, and therefore led to a regained resistance towards 8-ADP. Two possible different genotypes were the result of this procedure: 1) Either the wild-type genotype was reverted; or 2) the desired marker-less mutation was achieved, depending on whether the same recombination event as before, or the opposite recombination event

occurred (Moore and Leigh 2005). In general, one great advantage of marker-less mutagenesis compared to suicide vector constructs with only positive selection is the ability to excise the selectable marker for another round of positive selection from the genome. This renders the selectable marker as reusable. Thus, the generation of multi-gene deletion mutants was possible with the same selectable marker for positive selection and *hpt*/8-ADP for negative selection in several rounds of the described procedure.

Additional to the suicide vector constructs for genomic DNA integration, a shuttle-vector system for *M. maripaludis* was established. The first draft for this shuttle vector was pDLT44 (**Figure 2**) (Tumbula *et al.* 1997). Every existing shuttle vector for *Methanococcus* spp. up to now was based on this draft. The vector backbone possessed an *E. coli* pUC19 vector containing an origin of replication and antibiotic resistance as selectable marker for *E. coli*. As a selectable marker for *M. maripaludis*, the *pac* cassette conferring resistance towards puromycin was chosen, while a neomycin resistance was also possible. The major difference compared to the suicide vector constructs was the replicon for *M. maripaludis* for which the natural occurring cryptic plasmid pURB500 of *M. maripaludis* was implemented. The replicon pURB500 allowed the shuttle vector for extrachromosomal replication in the host microbe. Since the location of the origin of replication on pURB500 had not been defined yet, the entire plasmid was fused initially into the shuttle vector construct. This led to a shuttle-vector construct size of ~12 kb, which further resulted in low transformation frequencies. Therefore, the location of the origin of replication on pURB500 was investigated in more detail to reduce the size of the replicon sequence, and thus of the shuttle-vector constructs for *M. maripaludis*. In brief, the plasmid pURB500 contained two regions without open reading frames, ORFless1 and ORFless2. These were assumed to inhabit the origin of replication. ORFless 2 and ORF3 turned out to be not important for replication of pURB500. Therefore, these parts got excluded from the shuttle-vector constructs. This reduced the size of shuttle-vector constructs to around 6 kb. The reduced size improved the transformation efficiency considerably from 8-9 transformants/µg plasmid DNA to $5.3 \cdot 10^6$ transformations/µg plasmid DNA. (Sarmiento *et al.* 2011, Walters *et al.* 2011).

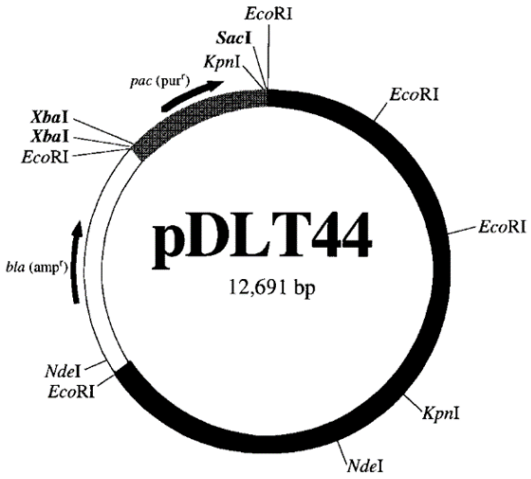

Figure 2. Vector map of the first shuttle vector draft pDLT44 for *M. maripaludis* (Tumbula *et al.* 1997). Besides an *E. coli* vector backbone containing ampicillin as selectable marker and an *E. coli* origin of replication, it inhabits *pac* as selectable marker and the cryptic plasmid pURB500 as replicon for *M. maripaludis*.

2.2. Genetic tools for *Methanosarcina* spp.

The model microbes of genetic systems for Methanosarcinales are *Methanosarcina mazei*, *Methanosarcina barkeri*, and *Methanosarcina acetivorans*. While *M. mazei* and *M. barkeri* are able to grow autotrophically from hydrogen and carbon dioxide, *M. acetivorans* is strictly heterotrophic. Substrates for heterotrophic growth are, for example, acetate or methanol as sole carbon and energy source (Madigan *et al.* 1997, Enzmann *et al.* 2018).

First genetic alterations in *Methanosarcina* spp. were published in 1996 using *M. mazei*. A suicide vector for genomic DNA integration was developed based on the high-copy number plasmid pUC19 for *E. coli*. Whereas the *hisA* gene was used for homologous recombination in *M. voltae (Gernhardt et al. 1990)*, parts of the genes *dnaK* and *grpE* with their intergenic regions containing an *Eco*RI restriction enzyme recognition site, were fused into the suicide-vector construct for *M. mazei*. Into this *Eco*RI site of the intergenic region, the *pac* cassette, including $P_{mcrB(M.v.)}$ and $T_{mcr(M.v.)}$ from *M. voltae* pMip1 (**Figure 1A**), was fused as a selectable marker for *M. mazei*. The first successful transformation of *M. mazei* with clonal populations that were resistant to puromycin were gained by chemical transformation of *M. mazei* cells in liquid culture using high-salt mineral media and heat shock (de Macario *et al.* 1996).

As it was stated for *M. maripaludis*, for *M. acetivorans* a deletion of the *hpt* gene also resulted in a resistance to toxic purine analogs (Pritchett *et al.* 2004, Moore and Leigh 2005). Therefore, the method for marker-less mutagenesis of *Methanosarcina* spp. was developed analog to *M. maripaludis* based on the toxic purine analog 8-ADP for counter selection (**Figure 3**). The marker-less mutagenesis could be carried out the same way as for *M. maripaludis* (Pritchett

et al. 2004). However, there was also an additional method where the second recombination event was forced by a *flp* recombinase instead of statistical probability (Rother and Metcalf 2005). This method reduced the screening effort, but left a scar of the *flp* recombinase recognition sequence in the genome. This method is based on a two-step homologous recombination. First, the *Methanosarcina* spp. Δ*hpt* strain was transformed with a suicide vector construct. It contained the *pac* cassette and the *hpt* gene as selectable markers which were flanked by two *flp* recombinase recognition sites. Those recognition sites were flanked by up- and downstream homologous flanking regions of the target gene (Orange X, **Figure 3**). After the recombination event at the target gene occurred, the genetically modified *Methanosarcina* spp. strain was positively selected with puromycin. In a second event, the mutant strain selected with puromycin was transfected with a second suicide vector, containing the *flp* recombinase gene, to delete the region between the up- and downstream homologous flanking regions of the gene of interest. The resulting marker-less mutant strain without *pac* and *hpt* regained resistance to 8-ADP, which was then selected for by negative selection (**Figure 3**) (Rother and Metcalf 2005).

Additional to the sophisticated method of marker-less mutagenesis, it was possible to generate deletion and insertion mutants of *M. acetivorans* with clustered regularly interspaced short palindromic repeats – CRISPR-associated protein 9 (CRISPR-Cas9)-mediated genome editing. With CRISPR-Cas9, scar-less editing of the genomic DNA is possible. In this case, the shuttle vector pJK027A, including replicons for *M. acetivorans* and *E. coli*, *pac*, and *hpt* gene for positive and negative selection in *M. acetivorans* was used as a template. Additionally, a sgRNA, repair template, and tetracycline-inducible *cas9* gene were fused to introduce a site-specific double strand brake in the genomic DNA of *M. acetivorans.* This double strand break was repaired through homologous flanking regions also added to the plasmid (Nayak and Metcalf 2017). Apart from the CRISPR-Cas9 approach, further genes for non-homologous end joining (NHEJ) from *Methanosarcina paludicola* were added to the shuttle vector without a repair template. Genetic modification of *M. acetivorans* with this shuttle vector led to viable cells with NHEJ based repaired genomic DNA and site-specific deletion of the target gene (Nayak and Metcalf 2017).

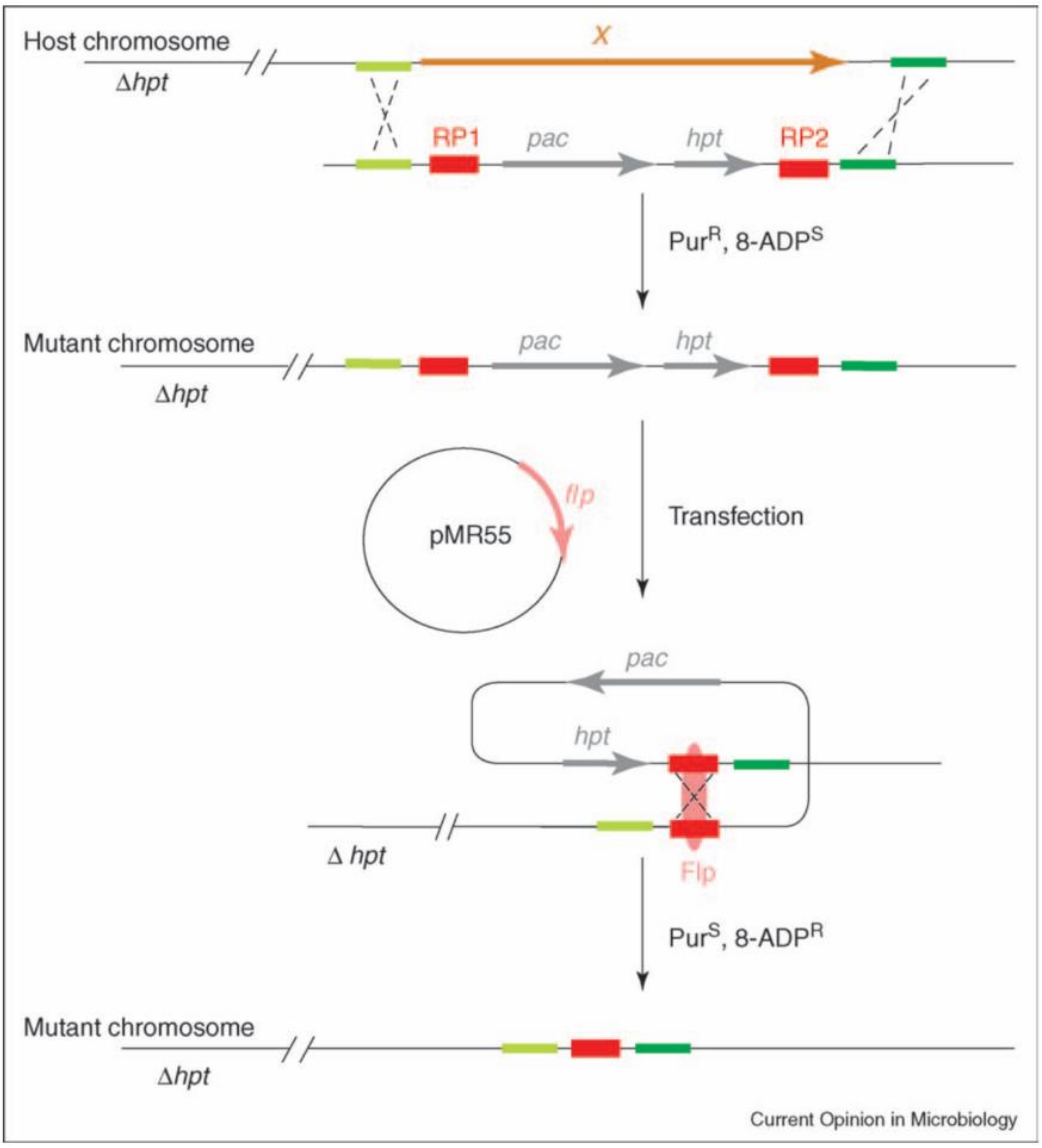

Figure 3. Scheme for a marker-less mutation technique. In the first step the Δ*hpt* strain is transformed by introduction of the puromycin resistance cassette (*pac*) and the *hpt* gene flanked by *flp* recombinase recognition sequence and homologous flanking regions of the target gene. After the recombination event (dotted lines), the mutant strain, selected by puromycin, is transfected by a *flp* carrying vector. After this second recombination event the marker-less mutant can be selected for *via* 8-ADP. Pur: Puromycin (Rother and Metcalf 2005)

A shuttle-vector system for *Methanosarcina* spp. was first published by Metcalf *et al.* (1997). It was based on implementation of the entire cryptic plasmid pC2A, which is native to *M. acetivorans*, as a replicon. The plasmid pC2A contains an origin of replication with a broad host range in the genus of *Methanosarcina* spp., since plasmid DNA was replicated extrachromosomally in 7 of 10 tested species of *Methanosarcina* spp. (Metcalf *et al.* 1997). As a selectable marker for *Methanosarcina* spp., the puromycin resistance gene (*pac*) was implemented. In the primal constructs, the $P_{mcrB(M.v.)}$ promoter and $T_{mcr(M.v.)}$ terminator of *M. voltae* were chosen (Metcalf *et al.* 1997). In follow up studies, also the $P_{mcrB(M.b.)}$ constitutive promoter from the methyl coenzyme M reductase gene of *M. barkeri* was fused directly

upstream of the *pac* gene (Guss *et al.* 2008). The replicon for *E. coli* was the *pir*-dependent R6K gamma origin of replication. This origin of replication could be induced to produce low and high plasmid copy numbers, depending on the toxicity of the expressed gene (Metcalf *et al.* 1994). Additionally, an ampicillin resistance gene (*bla*) was added as positive selectable marker in *E. coli*. The *lac*Zα provided a small multiple cloning site for genetic cargo and the opportunity for blue/white screening in *E. coli* (**Figure 4**).

Additional to *pac*, three selectable markers for positive selection have been implemented for *Methanosarcina* spp.; 1) a selectable marker based on mutagenesis of the *ileS* gene from *M. barkeri*, which confers resistance to mupirocin (Boccazzi *et al.* 2000); 2) a aminoglycoside phosphotransferase (*aph-IIb*), which confers resistance to neomycin (Mondorf *et al.* 2012); and 3) the streptothricin acetyltransferase (*sat*), which confers resistance to nourseothricin for positive selection (Farley and Metcalf 2019).

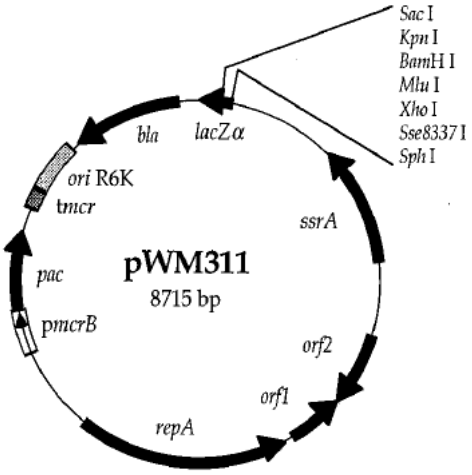

Figure 4. pWM311 shuttle-vector plasmid for *E. coli* and *Methanosarcina* spp. based on the native cryptic plasmid pC2A from *M. acetivorans* as replicon (Metcalf *et al.* 1997).

2.3. Genetic tools for the thermophilic methanogenic archaea *Methanocaldococcus jannaschii* and *Methanoculleus thermophilus*

Both systems for genetic modification of thermophilic methanogenic archaea are based on suicide-vector constructs for genome integration. For *M. jannaschii*, the native Hmg-CoA reductase conferred resistance as a selectable marker for positive selection towards lovastatin and simvastatin (Susanti *et al.* 2019). Hmg-CoA reductase as a selectable marker against simvastatin was also demonstrated for the thermophilic euryarchaea *Thermococcus kodakarensis* and *Pyrococcus furiosus* (Santangelo *et al.* 2010, Waege *et al.* 2010). Additionally, the F_{420}-dependent sulfite reductase (*fsr*) gene deletion led to sulfite toxicity in *M. jannaschii* and could, therefore, be implemented as a selectable marker for negative selection in future genetic tools (Susanti *et al.* 2019) .

For *M. thermophilus*, the neomycin resistance for *M. maripaludis* was used as a selectable marker (Argyle *et al.* 1996). Additionally, a thermostable neomycin resistance gene, that was adjusted to thermophilic conditions resulted in the desired phenotype of neomycin resistance (Hoseki *et al.* 1999). Genome integration was proven with deletion and complementation of genes responsible for expression of cell appendages. These were important for DNA transfer into the microbe, because a deletion resulted in the loss of ability for natural competence (Fonseca *et al.* 2020).

Even with potentially suitable extrachromosomal elements of *M. jannaschii* as replicons for shuttle-vector constructs (Wang *et al.* 2015, Susanti *et al.* 2019), both genetic systems still rely on the integration of heterologous DNA into genomic DNA *via* homologous recombination, and replicating shuttle-vector constructs in thermophilic methanogenic archaea have not been reported, so far.

3. Tools for regulation of gene expression and reporter genes in methanogenic archaea

DNA-transfer protocols and genetic tools form the basis for generation of genetically modified microbes. However, expression of heterologous genes may result in toxic side effects for the microbe or growth inhibition by energy limitation, especially for methanogenic microbes that are living at the thermodynamic limit of life (Thauer *et al.* 2008). Therefore, it is of utmost importance to implement tools for regulation of gene expression, and the level of expression, in existing genetic systems for methanogenic archaea.

For *Methanococcus* spp., currently three constitutive promoter systems are commonly used for gene expression. The P_{hmv} and $P_{mcrB(M.v.)}$ promoters from *M. voltae* are well established (Tumbula *et al.* 1997, Gardner and Whitman 1999). Additionally, a histone promoter from *Methanococcus vannielii* is available (Costa *et al.* 2013). The only established inducible promoter system for *Methanococcus* spp. is based on the native *nif* gene promoter. The expression is regulated by repression, based on the availability of nitrogen compounds. There is complete repression when *Methanococcus* spp. is cultivated in the presence of ammonium, intermediate repression in the presence of alanine, and no repression when cultivated in a dinitrogen-containing medium. The inducible-promoter system was tested for functionality with a mesophilic β-galactosidase as a reporter gene and quantitative o-Nitrophenyl-β-D-galactopyranosid ONPG assays (Lie *et al.* 2005). The *nif* inducible-promoter system is a native *Methanococcus* spp. system. Changes in the nitrogen source for the microbe, besides the expression level of the gene of interest, always changes the nitrogen and carbon metabolism of *Methanococcus* spp.. Therefore, more than one parameter is changed when analyzing the phenotypical behavior of mutant strains (Lie and Leigh 2002, Lie *et al.* 2005). An improvement

would be a tetracycline-inducible system as it is established for *Methanosarcina* spp., which was not successfully implemented in *Methanococcus* spp., so far (Leigh *et al.* 2011).

For *Methanosarcina* spp., besides the $P_{mcrB(M.v.)}$ promoter from *M. voltae*, the promoter and terminator system $P_{mcrB(M.b.)}$ and $T_{mcr(M.b.)}$ from *M. barkeri* is used (Guss *et al.* 2008). Karim *et al.* (2018) performed a more detailed study on these constitutive promoters and how the strength of gene expression was influenced by changes on a base level, especially with respect to the function of the transcription factor B recognition element (BRE) and transcription initiation site. Contrary to *Methanococcus* spp., for *M. acetivorans* promoter studies, a mesophilic β-glucuronidase has been used as a reporter gene with the corresponding quantitative 4-Nitrophenyl β-D-glucopyranoside (PNPG) assay to compare promoter strength in a quantitative fashion instead of a β-galactosidase.

To regulate the gene expression in microbes the *lac* repressor or the *tetR* repressor, are the most common systems (Berens and Hillen 2004). It was demonstrated that the *tetR* system is not only functioning in bacteria but also in archaea. For *Methanosarcina* spp. this system is well established (**Figure 6**) (Guss *et al.* 2008). The plasmid carries *pac* and *hpt* genes as selectable markers and the *tetR* gene for expression of the repressor of the constitutive $P_{mcrB(M.b.)}$ promoter, including a *tet*01 operator region as binding site for the repressor protein. When anhydrotetracycline, which is less harmful to *Methanosarcina* spp. than tetracycline, is added, the repressor protein binds anhydrotetracycline instead of the *tet*01 binding site and allows the expression of the gene of interest. The gene of interest is fused into the multiple cloning site downstream the $P_{mcrB(M.b.)}$(*tet*01) region. An additional promoter regulation system was described in which a thioredoxin system activates DNA in a redox-sensitive transcriptional operator region. In this case the reduction of cysteines back to thiols results in activation of the P_{mvsR} operator (Sheehan *et al.* 2015).

For *M. thermophilus*, the $P_{mcr(M.v.)}$ promoter was used for the selectable marker. For complementation studies with the gene of interest, however, $P_{hmtB(M.v.)}$ as an additional promoter from *M. voltae* was implemented (Fonseca *et al.* 2020). For *M. jannaschii*, the native constitutive promoter P_{sla}, that is located upstream of a putative S-layer protein, was implemented for gene expression of the selectable marker. For over-expression of the gene of interest, the promoter $P_{flaB1B2}$ from a putative flagellin gene of *M. jannaschii* was adopted (Susanti *et al.* 2019). So far, there are no inducible-promoter systems for thermophilic methanogenic archaea described in literature.

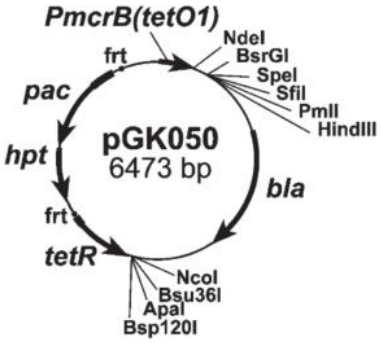

Figure 5. Vector map of a shuttle vector construct with anhydrotetracycline inducible gene of interest expression for *M. acetivorans* (Guss *et al.* 2008).

4. *Methanothermobacter thermautotrophicus* as microbe of interest

In the previous chapters, DNA-transfer methods, vector systems for integration into genomic DNA or replicative vector systems were described. Additionally, promoter systems and their regulation were presented. Within this section, the current status of genetic approaches and technical applications for the microbe *Methanothermobacter* spp. are presented. These results, combined with the developed systems mentioned above, are the basis for further development of a genetic system for *M. thermautotrophicus* ΔH.

M. thermautotrophicus ΔH is a rod-shaped thermophilic microbe with an optimal growth temperature of 65°C. It was first isolated in sewage sludge in Illinois in 1972 (Zeikus and Wolfe 1972). As a methanogenic archaeon, it is depending on methanogenesis, which is the biological production of methane. Hydrogenotrophic methanogenic archaea grow with hydrogen (electron donor) and carbon dioxide (electron acceptor and carbon source) as the substrates (Thauer *et al.* 2008). For decades, the Methanobacteriales species *M. thermautotrophicus* ΔH and *Methanothermobacter marburgensis* have been studied as model microbes for the biochemistry of the hydrogenotrophic methanogenic metabolism, and deep insights into their energy and carbon metabolism have been acquired (Thauer 1998, Thauer *et al.* 2008, Thauer 2015). For example, comparative genome analyses of *M. thermautotrophicus* ΔH and *M. marburgensis* revealed the genes that are most likely required for hydrogenotrophic methanogenesis (Kaster *et al.* 2011), and a plethora of studies unraveled the mechanism of key enzymes such as the methyl-coenzyme M reductase (reviewed in Thauer (2019)). Furthermore, the pseudomurein-containing cell wall, which is specific to Methanobacteriales, has attracted research on *Methanothermobacter* spp. (Kandler and König 1998). *M. thermautotrophicus* ΔH is an obligate anaerobic microbe at thermophilic conditions but it is able to withstand exposure to oxygen at room temperature (Kiener and Leisinger 1983, Kiener *et al.* 1988). Furthermore, no latency (*i.e.*, lag-phase or reduced growth rate) is

observed after reactivation from room temperature to 65°C, which qualifies *Methanothermobacter* spp. for power-to-gas applications.

4.1. *Methanothermobacter* spp. in power-to-gas applications

Photovoltaic and wind energy systems are the largest sites for renewable electric power production in Germany. Nevertheless, one of the major concerns is the inconsistency and fluctuation in electric power production. Therefore, the case of a surplus in electric power production exists. An additional issue is the low energy storage capacity. One powerful system to overcome these issues is the power-to-gas platform (Jentsch *et al.* 2014) (**Figure 6**).

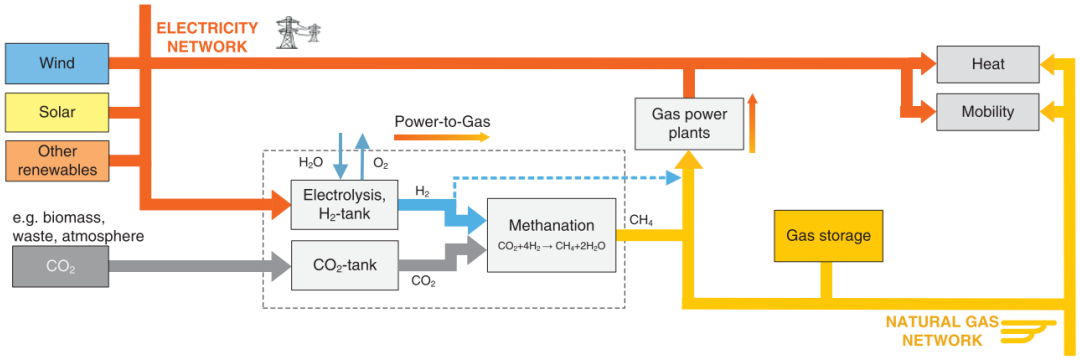

Figure 6. The general system of power-to-gas. A surplus in electric power from renewable energy plants drives electrolysis of water to hydrogen (H_2) and oxygen (O_2). The generated H_2 together with CO_2 from biogas plants gets processed to methane (CH_4) *via* biological or chemical methanation and directly introduced into the natural gas network (Jentsch *et al.* 2014).

Temporary overproduced electric power from renewable energy plants is transformed into hydrogen and oxygen by water electrolysis. While oxygen, as a byproduct, is collected for further applications, hydrogen is metabolized together with carbon dioxide from anaerobic digestion or industrial off-gases into methane in a methanation step. The resulting methane is supplied in the existing natural gas grid with a vast storage capacity (Jentsch *et al.* 2014, Burkhardt *et al.* 2015, Götz *et al.* 2016, Thema *et al.* 2019). The methanation process can be executed both chemically and biologically. The chemical synthesis of methane (Sabatier process) is described in Götz *et al.* (2016). This process is conducted with high temperature conditions and requires the purest form of gases to avoid damage to the catalysts by hydrogen sulfide gas or other impurities. Although, since an abiotic power-to-gas process is only a facultative process that gets switched on when a surplus of energy occurs, it is very energy consuming to initiate the process. A biomethanation process with methanogens can overcome these problems. Despite the fact that no genetic system for *M. thermautotrophicus* and *M. marburgensis* was available, so far, wild-type cultures of those microbes have been implemented as biocatalysts for a biological methanation step in the power-to-gas platform (Thema *et al.* 2019, Pfeifer *et al.* 2020, Thema *et al.* 2021). Coupled to the fast growth rate, the methane production rate is high compared to other methanogenic archaea (Martin *et al.*

2013, Seifert *et al.* 2014). For example, Electrochaea GmbH (Planegg, Germany) uses a proprietary (non-genetically modified) wild-type *M. thermautotrophicus* strain (Mets 2016). Additionally, hydrogen sulfide serves as a sulfur source for *M. thermautotrophicus*. Thus, hydrogen sulfide contamination in industrial off-gas or biogas, which causes damage to catalysts for thermo-chemical methanation, is not only unproblematic but even desired for biomethanation. With a productivity of roughly 95%, the efficiency of the biomethanation process of *M. thermautotrophicus* is high (Schill and von Stockar 1995, Schill *et al.* 1999). Nevertheless, there is a chance to increase the productivity to nearly 100% by natural selection or genetic modification of *M. thermautotrophicus* (Thema *et al.* 2021).

Genetic engineering will be necessary to further optimize *M. thermautotrophicus* as the biocatalysts for power-to-gas processes in a targeted fashion. With genetic engineering, the metabolism of the biocatalysts can, for example, be improved to maximize methane-production rates, or be amended for an expanded substrate or product spectrum, which would allow to convert the power-to-gas into a broader power-to-chemicals (*i.e.*, power-to-x) platform (Pfeifer *et al.* 2020). Furthermore, the long-lasting interest in the biochemistry and physiology of these model microbes led to extensive attempts to establish genetic tools for *Methanothermobacter* spp. in the past for purely research purposes (Meile and Reeve 1985, Leisinger and Meile 1993, Luo *et al.* 2001)

4.2. DNA transfer in *Methanothermobacter* spp.

Prior to further establishment of genetic tools in *M. thermautotrophicus* ΔH, DNA transfer needs to be possible. So far, three DNA-transfer techniques for *Methanothermobacter* spp. were described in literature: 1) virus-mediated transduction with virus ΨM1. In this method randomly mutated *M. marburgensis* strains with the respective phenotypes were infected with virus ΨM1. After lysis of *M. marburgensis*, the virus was purified from plaques and used for transduction of wild-type *M. marburgensis*. The transduction frequencies ranged from $5 \cdot 10^{-6}$ to $6 \cdot 10^{-4}$/plaque-forming units (pfu) (Meile *et al.* 1990); 2) DNA uptake *via* natural competence. A protocol for *M. thermautotrophicus* ΔH was published where genomic DNA of auxotrophic or antibiotic resistant *M. thermautotrophicus* ΔH strains was spot-plated together with wild-type *M. thermautotrophicus* ΔH, which resulted in the conversion to the mutant phenotype; and 3) chemical PEG treatment technique. This method was tested with wild-type *M. thermautotrophicus* ΔH (Worrell *et al.* 1988). So far, DNA transfer into *M. thermautotrophicus* ΔH with heterologous DNA from *E. coli*, or other model microbes with established genetic systems, has not been described.

A potential solution to overcome issues regarding DNA transfer and optimize DNA-transfer techniques for *M. thermautotrophicus* ΔH is the pseudomurein-degrading enzyme

pseudomurein endoisopeptidase (PeiP). PeiP and its homologue PeiW are proteases that are found in the *Methanothermobacter* spp. specific virus ΨM2 and *Methanothermobacter wolfei*, respectively. PeiP/PeiW belong to the best characterized proteases in methanogenic archaea. The pseudomurein-containing cell-wall is degraded by PeiP/PeiW, which cleave the iso-peptide bonds between the ε-amino group of an L-lysine residue and the α-carboxyl group of an L-alanine residue in the oligo-peptides that link the sugar chains of pseudomurein (Luo *et al.* 2002, Visweswaran *et al.* 2010, Schofield *et al.* 2015). This reaction removes the cell-wall of *Methanothermobacter* spp. resulting in protoplast formation (Sarmiento *et al.* 2011). Protoplast recovery was not achieved for *M. thermautotrophicus* ΔH, but the use of small concentrations of PeiP/PeiW might be helpful to permeabilize the cell-wall of *M. thermautotrophicus* ΔH, which could favor DNA transfer during DNA-transfer experiments.

4.3. Masking of heterologous DNA with DNA-methylation

DNA methylation is a crucial parameter in the establishment of new genetic systems for microbes. Restriction-methylation systems prevent heterologous DNA from replication and integration in the microbe by degradation. These systems recognize and break-down heterologous DNA through recognition of non- or differently methylated DNA sequences (Goldberg and Marraffini 2015). Since genetic modification of *E. coli* has been well established, it is common to use *E. coli* to produce genetically engineered heterologous DNA for modification of other microbes. In general, there are three genes of *E. coli* mainly responsible for methylation of *E. coli* DNA: 1) the gene *dam* expresses the Dam methyltransferase. This enzyme transfers a methyl group from S-adenosylmethionine (SAM) to the N6 position of the adenine residues of the sequence GATC; 2) the Dcm methyltransferase that is encoded by the *dcm* gene. This enzyme methylated the internal cytosine residues of the target sequences CCAGG and CCTGG at the C5 position; and 3) the *Eco*KI methyltransferase methylates adenine residues in the sequences AAC(N6)GTGC and GCAC(N6)GTT. While Dam recognition sites (1/256 bp) and Dcm recognition sites (1/512 bp) occur often in a random sequence of GC=AT, *Eco*KI sites are rare with around 1 in 8 kb (Marinus and Morris 1973, Marinus 1987). Deletions in all of those three genes are not lethal to *E. coli*. Therefore, to mask the DNA, which is used for genetic modifications in other microbes than *E. coli*, it is recommended to use an *E. coli* that is lacking at least the Dcm and Dam methyltransferases (dam$^-$/dcm$^-$ competent *E. coli*, New England Biolabs, Frankfurt, Germany). Additionally, helper plasmids with methyltransferases of the desired microbe can change the methylation state of heterologous DNA, and furthermore imitate the native DNA of the microbe, which is supposed to be genetically modified (Mermelstein and Papoutsakis 1993, Molitor *et al.* 2016).

4.4. Possible selectable markers for *M. thermautotrophicus* ΔH

Most of the common antibiotic substances that are used for the selection of bacteria, such as the model microbe *E. coli*, do not work for *Methanothermobacter* spp. (Hilpert *et al.* 1981). There are two problems. First, it is not possible for some antibiotic substances to enter the unique cell-wall structure of Methanobacteriales (pseudomurein). Second, the temperature stability of temperature-labile antibiotic substances is not given due to the incubation temperature of 65°C for *M. thermautotrophicus* ΔH. Puromycin meets both of these criteria (entering the cell and temperature stability). It incorporates into proteins as an amino acid analog and inhibits the metabolism of the microbe. It acts as a bacteriostatic antibiotic (Darken 1964). Thus, it is a candidate to be used in *M. thermautotrophicus* ΔH.

The kanamycin derivate neomycin has been shown to inhibit growth of *M. thermautotrophicus* ΔH, but also result in spontaneous resistant mutants (Majernik *et al.* 2003). However, thermostable variants of neomycin resistance genes as selectable markers for positive selection are available and already used in the genetic systems for the thermophilic *M. thermophilus* (Hoseki *et al.* 1999, Fonseca *et al.* 2020). This makes neomycin a candidate antibiotic for positive selection in *M. thermautotrophicus* ΔH. As for *Methanosarcina* (Boccazzi *et al.* 2000), pseudomonic acid has been shown to inhibit growth of *M. marburgensis*. Natural occurring mutations in the *ileS* gene of *M. marburgensis* resulted in resistance towards pseudomonic acid (Jenal *et al.* 1991). Thus, a mutated *ileS* gene is another candidate to act as a selectable marker.

The default carbon- and energy source of the thermophilic hydrogenotrophic methanogenic archaeon *M. thermautotrophicus* ΔH is carbon dioxide and hydrogen. Several strains of *M. thermautotrophicus,* however, owe the ability to use formate instead of hydrogen and carbon dioxide as their source of energy and carbon for growth and methane production (Nölling and Reeve 1997). The type strain *M. thermautotrophicus* ΔH lacks the ability for formate consumption (Touzel *et al.* 1992). Before the reclassification in the year 2000 towards the species of *M. thermautotrophicus*, strains with the ability to use formate were described as *Methanobacterium thermoformicium* (*M. thermoformicicum*); strains without this ability *Methanobacterium thermoautotrophicum* (Wasserfallen *et al.* 2000). Two of the formate using *M. thermautotrophicus* strains were analyzed in detail, the strains SF-4 (Yamamoto *et al.* 1989, Tanaka *et al.* 1994) and Z-245 (Nölling and Reeve 1997). However, a precise gene transcription analysis concerning formate usage is only available for *M. thermautotrophicus* Z-245. *M. thermautotrophicus* Z-245 shares a very similar formate dehydrogenase operon ($fdh_{Z\text{-}245}$) with the closely related species *Methanobacterium formicicum*, but also contains open reading frames (ORF) of *M. thermautotrophicus* ΔH in the same genetic region (**Figure 7**). It is still unclear whether the $fdh_{Z\text{-}245}$ operon was inserted into the genome of *M.*

thermautotrophicus Z-245 or excised from *M. thermautotrophicus* ΔH. The operon is located between ORF2 and DNA ligase (*lig*) (Nölling and Reeve 1997). The region up- and downstream of the $fdh_{Z\text{-}245}$ operon in *M. formicicum* contains the genes *fdhD* and *moaA*. *FdhD* is, similar to *moaA*, responsible for the biosynthesis of a molybdenum dependent chaperone. This chaperone is crucial for the function of related formate dehydrogenases (Hartmann *et al.* 2015). Therefore, it can be assumed that an increased concentration of molybdenum in the media would stimulate growth of *M. thermautotrophicus* Z-245 with formate. Since the entire genome of *M. thermautotrophicus* Z-245 has not been sequenced yet, the flanking regions of the $fdh_{Z\text{-}245}$ operon remain still unknown. Therefore, a heterologous expression of the formate dehydrogenase cassette in *M. thermautotrophicus* ΔH could lead to a formate prototrophy and thus, could act as a selectable marker.

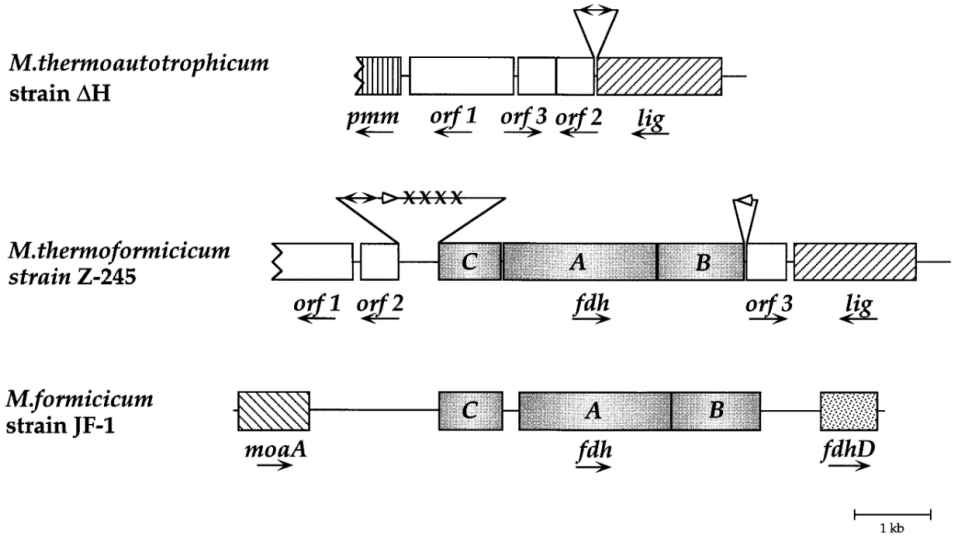

Figure 7. Genomic DNA section of *M. thermautotrophicus* ΔH, *M. thermautotrophicus* Z-245, and *M. formicicum* shows the locus of the $fdh_{Z\text{-}245}$ with additional up- and downstream regions. Since strain ΔH lacks the $fdh_{Z\text{-}245}$ operon, the potential excision site is highlighted (Nölling and Reeve 1997)

4.5. Genetic modification in *M. thermautotrophicus* ΔH

Up to now, no species in the order of Methanomicrobiales is genetically tractable. *M. thermautotrophicus* ΔH, which is a member of the order of Methanomicrobiales, is perfectly suitable for the establishment of a genetic system. It is more robust concerning oxygen contamination than most other methanogenic archaea (Kiener and Leisinger 1983). It has very short lag phases after transfer into fresh growth medium. Additionally, its doubling time of around 1.5 h at its optimal growing temperature is fast for methanogenic archaea (Nölling and Reeve 1997).

Furthermore, a transduction study was performed with the self-integrating virus ΨM1 specific to *M. marburgensis*. Genomic DNA of wild-type *M. marburgensis* with virus ΨM1 was used for transduction of leucine, adenosine, or tryptophan auxotrophic *M. marburgensis* strains. This

led to a regain of the metabolic pathways, and therefore to overcome the auxotrophy towards leucin, adenosine, or tryptophan, respectively. *M. marburgensis* was transformed successfully. However, the small burst size and low transformation frequencies lowered the interest in further analysis (Meile *et al.* 1990). In a second approach, wild-type *M. marburgensis* was transformed trough the addition of high-molecular-weight genomic DNA from a *M. marburgensis* strain that is resistant to 5-fluoruracil (5-FU). Wild-type *M. marburgensis* was spotted on solidified mineral media plates together with genomic DNA of the 5-FU resistant strain. 1.1% of all clonal populations tested were resistant to 5-FU. 5-FU-resistant *M. marburgensis* individual clonal populations, that were only detected on solidified mineral medium plates, containing gelrite instead of agar. However, in liquid media no transformants were detectable. Albeit, the transformation efficiency was negligibly low (Worrell *et al.* 1988).

Several approaches of genetic modification concerning *M. thermautotrophicus* ΔH were undertaken. Analogous to the cryptic plasmids pC2A in *Methanosarcina* spp. (Metcalf *et al.* 1997) and pURB500 in *Methanococcus* spp. shuttle-vector systems (Tumbula *et al.* 1997), there are the cryptic plasmids pME2001 (4.4 kb) and pME2200 (6.2 kb) of *M. marburgensis* and *M. thermautotrophicus* ZH3 (Bokranz *et al.* 1990, Stettler *et al.* 1995, Luo *et al.* 2001), respectively. The plasmid pME2001 from *M. marburgensis* was the first methanogenic plasmid isolated. Because *M. marburgensis* and *M. thermautotrophicus* ΔH are closely related, there is a high likelihood that *M. thermautotrophicus* ΔH is covered by the host range of the origin of replication on pME2001. That could enable pME2001 to act as a replicon in *M. thermautotrophicus* ΔH (Meile and Reeve 1985). The plasmids pME2001 and pME2200 share the same sequence of 4.35 kb. There are only 5 regions that differ between the plasmids, the inserted fragments 1-5 (IF1-IF5) (**Figure 8**). While IF1-IF4 are only present in pME2200, IF5 is the only inserted fragment that derives from pME2001. It was reported that putative shuttle vector constructs, containing pME2001 and standard *E. coli* low copy number vectors (pET, pBBR), were replicated in *E. coli*. A problem arose due to the toxic side-effects of proteins that were expressed from genes on pME2001 in *E. coli* (Meile and Reeve 1985). Additionally, a hot-spot site in which genomic DNA of *E. coli* is spontaneously inserted into pME2001 was found. This hot-spot site was determined as an IS10 locus (Luo *et al.* 2001). Further investigations towards using pME2001 as a replicon for *M. thermautotrophicus* ΔH failed due to assembly issues in *E. coli* (Luo *et al.* 2001). Another possibility for a replicon in *M. thermautotrophicus* ΔH would be the plasmids pFZ1 and pFZ2 from *M. thermautotrophicus* Z-245. These plasmids are ~12 kb in size and probably replicated by a rolling circle mechanism (Nölling *et al.* 1991). However, the large plasmid size poses an additional hurdle to use the entire plasmid as replicon in shuttle vector constructs (Wang *et al.* 2015). Further analysis of

the precise region of the origin of replication would be necessary before implementing pFZ1 or pFZ2 into shuttle vector constructs for *E. coli* and *M. thermautotrophicus* ΔH.

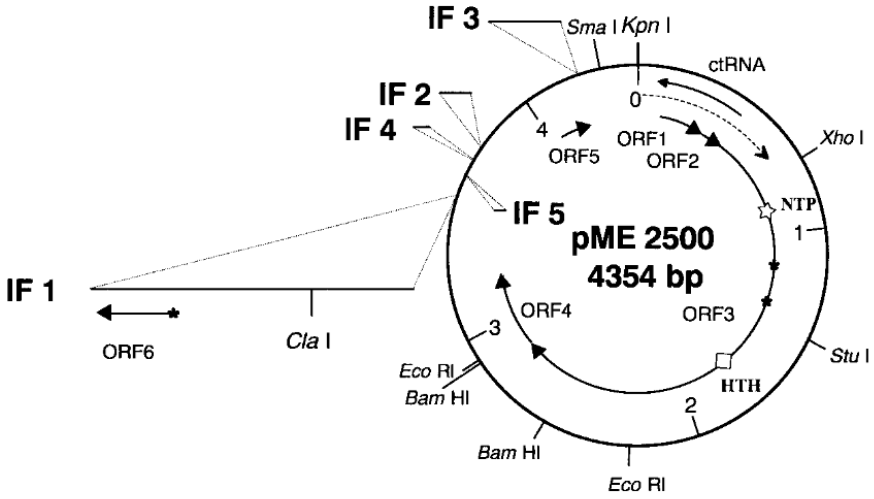

Figure 8. Vector map of plasmid pME2500. This theoretical plasmid is a fusion of the cryptic plasmids pME2001 and pME2200 from *M. marburgensis* and *M. thermautotrophicus* ZH3, respectively. The plasmids share the same backbone of 4,354 bp. Additional regions are marked as inserted fragments (IF). IF1-IF4 are only present in pME2200; IF5 only in pME2001 (Luo *et al.* 2001).

Spurred by the recurring interest in *Methanothermobacter* spp. as model microbes for biochemistry and physiology of methanogenic archaea with a long history, and as biotechnologically relevant microbes in power-to-gas processes, we set out to utilize modern molecular biology tools and the knowledge on the genetic tools for other methanogenic archaea and thermophilic microbes as described in the previous sections to develop a genetic system for *M. thermautotrophicus* ΔH.

Dissertation outline

Objective 1: Establishment of preliminary requirements for the development of genetic tools for *M. thermautotrophicus* ΔH

- Spot-, spread-, and pour-plating enables for isolation of individual clonal populations of *M. thermautotrophicus strain* ΔH and strain Z-245 with high plating efficiencies. (**See IV.1.1.**)
- *M. thermautotrophicus* ΔH is sensitive to antibiotic substances, that were commonly used in genetic systems for methanogenic archaea (**See IV.1.2.**)

Objective 2: Establishment of a DNA-transfer protocol for *M. thermautotrophicus* ΔH

- Interdomain conjugation with *E. coli* S17-1 allows for DNA transfer into *M. thermautotrophicus* ΔH (**See IV.2.1.**)
- Free plasmid DNA is not resulting in DNA transfer into *M. thermautotrophicus* ΔH (**See IV.2.2.**)

Objective 3: Establishment of genetic tools for *M. thermautotrophicus* ΔH

- The modular pMVS design (plasmid *Methanothermobacter* Vector System) acts as a replicative shuttle vector in *E. coli* and *M. thermautotrophicus* ΔH (**See IV.3.**)
- Suicide vector constructs facilitate genome integration in *M. thermautotrophicus* ΔH (**See IV.4.**)

Objective 4: Proof of principle for heterologous gene expression in *M. thermautotrophicus* ΔH *via* the pMVS design

- A thermostable ß-galactosidase (BgaB) from *Geobacillus stearothermophilus* is a functional reporter to investigate promoter sequences in *M. thermautotrophicus* ΔH (**See IV.5.**)
- The constitutive promoters P_{synth}, $P_{synth(BRE)}$, and P_{hmtB} initiate protein biosynthesis with different levels of gene expression (**See IV.5.**)

III. Materials and Methods

1. Microbial strains and cultivation conditions

In this study, we cultivated exclusively *Escherichia coli* and *Methanothermobacter* spp. strains for respective experiments. For preliminary molecular-vector fusion, the cloning strain *E. coli* NEB stable (New England Biolabs, Frankfurt, Germany) was applied. For heterologous gene expression, we used *E. coli* BL21(DE3) (Merck Millipore, Mannheim, Germany), and for interdomain conjugational DNA transfer we used *E. coli* S17-1 (Pozzi *et al.* 2016). *E. coli* S17-1 was kindly provided by Prof. Wolfgang Wohlleben (Biotechnology Department, University Tübingen, Tübingen, Germany). *M. thermautotrophicus* ΔH (DSM 1053), *M. thermautotrophicus* Z-245 (DSM 3720), and *M. marburgensis* (DSM 2133) were obtained from the DSMZ (Braunschweig, Germany).

E. coli was cultivated in LB medium, which contained (per liter): sodium chloride, 10 g; tryptone, 10 g; yeast extract, 5 g, and which was supplemented with appropriate amounts of chloramphenicol (30 µg/mL), ampicillin (100 µg/mL), or kanamycin (50 µg/mL). For cultivation of *E. coli* S17-1, trimethoprim (10 µg/mL) was added to stabilize the genome-integrated *tra* module, which is responsible for mobilization of plasmid DNA (Simon *et al.* 1986). Solidified LB media plates contained 1.5 weight% of Kobe I Agar (Carl Roth, Karlsruhe, Germany) and were incubated at 37°C. Liquid *E. coli* cultures were incubated at 37°C with shaking at 150 rpm (Lab companion ISS-7100R, Jeio Tech, Republic of Korea).

Methanothermobacter spp. were cultivated according to basic principles for methanogen cultivation as stated in Balch *et al.* (1979), with adjustments to state-of-the-art anaerobic handling equipment. The mineral medium contained (per liter): sodium chloride, 0.45 g; sodium hydrogen carbonate, 6.00 g; di-potassium hydrogen phosphate, 0.17 g; potassium di-hydrogen phosphate, 0.23; ammonium chloride, 0.19 g; magnesium chloride hexahydrate, 0.08 g; calcium chloride dihydrate, 0.06 g; ammonium nickel sulfate, 1 mL (0.2 weight%); iron(II)chloride pentahydrate, 1 mL (0.2 weight%); resazurin indicator solution, 4 mL (0.025 weight%); and trace element solution, 1 mL (10-fold as stated in Balch *et al.* (1979)). All chemicals were *p.a.* grade. No vitamin solution was added. For the formate growth experiments, the mineral medium was supplemented with 100-200 mM sodium formate, 10 µM sodium molybdate, 1 µM sodium selenite, and 0.125 weight% yeast extract. The medium was gassed using N_2/CO_2 (80/20 volume%) to eliminate dissolved oxygen. The pH value was adjusted to 7.2 using hydrochloric acid. As reducing agent and sulfur source, we added 0.5 g/L cysteine hydrochloride. For solid mineral medium, we additional supplied 0.3 g/L sodium sulfide monohydrate. Afterwards, the mineral medium was dispensed into serum bottles inside

of an anaerobic chamber with a 100% N_2 atmosphere (UniLab Pro Eco, MBraun, Garching, Germany). The headspace of the serum bottles was exchanged to 200 kPa H_2/CO_2 (80/20 volume%) and autoclaved (100 kPa, 20 min, 121°C). For the formate growth experiments, the headspace of the serum bottles was exchanged to 152 kPa N_2/CO_2 (80/20 volume%). All *Methanothermobacter* strains in liquid medium were incubated at 60°C with shaking at 150 rpm (Lab companion ISS-7100R, Jeio Tech, Republic of Korea). For cultivation of genetically modified *M. thermautotrophicus* ΔH, 250 µg/mL neomycin sodium salt was added when shuttle-vector constructs were used, and 100 µg/mL with suicide-vector constructs for genome integration. It was important to add freshly prepared anaerobic neomycin sodium salt solution. For solidified mineral medium, 1.5 weight% Bacto™ agar (BD Life Science, Berkshire, UK) was supplemented *prior* to autoclaving. Afterwards, solidified media plates were poured and dried for 2 h inside of the anaerobic chamber. *M. thermautotrophicus* ΔH was applied to solidified media plates by spot-plating, spread-plating, or pour-plating. For spot-plating, 50 µL of *M. thermautotrophicus* ΔH culture was spotted on a solidified media plate. Incubation was started after the drop was completely absorbed. For spread-plating, 50 µL of diluted or undiluted liquid culture was applied to a solidified media plate and spread with a Drigalski spatula until the liquid was completely absorbed. For pour-plating, 5 mL mineral medium containing 0.8 weight% Bacto™ agar (soft-agar) were mixed with a liquid *M. thermautotrophicus* ΔH culture and poured on top of a solidified media plate, which contained 1.5 weight% Bacto™ agar. For better gas-solid mass transfer and to avoid sealing of the plates by water, paper clips were added to the petri dish *prior* to incubation in a custom-made stainless-steel jar (Raff + Grund, Freiburg am Neckar, Germany) (**Figure 11**) inspired by Balch *et al.* (1979). The gas phase of the stainless-steel jar was exchanged to 200 kPa of $H_2/CO_2/H_2S$ (79.9/20/0.1 volume%). The pressurized anaerobic jar was incubated without shaking at 60°C in a heat incubator (Memmert, Schwabach, Germany).

2. Primers, plasmids, gBlocks, and genetically modified strains

All primers, gBlock™ DNA fragments (IDT, Coralville, IA, USA), and plasmids used in this study are summarized in **Tables 1-3.**

Table 1. List of primers used in this study

Name	Purpose	Sequence (5' -> 3')	Reference
Gib_CF1	pCF203	ATAAAATGCTTGGGAGATGACGCCCGCCCCAC	This study
Gib_CF2	pCF203	ATAATCTCCTCTATTTCCATGAGAATCACTCCTATTTTTTTG ATATATACATCATAACATTAC	This study
Gib_CF3	pCF203	AAAAAATAGGAGTGATTCTCATGGAAATAGAGGAGATTATAG AGAAAGTTGCTAGG	This study
Gib_CF4	pCF203	TGCGGGTCGTGGGGCGGGCGTCATCTCCCAAGCATTTTATGA GCCCTAGC	This study

Gib_CF5	pSB1	GCCGGTGGTTACCGTGATATTATCTATTACTATATCCCTATATAAAGAATACTCAAAAAATGGGC	This study
Gib_CF6	pSB1	GTAATAGATAATATCACGGTAACCACCGGCTAGCAGGTGATGCATATGGCTAAAATGAGAATATCAC	This study
Gib_CF7	pSV1_1	TATTTTGAATCCATTGCGTTGCGCTCACTG	This study
Gib_CF8	pSV1_1	TGGGCGGCCGGCCGCGTTAATATTTTGTTAAAATTCGCGTTAAATTTTTGTTAAATCAG	This study
Gib_CF9	pSV1_1	AAATATTAACGCGGCCGGCCGCCC	This study
Gib_CF10	pSV1_1	TGCATTTTTTTGCGGCGCGCCCTGACA	This study
Gib_CF11	pSV1_1	AGCGCAACGCAATGGATTCAAAATAGATTCATAATGGAGTCATCCACG	This study
Gib_CF12	pSV1_1	TCAGGGCGCGCCGCAAAAAAATGCAAATAAAATTTGGGGTGG	This study
Res_CF1	pSV1_2	CGTACTGCAGCGATCGCGGTCATATGGATACAGCGGCC	This study
Res_CF2	pSV1_2	GTTATGGATTATAAGCGGCCGGC	This study
Gib_CF13	pMVS1111A:P_{synth}-*bgaB*	CCACCCTGCCACCCCAAATTTTATTTGCATTTTTTTGCGGGTTAATTAAGCCTGGAGGAATGCCTTTATATAGG	This study
Gib_CF14	pMVS1111A:P_{synth}-*bgaB*	TTTATATATTTTTAATTCACTGGGGGCAATTCTGTCAGGGCGCGCCTGGGGTCGTGCGCTC	This study
Gib_CF15	pMVS1111A:P_{hmtB}/$P_{mrt(M.t.)}$-*bgaB*	CGGCTCTAGCTATGTCCGATC	This study
Gib_CF16	pMVS1111A:P_{hmtB}/$P_{mrt(M.t.)}$-*bgaB*	CACTGGGGGCAATTCTGTCAG	This study
Gib_CF21	pCF201	AATACAAGAAAGGCGCGCCAAATCATTATATAGGACCTTGATAAAATTTTTTAGAGGGC	This study
Gib_CF22	pCF201	ACCTGACGTGTGGCCGGCCCGATTCAAATATAACAGCCGTTATAACACCGC	This study
Gib_CF23	pCF201	AATCGGGCCGGCCACACGTCAGGTGGCACTTTTCG	This study
Gib_CF24	pCF201	CATCCACGGATGCGATCGCCTAAGAAACCATTATTATCATGACATTAACCTATAAAAATAGGC	This study
Gib_CF17	pCF202	AAAAAATAGGAGTGATTCTCATGGCTAAAATGAGAATATCACCGGAAT	This study
Gib_CF18	pCF202	TGCGGGTCGTGGGGCGGGCGCTAAAACAATTCATCCAGTAAAATATAATATTTTATTTTCTCCCAAT	This study
Gib_CF19	pCF202	GATATTCTCATTTTAGCCATGAGAATCACTCCTATTTTTTTGATATATACATCATAACATTAC	This study
Gib_CF20	pCF202	TACTGGATGAATTGTTTTAGCGCCCGCCCCACG	This study
Res_LM1	pMVS1111A:P_{hmtB}-*fdh*$_{z\text{-}245}$	ATCGGCTTAGGCGCGCCTGCTCATCGTCAATTCTAGTAGAGTCATGAATCATTATGCAGG	This study
Res_LM2	pMVS1111A:P_{hmtB}-*fdh*$_{z\text{-}245}$	GCTTAGCGCATTAATTAACCGCCCATTTTTTGAGTATTC	This study
Gib_LM1	pLM201	TAACAGCGGCGCTATCAAGGTCCTGCATAATGATTCATGACGCCCGCCCCACG	This study
Gib_LM2	pLM201	TTTGCCGTATCTGCAGGCGATTTAAAAGATGATCCCATGAGAATCACTCCTATTTTTTTG	This study
Gib_LM3	pLM201	TTATGATGTATATATCAAAAAAATAGGAGTGATTCTCATGGGATCATCTTTTAAATCGCC	This study
Gib_LM4	pLM201	TCCTTTCGGTCGGGCGCTGCGGGTCGTGGGGCGGGCGTCATGAATCATTATGCAGGACC	This study
Gib_LM5	pLM202	ATCCTATATAAATATATCGCTAATTTTAAGGTTTTTCTGAGCCATCGGTTGGTTCATGGGTTAATTAAGAATACTCAAAAAATGGGCG	This study
Gib_LM6	pLM202	CGATATATTTATATAGGATTATATGAATAGATAATATCACATAAAATGAGGTGGTTAATTATGGGATCATCTTTTAAATCGCCTGCAG	This study

Seq_CF1	specific for gDNA *M. t.*1.5 kb	CCACCAGTTCGACTCCCTGG	This study
Seq_CF2	specific for gDNA *M. t.*1.5 kb	CTGTTAAAGGCGGGGGTGG	This study
Seq_CF3	specific for gDNA *M. t.* 2.8 kb	CTTGGGTGATGATGGGATGTATTG	This study
Seq_CF4	specific for gDNA *M. t.* 2.8 kb	CGAGGAGAAACACATCCAGCTG	This study
Seq_CF5	specific for pME2001 replicon	GTTAATCCAGCACATCCTCC	This study
Seq_CF6	specific for pME2001 replicon	CCTGTCCAACTTATACCTTTGG	This study
Seq_CF7	analysis of *bgaB* constructs	CCCCATAACATCGGCACAGTAC	This study
Seq_CF8	analysis of *bgaB* constructs	CCTGGCTGGGGTTAATAAATGTTG	This study
Seq_LM1	analysis of $fdh_{Z\text{-}245}$ constructs	GATTTCTGGAATCCGCCATGGG	This study
Seq_LM2	analysis of $fdh_{Z\text{-}245}$ constructs	CTAATAGTCGCCGATCCAAG	This study
Seq_LM3	analysis of $fdh_{Z\text{-}245}$ constructs	GGTTCCTGGCTTGAATG	This study
Seq_LM4	analysis of $fdh_{Z\text{-}245}$ constructs	GAGAAGCAAAGGATGACTG	This study
Seq_LM5	analysis of $fdh_{Z\text{-}245}$ constructs	CAGCACCCATCTTATTCG	This study
Seq_LM6	analysis of $fdh_{Z\text{-}245}$ constructs	GCAGTTAAGAAGGGTTCG	This study
Seq_LM7	analysis of $fdh_{Z\text{-}245}$ constructs	GGCTCCGTTATAAGGGTTG	This study
Seq_LM8	analysis of $fdh_{Z\text{-}245}$ constructs	CTGAATGGATCGAGAAAGG	This study
Seq_LM9	analysis of $fdh_{Z\text{-}245}$ constructs	CATTCTTTCGAGATGGAAG	This study
Seq_LM10	analysis of $fdh_{Z\text{-}245}$ constructs	CCTATATTCGCATTCGTGG	This study
Seq_LM11	analysis of $fdh_{Z\text{-}245}$ constructs	ATGTTTGCCACACTGTG	This study
Seq_LM12	analysis of $fdh_{Z\text{-}245}$ constructs	GGTGGGGTTTTGGTGTGCG	This study
Res_CF3	upstream flank integration pCF702	TAGCCTATTCGGCGCGCCGAAATCCCAACCTTCATATAATATTGCAAG	This study
Res_CF4	upstream flank integration pCF702	TCATGGCTACGTCGACCGGGCCATAACACATACCAC	This study
Res_CF5	downstream flank integration pCF702	TCAGGATTCGGGCCGGCCTCCGTAAGAAGGGAATTGAACCTCC	This study
Res_CF6	downstream flank integration pCF702	CGTTGCAATGCATATGGGTACTGTGTGAGGGTCATATTCTG	This study
Res_CF7	pUC to pMTL exchange pCF702	TATTGCAATGGTCGACAGTGGGCAAGTTGAAAAATTCAC	This study

M13 FW	pUC to pMTL exchange pCF702	TGTAAAACGACGGCCAGT	Eurofins genomics (Konstanz, Germany) standard primer list
Res_CF9	Resistance gene exchange in pCF702 + pCF703	TACGTTGCCAGGCCGGCCCCCATGAACCAACCGATGGC	This study

Table 2. List of gBlocks used in this study

Name	Sequence (5' -> 3')	Reference
gBlock $P_{mcr(M.v.)}$-*pac*-$T_{mcr(M.v.)}$	GGTACCGAAAAGTGCCACCTGACCGATGGCCGGCCGCCCATTTTTTGAGTATTCAAATT CAAATTATTGTGTTATTAACATCTTATATATAAACTTTTCTATTTAATGTTAATGAAAA AGTGAATATATATACATAGAGTAATGTTATGATGTATATATCAAAAAAATAGGAGTGAT TCTCATGACCGAGTACAAGCCCACCGTTAGGCTCGCAACCAGGGATGATGTTCCCAGGG CAGTTAGGACCCTCGCAGCAGCATTCGCAGATTACCCCGCAACCAGGCACACCGTTGAT CCCGATAGGCACATAGAGAGGGTTACCGAGCTCCAGGAGCTCTTCCTCACCAGGGTTGG TCTCGATATAGGTAAGGTTTGGGTTGCAGATGATGGTGCAGCAGTTGCAGTTTGGACCA CCCCCGAGTCAGTTGAGGCAGGTGCAGTTTTCGCAGAGATAGGTCCCAGGATGGCAGAG CTCTCAGGTTCAAGGCTCGCAGCACAGCAGCAGATGGAGGGTCTCCTCGCACCCCACAG GCCCAAGGAGCCCGCATGGTTCCTCGCAACCGTTGGTGTTTCACCCGATCACCAGGGTA AGGGTCTCGGTTCAGCAGTTGTTCTCCCCGGTGTTGAGGCAGCAGAGAGGGCAGGTGTT CCCGCATTCCTCGAGACCTCAGCACCCAGGAACCTCCCCTTCTACGAGAGGCTCGGTTT CACCGTTACCGCAGATGTTGAGTGCCCCAAGGATAGGGCAACCTGGTGCATGACCAGGA AGCCCGGTGCATGACGCCCGCCCCACGACCCGCAGCGCCCGACCGAAAGGAGCGCACGA CCCCATGGCTCCGACCGAAGCCACCCGGGGCGGCCCCGCCGACCCCGCACCCGCCCCCG AGGCCCACCGCGGGGGACACACCGAACACGCCGACCCTGCTGAACACGCGGCGCAGTTC GGTGCCCAGGAGCGGATCGGGAATTAATTCGAAGCTGCTGGTGAAAGAGACCCTATCTT ACCTGCTAAAATCTAAGTTAATTACTAATTTATTATTAATTTATTATTAGATTGGGCAA AATAGTAAAAGAAAACTAAAGGAAACCTAATATGGTTTCCTTTTTTTATATATTTTTAA TTCACTGGGGGCAATTCTGTCAGGGCGCGCCTTCGGGCCATCGGGCCC	This study
gBlock P_{hmtB}-*Pac*I-*bgaB*	CGGCTCTAGCTATGTCCGATCAATCTTAATTAAGCCTGGAGGAATGCCCCCATGAACCA ACCGATGGCTCAGAAAAACCTTAAAATTAGCGATATATTTATATAGGATTATATGAATA GATAATATCACATAAAATGAGGTGGTTAATTATGAACGTTCTCAGTTCCATCTGCTATG GGGGGGATTACAAC	This study
gBlock $P_{mrt(M.t.)}$-*Pac*I-*bgaB*-cor	CGGCTCTAGCTATGTCCGATCAATCTTAATTAAGCCTGGAGGAATGCCCCATTTCCATG GATTATCGCTGGCAATCCCATAACCCCATCAGTTTTATTAATAAAATAGTAAATTTTAT TAATAAATAAATAAAACAAGAGGTGTGAATACCATGAACGTTCTCAGTTCCATCTGCTA TGGGGGGGATTACAAC	This study
gBlock codon-optimiz	CTGACAGAATTGCCCCCAGTGAATTAAAAATATATAAAAAAAGGAAACCATATTAGGTT TCCTTTAGTTTTCTTTTACTATTTTGCCCAATCTAATAATAAATTAATAATAAATTAGT AATTAACTTAGATTTTAGCAGGTAAGTGGGGTCGTGCGCTCCTTTCGGTCGGGCGCTGC	This study

ed GGGTCGTGGGGCGGGCGCTAGACCTTGCCGGCTTCGTCGTGTTCCCTAAGGACAGCGAC

bgaB GTCGACGCCCTGAATCCTGAGTTCACCCCCCCTGAAGCATTTGCCATCTATCATATTCT

GGTAGATCTTATCTTCCGGAAGGGAGAGTGTGACCTCATAGTCGTTGTGGTTAATTATA

ATAAGGTACTTCCATTCATCGGTCTCCCTCTGCTGAACTTCGACATTCTCAGCAACCTC

CAGTATAGGATTTATGTGGTGTTTAGCAAACACCTGTTCGAGAAGCCTGCCAAGGTAGT

TGCTGTCAGGGTATGTTCCTACGTATATGCCCTCCCCCTTTCCGTAGCAGTTCCTGGTA

ACAGCAGGAAGGCCGGCATACCAATCACCTTTGAATGTGGCGAGAGGCTCAGCACCTTC

CAGCCTTATTATATCGGCCCATGTGGTACAGTCATACTCGCCGTCGTTTGAGTAGATCT

TATTCACCTTTGTCTCGGGATAAGGAACGAATTCCTCCACGAAGATGCCGAGAATGTCC

CTCAGCGGTCCTGGATATCCCCCGAGGTGCACTCTATCGTTCTCATCGACTATCACACT

GAAAAAGCTTACAATCAGGGTTCCGCCGTTTGCGACAAACTGCCTAAGGTTCTCATCTT

CTCCCTCTTTCACCATATACAGCATCGGTGCAATAACAACCTTATATTTTGTGAGATCG

TCGGACGGTCTTACAAAGTCGACTGCTATGTTTCTCTTGTAAAGCTCTCTATAATATGC

CTCTACTATGGGAATATATCTGAGCTTGTTGTGCGGTTTGGAACTGAGCTCAACTGCCC

ACCAGTTTTCCCAGTCAAAGATAATTGCCACCTCTGCCTTTATTCTACTCCCCACGAGG

CAGTCAAGTTTTTTCAGCTCCTGGCCAAGCTGGGTAACTTCCCTGTATATTCTATTGTT

TTCGTTAAGAAAGTGGGGCACCATTGCTCCGTGAAACTTCTCAGCTCCTGCTCTGGACT

GCCTCCACTGAAAGAACATTATCCCATCGGCACCCCTGGCGATTGTTGCGTAACTCCAG

AGTCTCATAACCCCCGGCGGCTTTGGCACATTGATATCTCTCCAATTAACGTGACTGGT

GACCTGCTCCATAAGAATGAACGGCTGCCCCTTCCTAAGTGACCTCATGAGGTCATTCA

TCATTGCGTGCTGTATAGGGAGTCCCTCCCTGGGATCTGGGTAGCTATCCCAGGTAACG

ATATCTACGTGCTGAGCCCACTGAAAGTAGTTGAGTGGCTTGAATGATCCCATGAAATT

TGTGGAGACCGGGATATCGGGGGTTACTTCCCTGAGGATCTCCTTTTCTGTAAGGAAGA

GTTTGAGGATTGAATCATTCATGAATCTGTAGTAATCAAGCTCCTGGCTGGGGTTAATA

AATGTTGGTGCCTTCCTAGGGGGATTAATCTCATCCCAGTGGTTATATCTCTGGCCCCA

GAAGTTTGTACCCCATCTTTCATTAAGTTCATCAATGGTCTTATACCTTTCTTTAAGCC

ATTTTCTGAAAGCAACTGCGCAATTCTCACAGAAACACTTACTTACATGGCAAGCGTAT

TCGTTATTTACGTGCCACATTTTGAGGGCTGGATGATTTTTGTATCTCTCAGCTATAGC

CCTTACCAGCCTCTTTATATGTGTTATAAGCTGAGGGTGATTTGGGCAATAATGCTGTC

TACTCCCGAAACTCAGTATCACACCGGACTCGTCAATAGGGAGTGAATCAGGGTATTTC

TTCACGAACCAGGCGGGTGTGGTTGCGGTGGCGGTCCCCAGATTTATGTATACCCCATG

ATCGTAGAGGATGTCTATCACTTTGTCGAGCCATTCAAAATCAAATACACCGTCTGATG

GCTCGATTTTGGACCAGCTAAAGATTCCGAGTGAAACAAGATTAACACCGGCCTTCTGC

ATAAGTTTTGCGTCCTCGTACCATATCTCCTCGGGCCACTGTTCTGGGTTGTAATCCCC

CCCATAGCAGATGGAACTGAGAACGTTCATATGCATCACCTGCTAGCCGGTGGTTACCG

TGATATTATCTATTACTATATCCCTATATAAAGGCATTCCTCCAGGCTTAATTAAC

Table 3. List of plasmids used in this study

Name	Function	Reference	*M. t.* strain[1]
pMTL83151	Shuttle vector for *Clostridia* spp.	Heap *et al.* (2009)	-

pMU131	Shuttle vector for *Thermoanaerobacter* spp.	Shaw *et al.* (2010)	-
pME2001	Cryptic plasmid of *M. marburgensis*	Bokranz *et al.* (1990)	-
pBBR1-MCS2	Standard cloning vector in *E. coli*	Kovach *et al.* (1995)	-
pUC19	Standard cloning vector in *E. coli*	Yanisch-Perron *et al.* (1985)	-
pYS3	Shuttle vector for *Pyrococcus furiosus* including Sim^r	Waege *et al.* (2010)	-
pME2508	PeiP production in *E. coli*	Luo *et al.* (2002)	-
pCF200	pUC57 vector including synthesized $P_{mcrB(M.v.)}$_Pur^r codon-optimized for *M. thermautotrophicus* ΔH, T_{mcr}	This study	-
pCF201	pUC19 vector including native *M. thermautotrophicus* Z-245 $fdh_{Z\text{-}245}$ operon with putative promoter region	This study	-
pLM201	Exchange of Neo^r to coding region of $fdh_{Z\text{-}245}$ from pCF201 in pCF204	This study	-
pLM202	Exchange of $P_{mcrB(M.v.)}$ to P_{hmtB} in pLM201	This study	-
pCF203	Exchange of Pur^r to Sim^r in pCF200	This study	-
pCF204	Exchange of Pur^r to Neo^r in pCF200	This study	-
pCF404	pUC57 including 1 kb up- and downstream of annotated *pyrF* gene (MTH_RS00570) and $P_{mcrB(M.v.)}$_Pur^r	This study	-
pCF407	Exchange of $P_{mcrB(M.v.)}$_Pur^r to $P_{mcrB(M.v.)}$_Neo^r in pCF404	This study	-
pSB1	Exchange of $P_{mcrB(M.v.)}$ promoter to P_{synth} in pCF407	This study	-
pSV1_1	Shuttle vector construct containing $P_{mcrB(M.v.)}$_Sim^r and pBBR1MCS2 backbone and pME2001 replicon	This study	-
pSV1_2	Shuttle vector construct containing $P_{mcrB(M.v.)}$_Sim^r and pMTL backbone and pME2001 replicon	This study	-
pSV1_3	Shuttle vector construct containing $P_{mcrB(M.v.)}$_Neo^r and pMTL80151 backbone and pME2001 replicon	This study	-
pMVS-V1	Shuttle vector construct containing P_{synth}_Neo^r and pMTL backbone and pME2001 replicon	This study	x
pMVS1111A: P_{synth}-*bgaB*	Shuttle vector construct pMVS-V1 including β-galactosidase (*bgaB*)-gene and promoter P_{synth}	This study	x
pMVS1111A: P_{hmtB}-*bgaB*	Shuttle vector construct pMVS-V1 including β-galactosidase (*bgaB*)-gene and promoter P_{hmtB}	This study	x

pMVS1111A: $P_{mrt(M.t.)}$-*bgaB*	Shuttle vector construct pMVS-V1 including β-galactosidase (*bgaB*)-gene and promoter $P_{mrt(M.t.)}$	This study	x
pMVS1111A: $P_{synth(BRE)}$-*bgaB*	Shuttle vector construct pMVS-V1 including β-galactosidase (*bgaB*)-gene and promoter $P_{synth(BRE)}$	This study	x
pCF702	Integration vector containing P_{synth}_Neo^r and Mth60-fimbriae operons 1 kb homologous flanking regions upstream and downstream	This study	x
pCF703	Integration vector containing P_{hmtB}_fdh_{Z-245} from pLM202 and Mth60-fimbriae operons 1 kb homologous flanking regions upstream and downstream	This study	x

[1] Successful transformation of *M. thermautotrophicus* ΔH (*M.t.)* is marked with x.

3. Molecular methods for genetic modification of *E. coli*

3.1. PCR amplification with Q5 hot start high-fidelity polymerase

PCR products for fusion of constructs *via* Gibson assembly® or restriction/ligation cloning were amplified with Q5 hot start high-fidelity polymerase. We always derived template DNA from highly pure genomic DNA or plasmid DNA extractions (**See III.3.6, III.5.3**). Template DNA, that was derived from plasmid extractions was diluted 1/10. Samples (**Table 4**) were prepared at room temperature. After sample preparation, the samples were aliquoted in 0.2 mL PCR tubes and PCR was performed with Eppendorf Mastercycler pro S (Eppendorf, Hamburg, Germany) using the Q5 PCR program (**Table 5)**. After the PCR amplification, PCR products were pooled and PCR products meant for restriction/ligation cloning were digested immediately with 1 µL of *Dpn*I at 37°C for 1 h to eliminate template DNA. Gibson assembly® PCR products were *Dpn*I digested after the Gibson assembly®. All pooled PCR products, which were amplified with Q5 hot start high-fidelity polymerase, were PCR purified, according to the manufacturer manual *via* QIAquick PCR Purification Kit (Qiagen, Hilden, Germany) and eluted in 30 µL $H_2O_{millipore}$ twice.

Table 4. Q5 polymerase PCR sample mix

SUBSTANCE	AMOUNT (>5 KB) [µL]	AMOUNT (<5 KB) [µL]
Q5 polymerase buffer (5x)	20	40
Nucleotide mix (10 mM)	2	4
Primer A (10 µM)	1	2
Primer B (10 µM)	1	2
Template DNA	2	3
Q5 hot start high-fidelity polymerase	1	2
$H_2O_{millipore}$, ad	100	200

All samples were aliquoted á 10 µL *prior* to PCR amplification and pooled afterwards.

Table 5. Q5 polymerase PCR program

STEP	TEMPERATURE [°C]	DURATION
Initial denaturation	93	90 s
Denaturation[1]	93	20 s
Annealing[1]	60	10 s
Extension[1]	72	30 s/kb + 60 s
Final extension	72	Time for extension + 30 s
Hold	8	∞

[1] The steps in italics were included in the cycles. It was set per default to 30 cycles, in rare cases with low DNA yield they were raised to 35 cycles.

3.2. Restriction/ligation fusion of constructs

For the restriction digest, the template DNA, such as PCR purified PCR products or highly pure plasmid extractions (**See III.3.1., III.3.6.**) were digested, using restriction enzymes (**Table 6)** for 2 h at the optimal temperature for the respective enzyme (mostly 37°C). The vector backbone was additionally digested with calf- or shrimp-alkaline phosphatase (CIP, SAP) to dephosphorylate the 5' DNA ends. Digested DNA fragments were PCR purified *via* a QIAquick PCR purification kit and eluted in 30 µL $H_2O_{millipore}$ twice. The final DNA concentration was determined with 1 µL of DNA sample with a spectrophotometer (NP80, Implen, Munich, Germany).

For ligation, digested vector- and insert-DNA fragments were mixed in a ratio of 1:3 (fragment count/fragment count), which were calculated with NEBioCalculator tool (New England Biolabs, Frankfurt/Main, Germany), in 20 µL of T4 ligase (New England Biolabs, Frankfurt/Main, Germany) reaction mixture. A maximum of 50 volume% of the total reaction volume consisted of DNA sample and the minimal amount of vector was 100 ng of DNA. The ligation reaction was incubated at room temperature for 1-2 h and immediately used for chemical transformation of *E. coli* (**See III.3.5**).

Blunt-ended subcloning of PCR amplified fragments in the linearized vector pMiniT 2.0, was performed with the NEB® PCR Cloning Kit (New England Biolabs, Frankfurt/Main, Germany), according to manufacturer manual.

Table 6. Restriction digest sample mix

SUBSTANCE	AMOUNT [µL]
CutSmart Buffer® (10x)	5
Enzyme A	1
Enzyme B	1
(Optional CIP/SAP)	(1)
Template DNA	5-10 (0.5-2 µg of DNA)
$H_2O_{millipore}$, ad	50 µl

3.3. Gibson assembly® fusion of constructs

Two options were used for fusion of constructs *via* Gibson assembly®: 1) a restriction enzyme digested vector (**Table 6**) and an insert with corresponding overhangs of 40 bp and 2) two PCR amplified fragments with 40 bp overhang within each interface in total. For both options the vector to insert ratio was 1:3, which was calculated with the equation provided in the user manual (New England Biolabs, Frankfurt/Main, Germany), while the vector DNA concentration always exceeded 100 ng (**Table 7**). After mixing the reaction sample, it was incubated at 50°C in the Eppendorf Mastercycler pro S (Eppendorf, Hamburg, Germany) for 1 h. When the Gibson assembly® consisted of two PCR products, the assembled sample was immediately digested using 0.5 µL of *Dpn*I for 1 h at 37°C to eliminate non-assembled PCR template and reduce the background of false positive clones.

Table 7. Gibson assembly® sample mix

SUBSTANCE	AMOUNT [µL]
Gibson assembly® master mix	5
Vector template DNA	0.1-2 (~100 ng of DNA)
Insert template DNA	1-3 (three times exceeding vector)
$H_2O_{millipore}$, ad	10

3.4. Preparation of chemical competent *E. coli* cells (Sambrook *et al.* 1989), modified by Christian Klask (2017)

An overnight culture of *E. coli* was transferred to 100 mL sterile liquid LB medium in a 500-mL Erlenmeyer flask to an initial OD_{600} of ~0.05-0.1 and incubated at 37°C, while rotating with 150 rpm. When the OD_{600} reached 0.4-0.6, the culture was dispensed in two sterile 50-mL falcon tubes and centrifuged for 20 min at 3700 g and 4°C. The supernatant was discarded and each pellet was gently resuspended in 20 mL of ice-cold 100 mM calcium chloride dihydrate solution. The resuspended cells were centrifuged for 20 min at 3700 g and 4°C. The supernatant was discarded and each pellet was gently resuspended in 3 mL of ice-cold 100 mM calcium chloride dihydrate solution with 25 volume% of glycerol. After incubation of 20 min on ice, the

resuspended cells were aliquoted á 150 µL in ice-cold 1.5 mL Eppendorf reaction tubes and were immediately frozen in liquid nitrogen. The frozen cells were stored at -80°C for up to 3 months.

3.5. Transformation of chemical competent *E. coli* cells (Sambrook *et al.* 1989)

A frozen aliquot of chemical competent *E. coli* cells was thawed on ice. Afterwards, 10 µL of ligation reaction, Gibson assembly® reaction, or 1-2 µL of highly pure plasmid DNA extraction was added to the competent cells and mixed by swirling with the pipet tip and flicking the tube. After 30 min of incubation on ice, the cells were treated with a heat-shock at 42°C for 1 min and cooled down on ice for 3-5 min. We added 850 µL of sterile SOC media (VWR, Darmstadt, Germany). Afterwards, the tube was inverted for 5-7 times and incubated at 37°C for 1 h to allow *E. coli* expression of the resistance gene and recovery of the cells. During the 1 h recovery of the *E. coli* cells, plates with solidified LB medium, containing the respective antibiotic, were prewarmed at 37°C. Consecutively, the *E. coli* cells were centrifuged for 3 min at 13000 g and room temperature, the supernatant was discarded and the pellet resuspended in ~50 µL of remaining SOC medium, and plated on the prewarmed solidified LB medium plates. The inoculated plates were incubated at 37°C for 16-24 h.

3.6. Colony PCR using EconoTaq Master mix

Individual clonal populations of transformed *E. coli* can be immediately analyzed with colony PCR to reduce the workload to find the correct genetically modified *E. coli* strain. The individual clonal population was scratched from the plate with a sterile wooden applicator stick, transferred to a sterile selective solidified LB medium plate (rescue plate), dipped in the prepared colony PCR sample mix (**Table 8**), and then used for inoculation of 3 ml of sterile selective liquid LB medium in test tubes for test restriction enzyme digestion (**See III.3.7.**). The rescue plate was incubated at 37°C (non-rotating) and the test tubes were incubated at 37°C and a 150 rpm rotation. For this application, we used the EconoTaq® plus green 2x Master Mix (Lucigen Corporation, Middleton WI, USA), according to manufacturer manual. We reduced the amount from default 20 µL to 10 µL sample total volume and raised the amount of primer from 0.1 to 0.5 µL. The PCR protocol in the PCR cycler was set as stated in the manufacturer manual.

Table 8. Colony PCR sample mix

SUBSTANCE	**AMOUNT [µL]**
EconoTaq master mix	5
Primer A (10 µM)	0.5
Primer B (10 µM)	0.5
DNA template	Clonal population material
$H_2O_{millipore}$, ad	10

3.7. Plasmid-DNA extraction

Depending on the later purpose, two different methods for plasmid-DNA extraction were applied. For highly pure plasmid DNA for Sanger sequencing or fusion of constructs, the QIAprep Spin Miniprep Kit (Qiagen, Hilden, Germany) was used and plasmid DNA was eluted in 50 µL $H_2O_{millipore}$. For screening approaches of more than four samples, we aimed for a cheaper method for plasmid DNA extraction. The final plasmid DNA is less pure than with the QIAprep Spin Miniprep Kit, but the yield is sufficient for test restriction digestion and retransformation of *E. coli*. 1.5 mL of an overnight culture of *E. coli* was centrifuged at room temperature with 17000 g for 3 min. The supernatant was discarded and the pellet resuspended *via* pipetting in 150 µL Buffer P1 (**Table 9**). After addition of 150 µL Buffer P2 for alkaline lysis of *E. coli* cells (**Table 10**), the tube was inverted 6-8 times. To precipitate proteins and lipids, 250 µL Buffer P3 (**Table 11**) was added and the tube was 6-8 times inverted. Subsequently, the precipitated proteins and lipids were centrifuged for 10 min at room temperature with 17000 g for 10 min. During the centrifugation, sterile 1.5-mL Eppendorf reaction tubes were filled with 500 µL of 100 volume% 2-propanol. The plasmid DNA containing supernatant was transferred carefully to the 2-propanol containing reaction tubes and the pellet was discarded. The tubes were inverted 5 times followed by a centrifugation at room temperature with 17000 g for 5 min. Afterwards, the supernatant was discarded and the invisible pellet was washed once with 400 µL of ice-cold 70 volume% ethanol at room temperature with 17000 g for 5 min. The supernatant was discarded, the residual ethanol was removed by tapping the tube upside down on laboratory paper several times and incubation at 50°C for 20 min. The dry plasmid DNA pellet was finally resuspended in 40 µL of $H_2O_{millipore}$ and rehydrated for 30 min at room temperature *prior* to analysis.

Table 9. Composition of Buffer P1

SUBSTANCE	AMOUNT
Tris	50.0 mM
EDTA	10.0 mM
RNase A	100.0 µg/mL

The pH was adjusted to 8.0 using 4 M HCl, Buffer P1 was stored at 4°C.

Table 10. Composition of Buffer P2

SUBSTANCE	AMOUNT
Sodium hydroxide	200.0 mM
SDS	1 volume%

Table 11. Composition of Buffer P3

SUBSTANCE	AMOUNT
Potassium acetate	2.55 M

The pH was adjusted to 4.8 using concentrated acetic acid.

3.8. Test restriction enzyme digestion for analysis

The analysis of plasmid-DNA extraction from individual clonal populations was performed *via* test restriction enzyme digestion. Therefore, 5 µL of plasmid-DNA extraction was mixed as described in **Table 12**, and incubated for 1-2 h at 37°C. The fragment size was analyzed with agarose gel electrophoresis (**See III.3.8.**).

Table 12. Test restriction enzyme digestion sample mix

SUBSTANCE	AMOUNT [µL]
CutSmart Buffer® (10x)	2
Restriction enzyme A	0.5
(Restriction enzyme B)	0.5
Plasmid DNA extraction	5
$H_2O_{millipore}$, ad	20

3.9. Agarose gel electrophoresis

The analysis of PCR products, restriction enzyme digestions, or ligation reactions was performed with agarose gel electrophoresis. First, an agarose gel was prepared by mixing 100 mL of 1x TAE buffer (**Table 13**) with 1 g of agarose. The suspension was boiled for 2 min until the agarose was completely dissolved. Afterwards, 3 µL of Midori-green advance (Biozym, Hessisch Oldendorf, Germany) was added as a DNA intercalating UV stain, poured in a form with suitable comb, and solidified at room temperature for 15 min. PerfectBlue Gelsystems (VWR, Darmstadt, Germany) for electrophoresis were filled with 1x TAE buffer (**Table 13**), the solidified gel was inserted and loaded with suitable amount of DNA sample and GeneRuler 1 kb DNA Ladder (Thermo Scientific, Waltham MA, USA) as reference. Afterwards, the gel was run with a slow (45 min, 130 V) or fast (45 min, 140 V) program depending on fragment size.

Table 13. Composition TAE Buffer (1x)

SUBSTANCE	AMOUNT
Tris	4.48 g
Sodium-EDTA	0.37 g
Glacial acetic acid	1.15 mL
$H_2O_{millipore}$, ad	1,000 mL

3.10. Sanger sequencing

The analysis of correctly fused plasmid constructs on a base-pair resolution was performed with Sanger sequencing. All Sanger-sequencing reactions for analysis of fusion and retransformation of shuttle-vector constructs were performed with the genomics center of the Max-Planck institute for developmental biology. Sanger sequencing of constructs for genome integration of $fdh_{Z\text{-}245}$ and Neo^r at the Mth60-fimbriae operons locus (pCF702, pCF703) were performed with GeneWiz inc. (South Plainfield (NJ), USA).

3.11. Long term storage of *E. coli* strains

Correctly sequenced plasmid constructs in *E. coli* were prepared for long-term storage. Therefore, 1 mL of a fresh overnight culture of the respective *E. coli* strain was resuspended in 0.5 mL of sterile 80 volume% glycerol solution in a sterile 2 mL screw cap vial. After incubation on ice for 30 min, the vial was barcoded and stored in the Environmental Biotechnology Group culture collection for aerobic microbes at -80°C. All individual strains were prepared and stored in duplicates.

4. Strategies for generation of shuttle- and integration-vector constructs

4.1. Generation of the modular pMVS as replicative vector for *M. thermautotrophicus* ΔH

pCF200, which contains the puromycin acetyltransferase (*pac*)-gene (Pur^r) from *Streptomyces alboniger* as a codon-optimized version for *M. thermautotrophicus* ΔH under the control of the $P_{mcrB(M.v.)}$ promoter and the T_{mcr} terminator from *Methanococcus voltae* (Sarmiento *et al.* 2011), was completely synthesized (BioCat, Heidelberg, Germany). The *pac*-gene in pCF200 was exchanged to the 3-hydroxy-3-methylglutaryl-coenzyme A reductase (Hmg-CoA)-encoding gene (Sim^r) from *Thermococcus kodakarensis* by using pYS3 (Waege *et al.* 2010) and pCF200 as templates for Gibson Assembly®, resulting in pCF203. pCF203, pME2001 (extracted from wild-type *M. marburgensis*), and pBBR1-MCS2 (Addgene #85168) were used as templates for Gibson Assembly® with the Gibson Assembly® Ultra kit (Synthetic genomics, La Jolla CA, USA), and resulted in the putative shuttle vector pSV1_1. pSV1_1 was the basis for further shuttle vectors (Enkerlin 2020). For the introduction of a high-copy number replicon for *E. coli,* the *tra*-region, which includes the Ori-T for plasmid mobilization, and an additional *Asi*SI restriction enzyme-recognition sequence, the pBBR1-MCS2 backbone was exchanged *via* Gibson Assembly® to the *E. coli* vector backbone from pMTL83151 (Heap *et al.* 2009), including Cam^r, ColE1, and the *tra* minigene, resulting in pSV1_2. To implement the thermostable neomycin phosphotransferase gene (Neo^r) (Hoseki *et al.* 1999), the Pur^r from pCF200 was exchanged to Neo^r from pMU131 (Shaw *et al.* 2010) by Gibson Assembly®. Afterwards, based on pCF404, the Neo^r under the control of the $P_{mcrB(M.v.)}$ promoter and the T_{mcr} terminator, was used to construct a putative integration plasmid for the exchange of an annotated *pyrF* gene in *M. thermautotrophicus* ΔH, using *Asc*I and *Fse*I as restriction enzymes

and T4 ligase for ligation, resulting in pCF407. In pCF407 the $P_{mcrB(M.v.)}$ promoter was exchanged to P_{synth} by inverse PCR, resulting in pSB1. The fragments P_{mcrB}_Neo^r_T_{mcr} from pCF407 and P_{synth}_Neo^r_T_{mcr} from pSB1 were used to substitute the Sim^r in pSV1_2 by restriction-ligation cloning using *Asc*I and *Fse*I, resulting in pSV1_3 and pMVS-V1, respectively. To generate pMVS1111A:P_{synth}-*bgaB*, the PCR amplified gBlock with the thermostable β-galactosidase (*bgaB*) gene, which was codon-optimized for *M. thermautotrophicus* ΔH, and which was placed under the control of the P_{synth} promoter, was fused to *Asc*I-digested pMVS-V1 with Gibson Assembly®. The *Asc*I restriction enzyme-recognition sequence was recovered at the intersection with the selectable-marker module and a *Pac*I recognition sequence was introduced at the intersection with the *M. thermautotrophicus* ΔH-replicon module. Further promoters ($P_{synth(BRE)}$, P_{hmtB}, $P_{mrt(M.t.)}$) were amplified *via* overlap-extension PCR of the β-galactosidase gBlock and promoter gBlock and inserted by restriction/ligation cloning using restriction enzymes *Pac*I and *Asc*I.

4.2. Generation of suicide-vector constructs for genome integration in *M. thermautotrophicus* ΔH

To generate suitable suicide-vector constructs for genome integration at the Mth60-fimbriae operons, we developed a three-step cloning strategy. This includes the *E. coli* backbone with 1-kb homologous flanking regions up- and downstream of the Mth60-fimbriae operons with the neomycin resistance (Neo^r) and $P_{mcrB(M.v.)}$ as non-functional spacer in between. The spacer flanked by *Fse*I and *Asc*I as modular restriction enzyme recognition sites facilitate the exchange of the selectable marker module in further suicide-vector constructs.

The plasmid pCF204, which contains the pUC57 vector backbone and Neo^r with $P_{mcrB(M.v.)}$, flanked by the restriction enzyme recognition sites *Fse*I and *Asc*I, was used as a start point for the three-step cloning strategy. To exchange the vector backbone of pCF204 towards the *E. coli* vector backbone from pMTL83151 (Heap *et al.* 2009), including Cam^r, ColE1, and the *tra* minigene with Ori-T, the pMTL83151 backbone was PCR amplified to implement a *Sal*I restriction site and PCR purified. The resulting PCR product of pMTL83151 and pCF204 were restriction digested with *Kpn*I and *Sal*I, PCR purified, and ligated with T4 ligase. After confirmation of the backbone exchange, the up- (0.8 kb due to ORF not completely on the vector) and down-stream (1 kb) flanking regions were PCR amplified using Q5 hot start high-fidelity polymerase with primer combinations including the respective restriction site. The PCR products were PCR purified. The up- and down-stream flanking region fragments were digested with the restriction enzymes *Asc*I and *Sal*I (upstream) and *Fse*I and *Nde*I (downstream), respectively. The fragments were subsequently ligated into the backbone exchanged construct and digested with the corresponding restriction enzymes. The

downstream flanking region was implemented first, followed by the upstream flanking region in the third step after confirmation of downstream flanking region implementation.

After fusion of the suicide-vector backbone, including the up- and downstream homologous flanking regions, we exchanged the Neo^r with the non-functional $P_{mcrB(M.v.)}$ spacer to selectable markers that were proven to be functional in *M. thermautotrophicus* ΔH, which were the fdh_{Z-245} with P_{hmtB} from pLM202 (Fink *et al.* 2021) and Neo^r with P_{synth} from pSB1. This was performed *via* restriction/ligation cloning with the modular restriction sites *Fse*I and *Asc*I also facilitating the exchange of selectable markers for *M. thermautotrophicus* ΔH as a module in the pMVS design. The exchanges resulted in the final suicide-vector constructs pCF702 and pCF703.

5. Molecular methods for genetic modification of *M. thermautotrophicus* ΔH

5.1. Interdomain conjugational DNA transfer from *E. coli* to *M. thermautotrophicus* ΔH

E. coli S17-1 was chemically transformed with the respective shuttle vector or genome integration vector construct (**Figure 22A**). Overnight cultures of the respective *E. coli* S17-1 donor strains were inoculated. At the same time, 20 mL of liquid mineral medium was inoculated with wild-type *M. thermautotrophicus* ΔH (recipient). The overnight culture of *E. coli* S17-1, which contained the shuttle vector or genome integration vector construct, was diluted into 10 mL of fresh LB medium in a sterile 50 mL baffled flask for better aeration to give an OD_{600} of 0.3-0.5. When this culture reached an OD_{600} of 2.0-2.5, the incubation was stopped and the culture was harvested aerobically at 3700 g for 10 min at room temperature (Centrifuge 5920 R, rotor S-4x1000, Eppendorf, Hamburg, Germany). The supernatant was discarded and the *E. coli* S17-1 pellet was transferred into the anaerobic chamber. Wild-type *M. thermautotrophicus* ΔH was grown to an early stationary growth phase (OD_{600} of 0.25-0.35). 8 mL of *M. thermautotrophicus* ΔH culture was centrifuged stepwise at 8500 g for 4 min at room temperature (MySPIN™ 12 Mini Centrifuge, Thermo Scientific Waltham MA, USA) inside the anaerobic chamber. The final pellet was resuspended in 250 µL of the original non-concentrated *M. thermautotrophicus* ΔH culture, and gently mixed with the *E. coli* S17-1 pellet. 100 µl of cell suspension were anaerobically spotted on solid LB-MS medium, which was a mixture that consisted of 50 volume% of mineral medium and 50 volume% of LB medium without the 10 g/L sodium chloride. The spot was dried, while the lid of the petri dish was kept slightly open for 1 h at 37°C in the incubator (Coy laboratory products, Green Lake MA, USA) within the anaerobic chamber. When the spot was completely absorbed, the plates were provided with paper clips and transferred to a stainless-steel jar. The gas phase of the jar was exchanged to 200 kPa $H_2/CO_2/H_2S$ (79.9/20/0.1 volume%) and incubated at 37°C without shaking for 16-20 h. The spot-mated *E. coli* S17-1 and *M. thermautotrophicus* ΔH cells were washed from the LB-MS plates using 1 mL non-selective mineral medium and transferred to 4

mL non-selective mineral medium in a 50-mL serum bottle with a H_2/CO_2 (80/20 volume%) gas phase. After recovery for 3-4 h at 60°C with shaking at 150 rpm, 1 mL of the culture was transferred to 20 mL selective liquid mineral medium in a 100-mL serum bottle and incubated at 60°C with shaking at 150 rpm. Growth of *M. thermautotrophicus* ΔH after 24-48 h of incubation indicated successful DNA transfer into *M. thermautotrophicus* ΔH, while growth only later than 48 h indicated the appearance of spontaneously neomycin-resistant *M. thermautotrophicus* ΔH cells. 50 µL from this selective-enrichment culture was spread-plated on selective solidified media plates, and individual clonal populations were analyzed after two days of incubation at 60°C.

To determine the conjugation frequency, the following modifications to the standard protocol were made: 1) the cell count of *M. thermautotrophicus* ΔH in liquid culture was determined by counting in a Petroff-counting chamber. The initial recipient cell number in 100 µL of the stepwise-concentrated culture was calculated based on this cell count; 2) the 5-mL non-selective recovery culture from the washed spot after spot-mating was incubated for ~16-20 h instead of 3-4 h; and 3) 100 µL of the non-selective recovery culture was directly spread-plated on selective solidified media plates, without a liquid selective-enrichment step.

For integration vectors, the $fdh_{Z\text{-}245}$ was applied as an alternative selectable marker in *M. thermautotrophicus* ΔH. Therefore, the recovery medium contained mixotrophic conditions with 100 mM formate and H_2/CO_2 to recover cells and immediately enrich the correct transformants. Thus, the incubation time was set from 24 h to 48 h. Afterwards, 0.5 mL of recovered cell suspension was transferred to formate-containing liquid mineral medium and additionally pour-plated in 3 mL of soft agar on solidified mineral medium. Individual clonal populations were obtained after 3 days of incubation. The clonal populations were transferred to formate-containing liquid mineral medium and analyzed as described in **III.5.4. and III.5.6**.. No clonal populations were obtained from spread-plating approaches with recovered cell suspensions, so far.

5.2. Plasmid-DNA extraction from genetically modified *M. thermautotrophicus* ΔH strains and *M. marburgensis*

Plasmid DNA from wild-type *M. marburgensis* cells or (genetically modified) *M. thermautotrophicus* ΔH was extracted with the QIAprep Spin Miniprep kit (Qiagen, Hilden, Germany), according to the manufacturer manual in combination with an enzymatic lysis step with the cell wall-degrading pseudomurein endoisopeptidase (PeiP) *prior* to extraction. The samples were resuspended in 100 µL Buffer P1 (from Qiagen QIAprep Spin Miniprep Kit), which was supplemented with sucrose (30 weight%), and lysed by adding 100 ng/mL PeiP, followed by incubation for 30 min at 60°C.

5.3. Genomic-DNA extraction of *Methanothermobacter* spp.

High molecular-weight genomic DNA for next generation sequencing (NGS) was extracted with the Fast DNA™ SPIN Kit for soil (VWR, Darmstadt, Germany), according to the manufacturer manual. 6 mL of stationary *M. thermautotrophicus* ΔH culture (OD_{600} 0.3-0.35) were stepwise centrifuged á 1.5 mL aerobically at room temperature with 17000 g for 4 min *prior* to extraction.

Genomic DNA for subsequential PCR analysis was extracted with the NucleoSpin Microbial DNA Kit (Macherey+Nagel, Düren, Germany) according to the manufacturer manual. 3 mL of stationary *M. thermautotrophicus* ΔH culture (OD_{600} 0.3-0.35) were stepwise centrifuged á 1.5 mL aerobically at room temperature with 17000 g for 4 min *prior* to extraction. The cell lysis step with supplied glass beads was performed with vortexing for 1 min at level 10 (Vortex Genie2, VWR, Darmstadt, Germany). The DNA was eluted in 50 µL $H_2O_{millipore}$ instead of 100 µL elution buffer and centrifuged for 1 min instead of 0.5 min.

5.4. PCR analysis of genetically modified *M. thermautotrophicus* ΔH strains

PCR analysis was performed from liquid cultures and directly from individual clonal populations, or genomic-DNA extractions for fragments with a size of over 4.5 kb. 100 µL of liquid culture or one individual colony, which was resuspended in 40 µL of deionized water, were boiled for 12 min at 100°C (ThermoMixer C, Eppendorf, Hamburg, Germany). After cooling the sample on ice, 1 µL of boiled crude extract or genomic DNA extraction was added to a 10-µL PCR reaction mix. PCR was performed using Phire plant PCR master mix (Thermo Scientific, Waltham MA, USA). The denaturation and annealing times were increased from 5 sec to 20 sec and to 10 sec, respectively. 30 cycles were performed for all analyses. We observed false positive PCR signals for shuttle-vector DNA due to residual plasmid DNA from *E. coli* for two transfers after the non-selective liquid recovery step. After the third transfer, plasmid DNA from *E. coli* was not detectable in any of our experiments, anymore. For robust PCR amplifications of individual clonal populations from *M. thermautotrophicus* ΔH, it was crucial to keep the agar contamination of the PCR sample as little as possible. Therefore, even though the plating efficiency is higher with pour-plating, genetically modified *M. thermautotrophicus* ΔH strains were spread-plated instead of pour-plated. This led to a lower total colony count, but to more reliable PCR results.

5.5. Retransformation analysis of *E. coli* with plasmid extraction from *M. thermautotrophicus* ΔH

Additional to PCR analysis, plasmid DNA from genetically modified *M. thermautotrophicus* ΔH strains was extracted. The purified plasmid DNA was used for retransformation of *E. coli* NEB stable. Analysis of *E. coli* NEB stable clonal populations was performed *via* test restriction

digestions and Sanger sequencing for further confirmation of segregational stability of shuttle vectors in *M. thermautotrophicus* ΔH.

5.6. Nanopore sequencing of *M. thermautotrophicus* ΔH strains

First, high molecular-weight genomic DNA from the respective *M. thermautotrophicus* ΔH strains was extracted. Second, for further concentration, size exclusion, and higher purification, the genomic DNA AMPure XP (Beckmann Coulter, Brea (CA), USA) magnetic bead clean-up was performed. The ratio of magnetic beads to genomic DNA volume was 2:1, which should exclude most of genomic DNA fragments smaller than 3 kb. The protocol was performed as described in the user manual for PacBio library preparation (PacBio template preparation and sequencing). Genomic DNA was eluted in 15 µL $H_2O_{millipore}$ and stored at 6°C.

We chose the rapid barcoding Kit (Oxford Nanopore Technologies, Oxford Science Park, UK) for library preparation by multiplexing of up to 12 samples for the three different *M. thermautotrophicus* ΔH strains to include all three strains multiplexed in the same flow-cell run. All steps were performed as described in the manufacturer manual. The run performance was adapted from Esquivel-Elizondo *et al.* (2021).

5.7. Long-term storage of *Methanothermobacter* spp. strains

Wild-type *Methanothermobacter* spp. strains and genetically modified *M. thermautotrophicus* ΔH that were confirmed with retransformation and subsequential Sanger sequencing were prepared for long-term storage at -80°C in the Environmental Biotechnology Group culture collection for anaerobic microbes. Therefore, 1 mL of overnight culture in the late exponential growth phase (OD_{600}~0.3) was transferred to a sterile 10-mL serum vial containing 2 mL of 80 volume% glycerol. The suspension was briefly mixed by vortexing, incubated for 30 min on ice, barcode labelled, and stored in the culture collection. All individual strains were prepared and stored in triplicates.

6. B-Galactosidase enzyme assays

For a β-galactosidase enzyme activity assay with the lactose analogue 3,4-cyclohexenoesculetin-β-D-galactopyranoside (S-Gal), 2 mL of overnight cell cultures that carried pMVS-V1 or pMVS1111A:P_{Synth}-*bgaB* were harvested by centrifugation for 4 min at 15000 g at room temperature (Centrifuge 5424, rotor FA-45-24-11, Eppendorf, Hamburg, Germany). The supernatant was discarded and the samples were stored at -20°C until further use. All samples were resuspended in 100 µL Buffer P1 (from Qiagen QIAprep Spin Miniprep Kit) containing sucrose (30 weight%), and lysed by adding 100 ng/mL PeiP, which was followed by incubation for 30 min at 60°C. 50 µL of the cell lysate were incubated with 250 µg/mL S-Gal and 250 µg/mL ammonium ferric citrate in 1 mL LB medium, which provided any potentially

required trace compounds. The samples were incubated for 1 h at 60°C. After ~30 min, a color change was visible.

For a β-galactosidase enzyme activity assay with the lactose analogue 2-Nitrophenyl β-D-galactopyranoside (ONPG), 4 mL of cell culture were harvested aerobically by step-wise centrifugation for 4 min at 15000 g. Afterwards, the same lysis procedure for samples was applied as for the S-Gal assay. The resulting cell lysate was used for a quantitative *in-vitro* β-galactosidase enzyme activity assay with ONPG as chromogenic substance, according to Jensen *et al.* (2017). In brief, 12.5 µL of cell lysate (equals to 0.5 mL of original cell culture) were mixed with 600 µL of ONPG (1 mg/mL)-containing substrate solution. The mixture was incubated for 2 h at 60°C. Afterwards, 200 µL were added to 200 µL of 1 M sodium bicarbonate stop-solution to a 96-well plate. The absorbance at 420 nm was measured in a micro-plate reader (Multiskan Go, Thermo Scientific Waltham MA, USA). For the preliminary experiment (**Figure 29**), 25 µL of cell lysate were mixed with 675 µL of ONPG substrate solution instead. After the incubation for 2 h at 60°C, 350 µL of substrate solution were added to 350 µL of stop solution, and the absorbance at 420 nm was measured in a cuvette (1-cm path length) with a spectrophotometer (NP80, Implen, Munich, Germany). For the analysis, Miller units were calculated with the equation $Absorbance_{420}$/(Incubation time [h]·OD_{600}·volume [L]). Values for 2 h of incubation time were used for the calculation.

7. Protein biochemical methods for extraction and purification of PeiP

The pseudomurein-degrading enzyme PeiP, which lyses pseudomurein-containing Methanobacteriales cell-walls, was produced as a heterologous 6xHistidine-tagged protein from pME2508-carrying *E. coli* BL21(DE3) as described in Kiener *et al.* (1987). The recombinant protein was purified *via* a Protino Ni-TED column according to the manufacturer manual (Macherey+Nagel, Düren, Germany). Protein concentrations were defined with Microplate BCA Protein Assay Kit - Reducing Agent Compatible according to the manufacturer manual (VWR, Darmstadt, Germany).

8. Software for *in-silico* and sequence analysis

8.1. SnapGene software (from Insightful Science; available at snapgene.com)

We used SnapGene for *in-silico* generation of restriction/ligation or Gibson assembly® cloning strategies, primer design, agarose gel simulations, analysis of unspecific DNA binding, and analysis of Sanger sequencing results. Additionally, we used SnapGene for *in-silico* predictions and to generate genome sequences of gene deletion or gene substitution mutant strains of *M. thermautotrophicus* ΔH as reference template for analysis of Sanger sequencing results or Nanopore sequencing reads.

8.2. QIAGEN CLC Genomics Workbench

We performed analyses of the Nanopore sequencing reads with QIAGEN CLC Genomics Workbench. We generated a workflow in which the raw sequences were first trimmed according to **Table 14**. Short and low-quality sequencing reads were discarded. Afterwards, the trimmed sequencing reads were aligned to reference sequences created in SnapGene and exported in genbank format (workflow input (2)) mapped by the Long Reads (beta) algorithm, according to **Figure 9**. Furthermore, we connected the reads tracks to the annotation tracks of the reference sequence genbank files for final analysis of the alignment. Unmapped reads were discarded. The schematic workflow is depicted in **Figure 10**.

Table 14. Set-up for trimming Nanopore sequencing reads

TRIM READS	
Trim using quality scores	true
Quality limit	0.05
Trim ambiguous nucleotides	true
Maximum number of ambiguities	2
Automatic read-through adapter trimming	false
Trim adapter list	
Trim homopolymers from 5'	false
Trim homopolymers from 3'	false
polyA	false
polyC	false
polyG	true
polyT	false
Remove 5' terminal nucleotides	false
Number of 5' terminal nucleotides	1
Remove 3' terminal nucleotides	false
Number of 3' terminal nucleotides	1
Trim to a fixed length	false
Maximum length	150
Trim end	Trim from 3'-end
Discard short reads	true
Minimum length	50
Discard long reads	false
Maximum length	1000

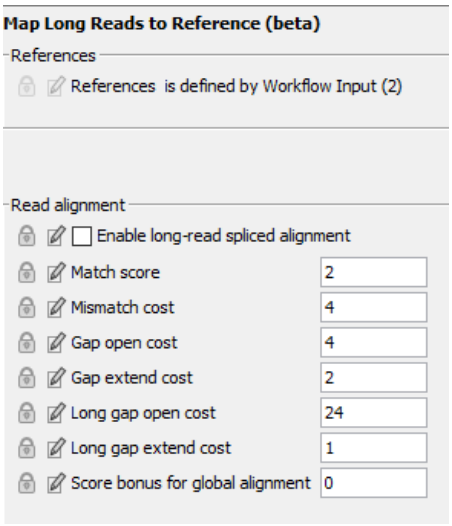

Figure 9. Default settings for Nanopore sequencing reads alignment by mapping Long Reads to Reference (beta).

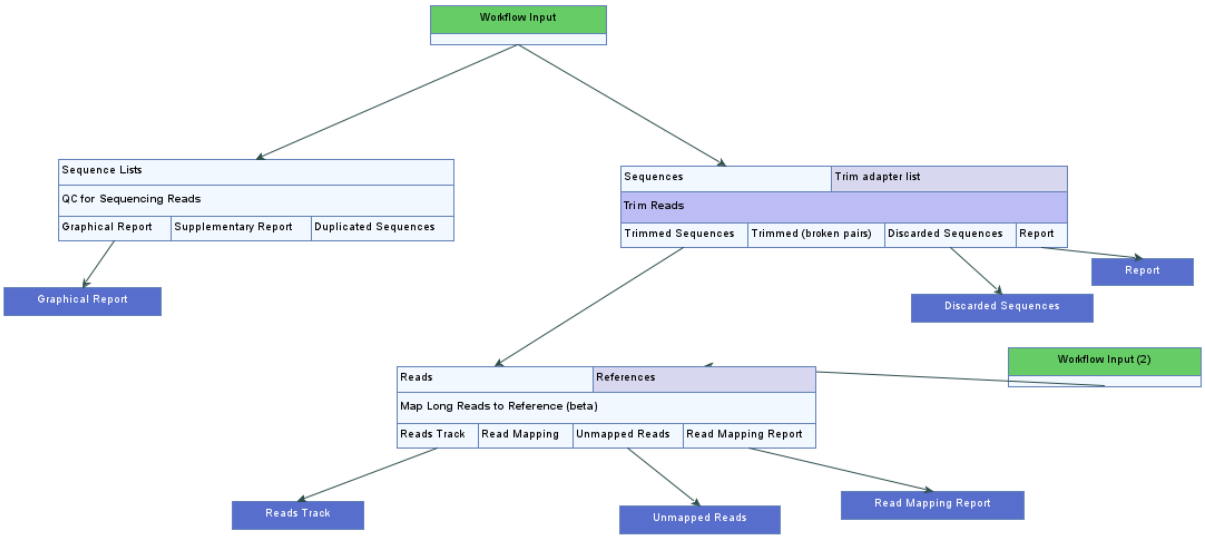

Figure 10. Workflow scheme for analysis of Nanopore sequencing reads by alignment to reference sequences. Sequencing reads (**workflow input**) underwent a quality control and were trimmed according to quality control and parameters in **Table 14**. Trimmed sequencing reads were afterwards aligned to reference sequences (**workflow input (2)**). Final results of the alignment were analyzed with reads track aligned to the annotation track from reference genbank files.

IV. Results

1. *M. thermautotrophicus* ΔH can be plated with high plating efficiencies and is sensitive to common antibiotic substances for methanogenic archaea

For the establishment of genetic systems two important prerequisites have to be accomplished before genetic work can be initiated: 1) Individual clonal populations need to be obtained from solidified media plates to be able to isolate individual genetically modified microbes; and 2) the microbe needs to be sensitive to antibiotic substances for which suitable selectable markers are available. With these two requirements, the establishment of a genetic system can be initiated.

The generation of individual clonal populations of *Methanothermobacter* spp. with high efficiencies was already demonstrated (Kiener and Leisinger 1983, Rospert *et al.* 1990). Yet, there were several difficulties to overcome to achieve similar plating efficiencies. In the following section, different plating techniques and incubation parameters are compared that were crucial for high plating efficiencies of wild-type *M. thermautotrophicus* ΔH. In the second section of this chapter, we describe our investigations on the sensitivity of wild-type *M. thermautotrophicus* ΔH towards antibiotic substances in selective liquid mineral media and on selective solidified mineral medium plates. These antibiotic substances were shown to inhibit growth of mesophilic and/or thermophilic methanogenic archaea. Additionally, these antibiotic substances are already used in genetic systems of respective methanogenic archaea (**See II.**).

1.1 Spot-, spread-, and pour-plating enable for isolation of individual clonal populations of *M. thermautotrophicus* ΔH with high plating efficiencies

In the very first stage of working with the thermophilic methanogenic archaeon *M. thermautotrophicus* ΔH, we reproduced cultivation in liquid mineral medium as stated in section **III.1.** After small optimizations, such as to omit sodium sulfide from liquid mineral medium for better measurements of optical density (sodium sulfide addition leads to precipitation), we focused on the technical issues of cultivating microbes at elevated temperatures with high pressure of hydrogen and carbon dioxide on solidified media plates. Together with the descriptions in Balch *et al.* (1979), Luis Antoniotti (Workshop of Max-Planck-Institute for Developmental Biology, Tübingen, Germany), and the company Raff + Grund (Freiburg am Neckar, Germany) that is specialized in production of stainless-steel containers, we were able to produce publicly available stainless-steel jars, which meet the technical requirements for safe handling to cultivate thermophilic anaerobic microbes at over-pressure with explosive gas mixtures (**Figure 11**).

Figure 11. Two customized stainless-steel jars from Raff + Grund (Freiburg am Neckar, Germany) for cultivation of anaerobic autotrophic microbes on solidified medium plates with a pressure capacity of up to 2 bar over-pressure and maximal handling temperature of -10°C to +80°C.

With accessible cultivation of *M. thermautotrophicus* ΔH in liquid mineral medium and anaerobic stainless-steel containers, we started to investigate three common plating techniques (spot-, spread-, and pour-plating), and compared factors that influenced the plating efficiency (*i.e.*, individual populations per cell-count of plated microbial cells, **see III.1.**). With spot-plating, individual populations were barely distinguishable, but concentrated and dense growth was obtained (**Figure 12A**). With spread- and pour-plating, we obtained individual populations (**Figure 12B, C**), and therefore we further investigated factors that influence plating efficiencies with these techniques. While the experimental variance was high in individual experiments and strongly depended on many different factors, which is further discussed below, some factors had a distinct impact on the plating efficiency. After we had optimized the plating conditions, we performed a set of experiments to compare the plating efficiency with as little experimental variance as possible (**Figure 12D**). The addition of 0.1 volume% hydrogen sulfide to the headspace gas mixture, as additional reducing agent and sulfur source, resulted in an increase of the number of individual populations by one order of magnitude when compared to the same plating procedure without hydrogen sulfide gas (**Figure 12D**). With hydrogen sulfide gas and with spread-plating of cells in the stationary growth phase, the plating-efficiency was found to be 1.2±0.5% (*N*=6; **Figure 12D**), while with spread-plating of cells in the exponential growth phase, a plating efficiency of 5±2% (*N*=4) was reached (**Figure 12D**). When we used pour-plating with the same number of cells in the stationary growth phase as with spread-plating, and with hydrogen sulfide gas, the number of individual populations increased drastically by two orders of magnitude with a plating efficiency of up to 50% (**Figure 15B**) or higher (135±10%, *N*=3; **Figure 12D**), whereas the colony size decreased when compared to individual populations from spread-plating (**Figure 12B, C**).

However, larger individual populations on top of the pour-plated solidified media plates were also observed (**Figure 12B**). Plating efficiencies of more than 100% and high standard-deviations in independent experiments appeared from incomplete counting, because of the formation of filaments or clumps of cells, and from a degree of sensitivity of the plating procedure to variations in the experimental handling such as differences in the exact growth phase of the plated culture or mineral media batches. In many experiments, we realized that the plating efficiency decreased considerably, when water accumulated inside the plate and formed a layer on the side of the plate, which led to a seal between the bottom of the petri dish-plate and the lid and prevented sufficient gas exchange. As a protective measure, we implemented the addition of paper clips on the edges of the plate to lift up the lid slightly, which efficiently prevented water from sealing the plates (**Figure 12E**).

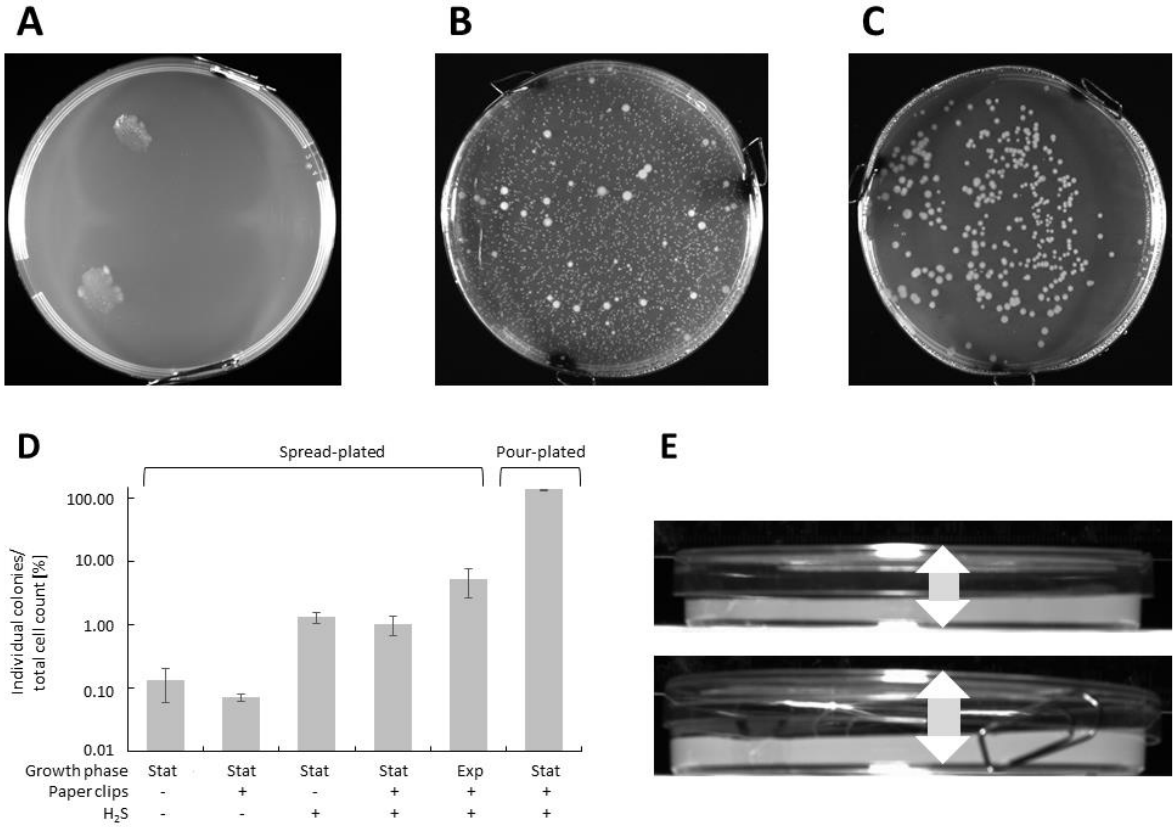

Figure 12. **A)** Spot-plating of *M. thermautotrophicus* ΔH cells on solidified media plates. **B)** Pour-plating of $1{\cdot}10^4$ *M. thermautotrophicus* ΔH cells on solidified media plates. **C)** Spread-plating of $1{\cdot}10^4$ *M. thermautotrophicus* ΔH cells on solidified media plates. **D)** Comparison of the influence from various factors on the plating efficiency with spread-plating of $1{\cdot}10^4$ *M. thermautotrophicus* ΔH cells and pour-plating of $1{\cdot}10^3$ *M. thermautotrophicus* ΔH cells, including the influence of paper clips, 0.1 volume% hydrogen sulfide (**H_2S**) in the head-space gas mixture, exponential growth phase (**Exp**), and stationary growth phase (**Stat**). The bars give the average percentage (log-scale) of individual populations per cell-count of initial microbial cells used for plating from technical replicates (*N*=3; *N*=4 for spread-plating with paper clips and hydrogen sulfide (**H_2S**) in exponential growth phase) with error bars indicating standard deviation. **E)** Influence of paper clips on the lid elevation. The arrow demonstrates the increase of lid/plate space compared for a plate without paper clips (upper picture) and with paper clips (lower picture).

In additional preliminary experiments, we tested wild-type *M. thermautotrophicus* Z-245 towards growth on 100 mM sodium formate-containing solidified mineral media plates. With this test we were able to predict the possibility of screening for individual clonal populations of genetically modified *M. thermautotrophicus* ΔH strains with the formate dehydrogenase operon ($fdh_{Z\text{-}245}$) that enabled wild-type *M. thermautotrophicus* Z-245 for growth on formate. It turned out that undiluted wild-type *M. thermautotrophicus* Z-245 culture (OD_{600}~0.3) did not result in individual clonal populations or a microbial lawn when spread-plated on top of the formate containing solidified media plates. Only aggregations of populations in slightly scratched parts of the solidified media plate were visible (**Figure 13A, red arrow**). When undiluted *M. thermautotrophicus* Z-245 culture was pour-plated with soft-agar on top of solidified mineral media plates without formate but with hydrogen and carbon dioxide (80/20 volume%) lawn formation was obtained (**Figure 13C, brighter shadow in red box**), while in solidified media plates with formate and without hydrogen and carbon dioxide indistinguishable microbial accumulations in gas bubbles inside the agar were visible (**Figure 13B, red arrows**). The agar was completely interspersed with gas accumulations, that had formed by carbon dioxide and methane, that was produced during growth on formate as the sole carbon- and energy source. The issue of gas bubble formation could only be overcome, to pick individual clonal populations, by drastic reduction of microbial cell count (maximum 10^4 cells) and transfer of individual clonal populations when they were very small (diameter >1 mm). With these optimizations it was possible to gather individual populations on formate containing solidified mineral media plates.

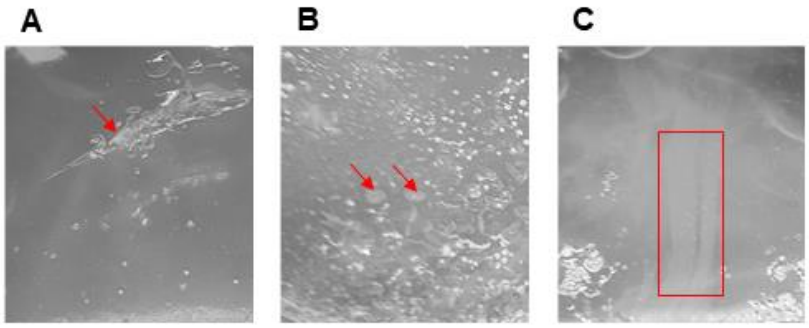

Figure 13. Comparison of spread-plating with formate in solidified mineral medium (**A**), pour-plating with formate in solidified mineral media plate with nitrogen/carbon dioxide gas phase (**B**), and pour-plating without formate but with hydrogen/carbon dioxide as gas phase (**C**) of undiluted liquid culture of *M. thermautotrophicus* Z-245 after two days of incubation at 60°C.

1.2 *M. thermautotrophicus* ΔH is sensitive to antibiotic substances commonly used in genetic systems for methanogenic archaea

In general, there are two alternatives for the use of antibiotic substances for selection of genetically modified microbes - positive and negative selection. Positive selection is achieved with an antibiotic substance and the corresponding antibiotic resistance gene as selectable marker. The genetically modified microbe is selected after transformation for the phenotypical trait (antibiotic resistance). Negative selection works *vice versa* to positive selection due to the phenotypical trait (antibiotic resistance) appearing when the respective selectable marker gene is not present. The selectable marker gene needs to be deleted to make the antibiotic substance harmless for the microbe. Negative selection is important for more sophisticated techniques of genetic modification such as marker-less mutagenesis. Nevertheless, we performed experiments towards growth inhibition with these substances to gather preliminary insights into possibilities for negative selection in future applications.

1.2.1 Antibiotic substances for positive selection

To find a suitable selection pressure for the positive selection of genetically modified cells, we analyzed puromycin, simvastatin, and neomycin for the inhibition of *M. thermautotrophicus* ΔH. For all three antibiotics, selectable marker genes are available. While puromycin and its mesophilic selectable marker *pac* are commonly applied to genetic systems for mesophilic methanogenic archaea (Enzmann *et al.* 2018), the thermophilic selectable markers for simvastatin and neomycin have been successfully used in thermophilic non-methanogenic microbes such as *Pyrococcus furiosus*, *Thermococcus kodakarensis* (simvastatin) (Santangelo *et al.* 2008, Waege *et al.* 2010), as well as *Thermoanaerobacter* spp. (neomycin) (Shaw *et al.* 2010). Recently, they were also applied to genetic systems of the thermophilic methanogenic archaea *M. jannaschii* (simvastatin) and *M. thermophilus* (neomycin) (Susanti *et al.* 2019, Fonseca *et al.* 2020).

We found that non-selective conditions result in a densely grown *M. thermautotrophicus* ΔH culture in liquid mineral media within 24 h (**Figure 14**). For simvastatin, we tested concentrations ranging from 0-21.5 µg/mL (0-50 µM) on ~$5 \cdot 10^5$ cells/mL, and found that 13 µg/mL (30 µM) inhibited growth at least for 48 h. We also tested the inhibition by the simvastatin-analog mevinolin but did not find a growth-inhibiting effect on *M. thermautotrophicus* ΔH up to a concentration of 21.5 µg/mL (50 µM). For neomycin, we tested concentrations ranging from 0-250 µg/mL on ~$5 \cdot 10^5$ cells/mL initial cell density. We found that 50 µg/mL inhibited growth for less than 24 h, 100 µg/mL inhibited growth for at least 48 h, and 250 µg/mL neomycin for at least 60 h of incubation, while we did not analyze the growth-inhibiting effect beyond an incubation period of 60 h (**Figure 14**). We further tested puromycin in liquid mineral medium and we found an inhibitory effect from 50 µg/mL on ~$5 \cdot 10^5$ cells/mL

initial cell density for at least 72 h. However, the available *pac*-gene as a selectable marker has not been adapted to thermophilic conditions yet to confer resistance against puromycin at elevated temperatures. Thus, the substance was not further investigated due to the absence of a thermophilic resistance gene.

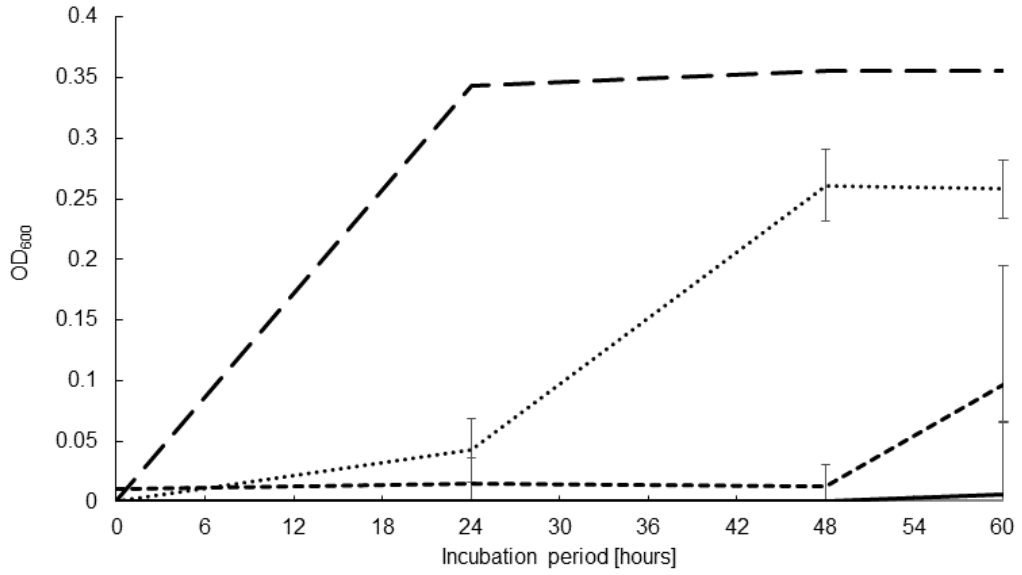

Figure 14. Measurement of OD_{600} after different incubation periods at 60°C (0 h, 24 h, 48 h, and 60 h) with initially $5 \cdot 10^5$ cells/mL of wild-type *M. thermautotrophicus* ΔH in liquid mineral medium containing neomycin concentrations of 0 µg/mL (**long-dashed line**, *N*=1), 50 µg/mL (**dotted line**), 100 µg/mL (**short-dashed line**), and 250 µg/mL (**black solid line**) for comparison to wild-type *M. thermautotrophicus* ΔH. Average (*N*=3) with error bars indicating standard deviation.

With having the plating efficiency defined (**See III.1.1.**), we further investigated simvastatin and neomycin for their inhibitory effects on solidified media plates. For simvastatin, we tested concentrations ranging from 0-21.5 µg/mL (0-50 µM) on the inhibition of $1 \cdot 10^8$ cells with pour-plating (**Figure 15A**). While up to 8.7 µg/mL (20 µM) simvastatin resulted in a microbial lawn formation of *M. thermautotrophicus* ΔH cells and inhibition was recognizable from 13 µg/mL (30 µM) upwards. At 21.5 µg/mL (50 µM), we observed only 27±10 (*N*=3) individual populations after an incubation period of 48 h (**Figure 15A**), which corresponds to a growth inhibitory efficiency of close to 100%. For neomycin, we tested concentrations ranging from 0-250 µg/mL on the inhibition of $1 \cdot 10^3$ cells with pour-plating (**Figure 15B**). At 50 µg/mL, no significant reduction of the number of individual populations was observed when compared to non-selective conditions for which we achieved a plating efficiency of ~50% (**Figure 15B**). With 100 µg/mL, only 30±5 (*N*=3) individual populations were observed, and with 250 µg/mL only 3±1 (*N*=3) individual populations were observed after an incubation period of 48 h, respectively (**Figure 15B**). Therefore, we concluded that 250 µg/mL of neomycin inhibits growth of wild-

type *M. thermautotrophicus* ΔH on solidified media plates with an efficiency of >99.9% for at least 48 h (**Figure 15B**)

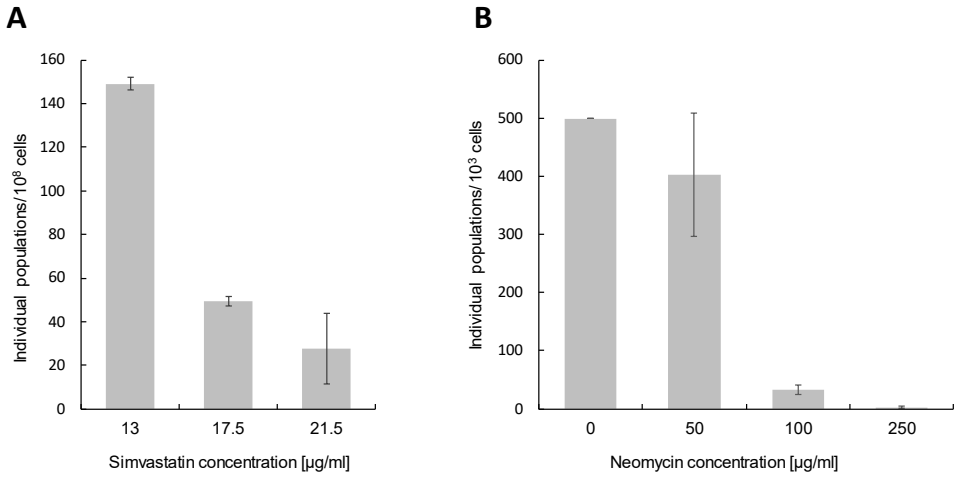

Figure 15. A) Individual populations from $1 \cdot 10^8$ wild-type *M. thermautotrophicus* ΔH cells (**grey bars**), which were pour-plated on solidified media plates containing simvastatin concentrations ranging from 13 µg/mL to 21.5 µg/mL. **B)** Individual populations from $1 \cdot 10^3$ wild-type *M. thermautotrophicus* ΔH cells (**grey bars**), which were pour-plated on solidified media plates containing neomycin concentrations ranging from 0 µg/ml to 250 µg/mL. Average (*N*=3) with error bars indicating standard deviation for wild-type *M. thermautotrophicus* ΔH.

1.2.2 Antibiotic substances for negative selection

For potential negative selection, we analyzed the sensitivity of wild-type *M. thermautotrophicus* ΔH to 6-aza-uracil and 8-aza-hypoxanthine. Both antibiotic substances are commonly used together with deletion of the corresponding uracil-phosphoribosyl-transferase (*upt*) and hypoxanthine-phosphoribosyl-transferase (*hpt*) genes, respectively, as negative selectable markers in marker-less mutagenesis tools for mesophilic methanogenic archaea (Pritchett *et al.* 2004, Moore and Leigh 2005).

With concentrations ranging from 50 µg/mL - 500 µg/mL in solidified mineral media plates, we tested the 6-aza-uracil sensitivity of $5 \cdot 10^3$ and $5 \cdot 10^6$ spread-plated wild-type *M. thermautotrophicus* ΔH cells. In controls without selective pressure, $5 \cdot 10^3$ cells resulted in ~1500 individual populations, and $5 \cdot 10^6$ cells resulted in a microbial lawn of wild-type *M. thermautotrophicus* ΔH after 80 h of incubation at 60°C. On 6-aza-uracil containing plates, no individual populations were observed with any tested concentration. Therefore, 50 µg/mL of 6-aza-uracil seems to be sufficient to inhibit growth of *M. thermautotrophicus* ΔH on plates for at least four days (**Figure 16A**). However, the plating experiments with 6-aza-uracil were performed without replicates (*N*=1). Therefore, the results are only providing a rough estimation of the inhibitory concentration. Nevertheless, *N*=5 plates indicated that at least 500

µg/ml of 6-aza-uracil is sufficient to inhibit growth of wild-type *M. thermautotrophicus* ΔH for at least 80 h of incubation.

We tested the 8-aza-hypoxanthine sensitivity of $1 \cdot 10^4$ spread-plated wild-type *M. thermautotrophicus* ΔH cells with 8-aza-hypoxanthine concentrations ranging from 50 µg/mL – 500 µg/mL on solidified mineral medium plates. After 80 h of incubation at 60°C, ~2300 individual populations were observed with the non-selective wild-type *M. thermautotrophicus* ΔH control, and ~1100 individual populations were observed with 50 µg/mL 8-aza-hypoxanthine-containing plates. Concentrations higher than 50 µg/mL did not result in formation of individual populations. Therefore, 100 µg/mL of 8-aza-hypoxanthine seems to be sufficient to inhibit growth of wild-type *M. thermautotrophicus* ΔH (**Figure 16B**). Also, the plating experiments with different 8-aza-hypoxanthine concentrations were performed without replicates (*N*=1). Therefore, the results are only providing a rough estimation of the minimum inhibitory concentration, but at least 500 µg/mL of 8-aza-hypoxanthine is sufficient to inhibit growth of wild-type *M. thermautotrophicus* ΔH for at least 80 h of incubation.

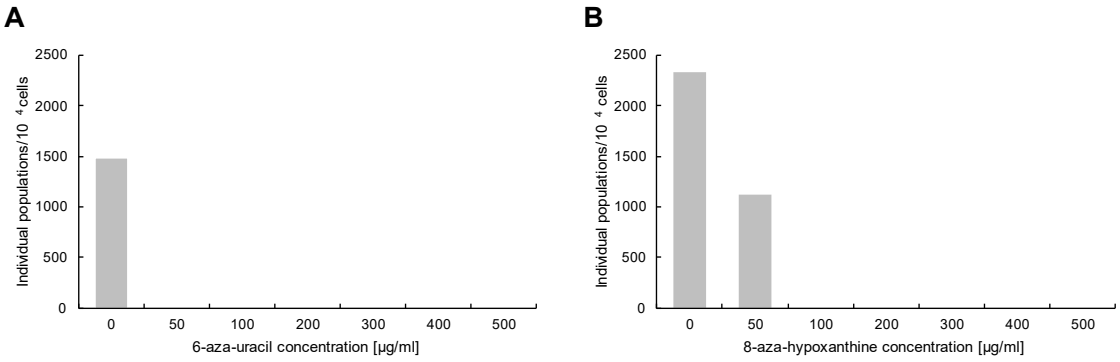

Figure 16. **A**) Number of Individual populations from $5 \cdot 10^3$ wild-type *M. thermautotrophicus* ΔH cells (**grey bars**), which were spread-plated on solidified media plates containing 6-aza-uracil concentrations ranging from 0 µg/mL to 500 µg/mL. Experimental sets *N*=1, *N*=5 for 500 µg/mL with no standard deviation calculatable. **B**) Number of individual populations from $1 \cdot 10^4$ wild-type *M. thermautotrophicus* ΔH cells (**grey bars**), which were spread-plated on solidified media plates containing 8-aza-hypoxanthine concentrations ranging from 0 µg/mL to 500 µg/mL. Experimental sets *N*=1, *N*=4 for 500 µg/mL with no standard deviation calculatable.

2. Interdomain conjugation with *E. coli* S17-1 allows for DNA transfer into *M. thermautotrophicus* ΔH

The two basic requirements, generation of high plating efficiencies and sensitivity of wild-type *M. thermautotrophicus* ΔH to antibiotic substances, enabled us to proceed with initiating the work on a genetic system for *M. thermautotrophicus* ΔH. One crucial step in the establishment of a genetic system is the DNA transfer into the host microbe. Following our broad approach, we investigated several published protocols (and modified versions) for potential DNA transfer into *M. thermautotrophicus* ΔH by using our various plasmids and shuttle vectors (**Supplement**

S1). These DNA-transfer protocols included: 1) natural competence protocols (Worrell *et al.* 1988, Susanti *et al.* 2019); 2) chemically/physically-induced DNA-transfer protocols, such as elevated calcium- and magnesium concentrations in the mineral medium, or low temperature incubation of pre-cultures to induce stress conditions; 3) an electroporation protocol (Molitor *et al.* 2016); and 4) an interdomain conjugation protocol with *E. coli* (Dodsworth *et al.* 2010) (**Supplement S1**). Most attempts did not result in cells with the expected selectable phenotype, and if so, could not be linked to the respective anticipated genotype, and appeared to be spontaneous-resistant cells (**Supplement S2**). The protocol that finally led to a successful DNA transfer into *M. thermautotrophicus* ΔH was an interdomain conjugation protocol with *E. coli* S17-1 (**Figure 17; see III.5.1.**), which was a modified version of the protocol for conjugational DNA transfer from *E. coli* S17-1 into *M. maripaludis* (Dodsworth *et al.* 2010).

To achieve a successful conjugational DNA transfer of the archetype shuttle vector pMVS-V1 (**Figure 22A; see IV.3.**) from *E. coli* S17-1 (donor) to *M. thermautotrophicus* ΔH (recipient), we increased the recipient cell concentration to ~$1.6 \cdot 10^9$ cells from a culture in the early stationary growth phase, which is a 5-fold higher cell concentration compared to Dodsworth *et al.* (2010). Furthermore, we used a spot-mating procedure to allow close physical contact between donor and recipient cells during an incubation period at 37°C on solidified media plates, which supported metabolic activity of *E. coli* S17-1 (**Figure 17A**), in contrast to direct spread-plating as in Dodsworth *et al.* (2010). After resuspending the spot-mated cells (donor + recipient) from the solidified media plate, we recovered *M. thermautotrophicus* ΔH in liquid mineral medium without any complex media additions (no organic carbon source) and without antibiotics additions at 60°C under a hydrogen/carbon dioxide atmosphere (**Figure 17B; see III.5.1.**). These incubation conditions decreased the viability of *E. coli* S17-1 to a very minimum, and therefore no counter-selection with antibiotic substances against donor cells were required. After a short incubation period (3-4 h) to recover *M. thermautotrophicus* ΔH under non-selective conditions, the cells were transferred to liquid medium, which contained neomycin for a selective-enrichment step. Importantly, the required incubation period for the cells to grow in this step was key for a successful identification of transconjugants (*i.e.*, recipient cells that received the shuttle vector). Neomycin at a concentration of 250 µg/mL inhibits growth of *M. thermautotrophicus* ΔH for at least 60 h in liquid medium (**Figure 14**). Therefore, when the cells did not grow within less than 60 h (typically growth appeared after 24-48 h in a successful experiment) in the selective-enrichment step, the conjugation experiment was regarded as unsuccessful, because the number of spontaneous-resistant cells is considerably higher compared to potential transconjugants, which renders screening essentially impossible.

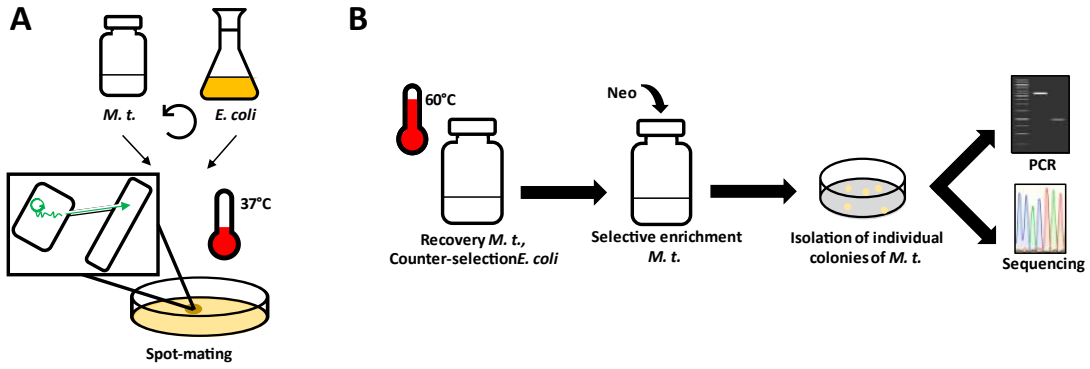

Figure 17. Schematic depiction and analysis of interdomain conjugation between *E. coli* S17-1 and *M. thermautotrophicus* ΔH. **A)** Wild-type *M. thermautotrophicus* ΔH (***M. t.***) and the shuttle vector-carrying *E. coli* were harvested by centrifugation, mixed, and spotted on solidified media plates that support growth of both microbes. During the spot-mating step at 37°C, the DNA-transfer process *via* conjugation takes place (**small scheme**). **B)** The process to isolate and identify individual clonal populations of genetically modified *M. thermautotrophicus* ΔH in the standard protocol. After the spot-mating step, *M. thermautotrophicus* ΔH cells were recovered in non-selective liquid mineral medium at 60°C, and afterwards, transconjugants were enriched in neomycin (**Neo**)-containing selective liquid mineral medium at 60°C. Individual populations were obtained from plating the enrichment culture. Those individual populations were analyzed by PCR and Sanger sequencing.

2.1. Successful conjugation leads to an antibiotic-resistant phenotype and stable replication of shuttle-vector DNA in *M. thermautotrophicus* ΔH

The first evidence whether conjugation experiments were successful were gathered through analysis of the phenotypical behavior. Successfully enriched selective cultures, which were obtained within 24-48 h after the conjugation experiment, showed in consecutive transfers wild-type-like growth behavior in the presence of 250 µg/mL neomycin. At the same time, with selective conditions wild-type *M. thermautotrophicus* ΔH did not grow to the same cell densities (**Figure 18A**). During pour-plating approaches on selective solidified media plates, we further achieved above 50% plating efficiency with the shuttle vector-containing *M. thermautotrophicus* ΔH transconjugants with 100 µg/mL and 250 µg/mL neomycin, while wild-type *M. thermautotrophicus* ΔH barely resulted in individual populations under selective conditions (**Figure 18B**).

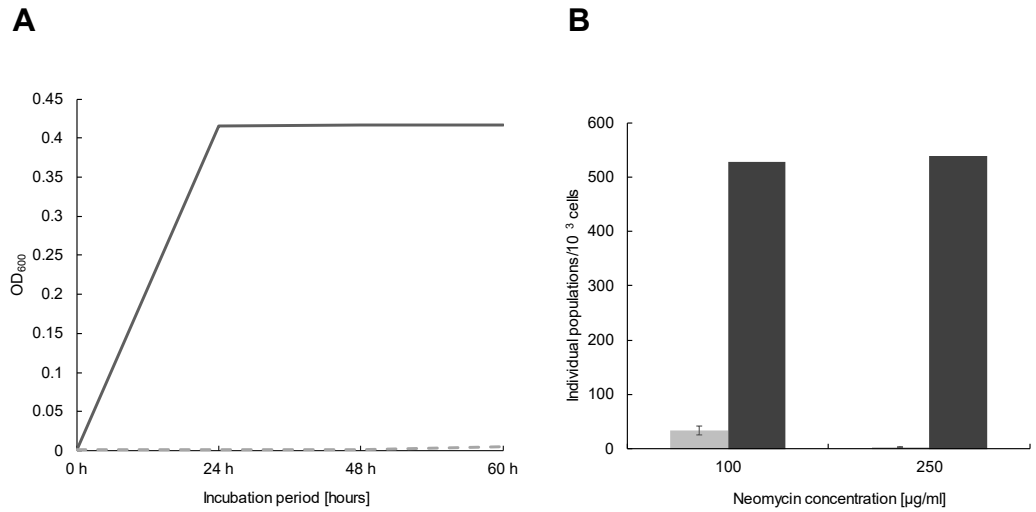

Figure 18. Comparison of shuttle vector-containing *M. thermautotrophicus* ΔH with wild-type *M. thermautotrophicus* ΔH in selective liquid media (A) and on solidified media plates (B). **A**) Measurement of OD_{600} after different incubation periods at 60°C (0 h, 24 h, 48 h, and 60 h) with initially $5 \cdot 10^5$ cells/mL pMVS-V1-carrying *M. thermautotrophicus* ΔH (**black solid line**, *N*=1) and wild-type *M. thermautotrophicus* ΔH (**grey dashed line**, *N*=1) were incubated in selective liquid mineral medium with 250 µg/mL neomycin **B**) Number of individual clonal populations of $1 \cdot 10^3$ pour-plated and pMVS-V1-carrying *M. thermautotrophicus* ΔH (**black bars**, *N*=1) and wild-type *M. thermautotrophicus* ΔH (**grey bars**, *N*=3).

After we found the expected phenotypical selective growth of putative transconjugant cells, we analyzed the genotype of genetically modified *M. thermautotrophicus* ΔH strains *via* site-specific PCR amplifications with: 1) a primer combination (**Table 1**), which specifically amplifies a 1-kilobase fragment of the pME2001 replicon; and 2) primer combinations (**Table 1**), which specifically amplify either a 1.5-kilobase or a 2.8-kilobase fragment of genomic DNA from *M. thermautotrophicus* ΔH to confirm the integrity of the genetically modified strains (**Figure 19A; see III.5.4.**). In preliminary experiments with high densities of *E. coli* S17-1, we found that PCR signals for the presence of our high-copy number shuttle vectors (with regards to copy number in *E. coli*) could be obtained after up to three transfers in liquid media, and also from areas of solidified media plates at which no growth was observed (after up to two transfers). Therefore, to gather reliable results on the stable replication of shuttle vectors in *M. thermautotrophicus* ΔH, and to exclude false positive results from residual *E. coli* DNA (**Supplement S3**), we first transferred cell material from individual clonal populations of putative *M. thermautotrophicus* ΔH transconjugants into selective liquid mineral medium. This enrichment culture was plated by streaking some culture with an inoculation loop on selective solidified media plates. From these plates, we inoculated another selective liquid mineral medium with cell material from individual clonal populations, and these liquid enrichment cultures were analyzed by PCR

amplification. Successful DNA transfer into *M. thermautotrophicus* ΔH was reproducibly confirmed (**Figure 19A**).

As a second approach to confirm the presence and integrity of the shuttle vector in *M. thermautotrophicus* ΔH, we extracted plasmid DNA from genetically modified *M. thermautotrophicus* ΔH cultures and used this plasmid DNA for retransformation of *E. coli* NEB stable (**See III.5.5.**). Individual clonal populations of *E. coli* NEB stable were analyzed with restriction-enzyme digestion and Sanger sequencing. We found that all analyzed individual clonal populations contained the entire shuttle vector, which was deduced from the correct fragment sizes in the restriction-enzyme digestion (**Figure 19B**), and did not contain any mutations in the *M. thermautotrophicus* ΔH replicon as well as the neomycin-selectable marker (**Figure 19C**). We did not re-sequence the entire *E. coli* replicon and selectable marker (**Figure 19C**).

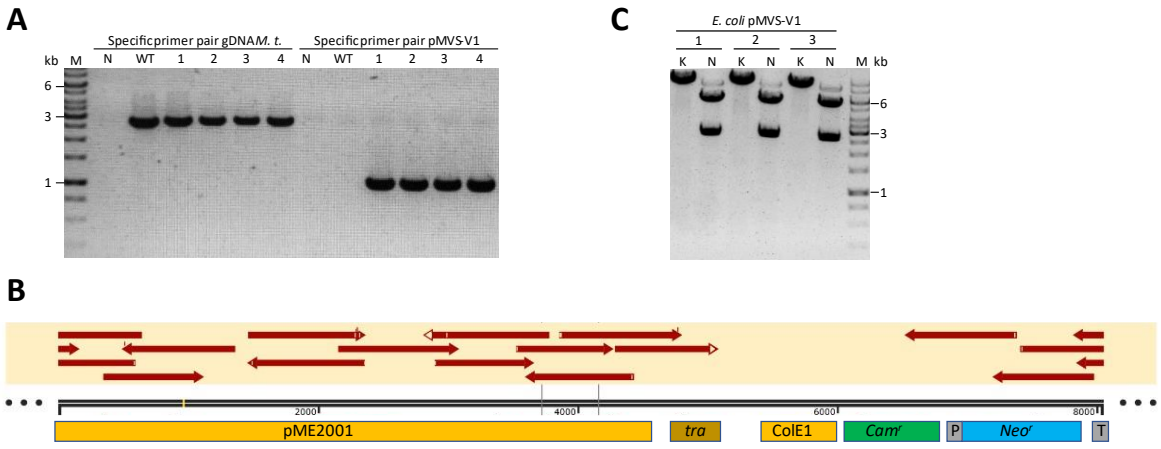

Figure 19. Molecular analysis of shuttle vector containing *M. thermautotrophicus* ΔH with site-specific PCR (A), plasmid retransformation (B), and Sanger sequencing (C) **A)** PCR analysis of four respective transconjugants (**1-4**) with primer combinations specific for the shuttle vector pMVS-V1 replicon (1-kilobase fragment) and for genomic DNA of *M. thermautotrophicus* ΔH (2.8-kilobase fragment). **N**, water negative control; **WT**, control with wild-type *M. thermautotrophicus* ΔH; **M**, GeneRuler 1 kb DNA Ladder (Thermo Scientific, Waltham MA, USA). **B)** Restriction-enzyme digestion of plasmid DNA, which was extracted from three independent *E. coli* pMVS-V1 enrichment cultures (**1-3**). The *E. coli* strains were generated with plasmid DNA, which was extracted from genetically modified *M. thermautotrophicus* ΔH. The unique cutter *Kpn*I (**K**), resulting in one 8.2-kilobase fragment, and the dual cutter *Nde*I (**N**), resulting in 2.7-kilobase and 5.5-kilobase fragments were used. **M,** GeneRuler 1 kb DNA Ladder (Thermo Scientific, Waltham MA, USA). **C)** Exemplified sequence alignment of Sanger sequences from retransformed *E. coli* plasmid DNA to the original pMVS-V1 sequence. Red arrows indicate the sequence and its direction. No deletions, insertions, or nucleotide exchanges were detected.

2.2. Free plasmid DNA is not resulting in DNA transfer into *M. thermautotrophicus* ΔH

By having demonstrated DNA transfer into *M. thermautotrophicus* ΔH, we further analyzed whether this transfer was, indeed, depending on conjugational DNA transfer from *E. coli* S17-1 or whether it was rather by uptake of free DNA under the utilized cultivation conditions during the conjugation protocol (**See III.5.1.**). Uptake of free plasmid DNA could occur, because *E.*

coli S17-1 donor cells contain a large amount of pMVS-V1 plasmid DNA due to the high-copy number ColE1 replicon, which might be released into the liquid medium from lysing *E. coli* S17-1 cells.

Therefore, we conducted control experiments. First, we added 200 ng/mL of purified pMVS-V1 plasmid DNA (extracted from *E. coli* NEB stable) to a freshly inoculated non-selective *M. thermautotrophicus* ΔH culture (~$1 \cdot 10^5$ cells/mL). After growth of this culture to the stationary growth phase and to allow for potential natural competence to occur during all growth phases, we treated the cells similar to our standard conjugation protocol, including the non-selective recovery and selective-enrichment steps, and selective spread-plating, but without the spot-mating/plating step. Second, we substituted *E. coli* S17-1 with the non-conjugative *E. coli* NEB stable, which carried pMVS-V1, to analyze the importance of mobilization for DNA transfer into *M. thermautotrophicus* ΔH. Third, we heated *E. coli* S17-1, which carried pMVS-V1, to 60°C for 20 min *prior* to spot-mating, to check whether *E. coli* needs to be viable to mediate the DNA transfer into *M. thermautotrophicus* ΔH. Fourth, we added 250 U/mL DNase I to the *E. coli* S17-1 pre-culture during the last 30 min of incubation at 37°C, to reduce the amount of initial free DNA during the spot-mating process. None of these experiments resulted in DNA transfer into *M. thermautotrophicus* ΔH except for DNase-I treatment of the *E. coli* S17-1 donor cells (**Figure 20A**). DNase I treated *E. coli* S17-1 and the standard protocol resulted in individual populations (**Figure 20B, C**). Analysis of two respective individual populations *via* PCR amplification revealed the presence of pMVS-V1 (**Figure 20D**).

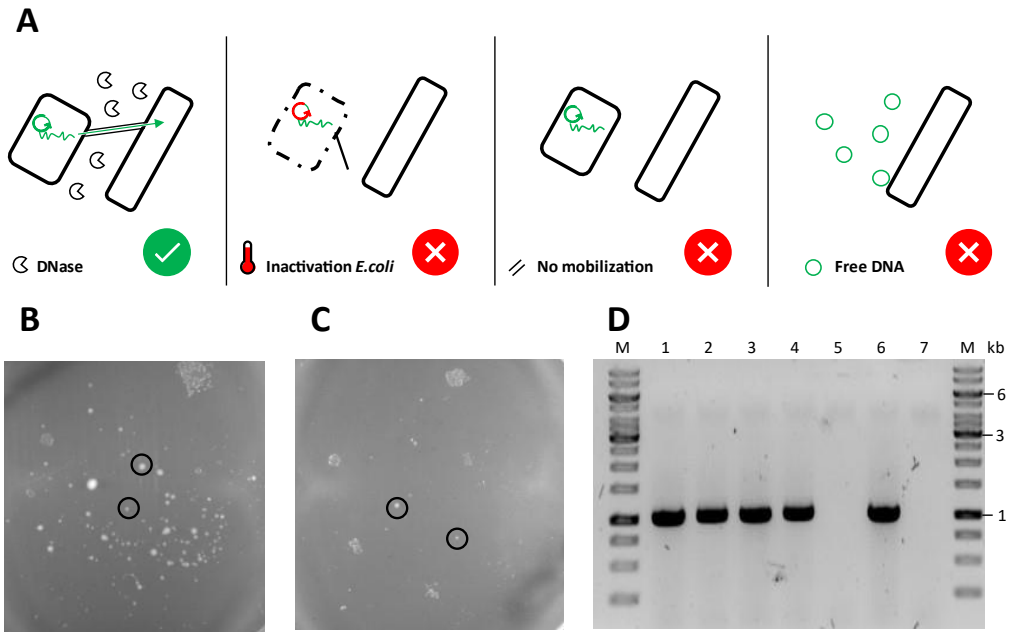

Figure 20. A) Experimental conditions for the confirmation of conjugation as the mechanism for DNA transfer were (from left to right): DNase I treatment, heat inactivation of *E. coli* S17-1, conjugation with non-conjugative *E. coli* NEB stable, and addition of free plasmid DNA directly to *M. thermautotrophicus* ΔH cell culture. **B)** Spread-plated *M. thermautotrophicus* ΔH using selectively enriched culture conjugated with standard protocol. Black circles represent individual populations, which were used for PCR analysis. **C)** Spread-plated *M. thermautotrophicus* ΔH using selectively enriched culture conjugated with DNase I treated *E. coli* S17-1. Black circles represent individual populations, which were used for PCR analysis. **D)** PCR analysis of the four individual populations from B and C **(1-4)**, wild-type *M. thermautotrophicus* ΔH **(5)**, purified shuttle-vector DNA as positive control **(6)**, and water as negative control **(7)**. A primer combination, which amplifies a 1-kilobase fragment from the pME2001 replicon was used for PCR amplification. **M,** GeneRuler 1 kb DNA Ladder (Thermo Scientific, Waltham MA, USA).

2.3. Interdomain conjugation frequencies into *M. thermautotrophicus* ΔH

With different shuttle vector constructs in independent experiments, we achieved reliable DNA transfer into *M. thermautotrophicus* ΔH with our standard protocol, which includes a selective-enrichment step (**Figure 19A**). To determine the conjugation frequencies, we performed experiments without the selective-enrichment step, but with a prolonged non-selective-recovery step. The determination of the conjugation frequency, which we define as transconjugants per initial recipient cells, is accompanied by several unknown parameters, such as the different incubation periods during the spot-mating, and the non-selective-recovery and selective-enrichment steps, before the selective spread-plating step to obtain individual clonal populations (**Figure 17**). This method reliably resulted in a high number of individual clonal populations. However, to quantify the conjugation frequency more accurately, we performed a subset of experiments in which we did not include the selective-enrichment step,

but instead we prolonged the incubation period for the non-selective-recovery step. Still, we had to take different parameters into account, and we corrected the conjugation frequency according to **Equation 1**:

$$f = \frac{N_P \cdot V_R}{E \cdot N_0 \cdot R_W \cdot 2^{(D_S + D_R)}} \quad \textbf{(Equation 1)}$$

where **f** represents the conjugation frequency; $\mathbf{N_P}$ represents the number of individual clonal populations obtained after the final selective spread-plating step; $\mathbf{V_R}$ represents the dilution factor for the amount of plated cells in relation to overall culture volume; **E** represents the spread-plating efficiency as a fraction; $\mathbf{N_0}$ represents the initial recipient cell number used for spot-mating; $\mathbf{R_W}$ represents the fraction of cells that are recovered from the washing step after the spot-mating; $\mathbf{D_S}$ represents the number of cell divisions during spot-mating; and $\mathbf{D_R}$ represents the number of cell divisions during non-selective recovery.

We calculated a range of parameters in a simple sensitivity analysis assuming the worst- and best-case scenarios (**Table 15**). The parameters $\mathbf{V_R}$, $\mathbf{N_P}$, and $\mathbf{N_0}$ are either known (dilution factor $\mathbf{V_R}$ is 50 in our experiments) or can be experimentally determined by cell counting before the conjugational DNA transfer and colony counting of transconjugants after the selective spread-plating step. The parameter **E** can be experimentally defined with a relatively good certainty, based on our plating efficiencies (**Figure 12D**). However, the parameters $\mathbf{R_W}$, $\mathbf{D_S}$, and $\mathbf{D_R}$ needed to be estimated in a certain range for the sensitivity analysis, for example, based on assumptions that are made from other experiments. For $\mathbf{D_S}$ this is because in the spot-mating step, *E. coli* and *M. thermautotrophicus* ΔH cells were combined and potential growth (number of cell divisions) of *M. thermautotrophicus* ΔH at 37°C cannot be determined. For our estimations, we define $\mathbf{D_S}$ as either 0 or 1 cell divisions. For $\mathbf{R_W}$, the washing step after the spot-mating step is critical. While with careful suspension of the entire spot a recovery of all cells can be assumed, for our estimations, we define $\mathbf{R_W}$ between 0.5 and 1.0 (for 50-100% recovery of cells). For $\mathbf{D_R}$, the overall number of cell divisions during the non-selective recovery step is critical. Based on typical growth experiments similar to these conditions (16-20 h without selection), we assume $\mathbf{D_R}$ to be between 5 and 8 cell divisions. These assumptions result in an estimated conjugation frequency between $6 \cdot 10^{-6}$ and $4 \cdot 10^{-9}$ (**Table 15**).

Table 15. Example calculations for conjugation frequencies for DNA transfer into *M. thermautotrophicus* ΔH based on Equation 1

Parameters	N_P	E	V_R	D_R	N_0	R_W	D_S	Conjugation frequency
Best-case scenario	10	0.01	50	5	$5 \cdot 10^8$	0.5	0	$6 \cdot 10^{-6}$
Worst-case scenario	1	0.05	50	8	$5 \cdot 10^8$	1	1	$4 \cdot 10^{-9}$

2.4. Segregational stability of shuttle vector with non-selective conditions

Once the plasmid DNA was transferred into *M. thermautotrophicus* ΔH, it was maintained with high segregational stability over many cell divisions in selective liquid media. However, the segregational stability with non-selective growth conditions of shuttle vectors in *M. thermautotrophicus* ΔH is of interest for longer incubation periods (*e.g.*, in bioreactors), but also required to be known for potential plasmid-curing techniques. Therefore, we performed an experiment to assess the segregational stability of pMVS-V1 in *M. thermautotrophicus* ΔH. We inoculated both selective and non-selective liquid mineral medium with ~$5 \cdot 10^5$ cells/mL from a selectively grown pre-culture of pMVS-V1-carrying *M. thermautotrophicus* ΔH. After growth to ~$1 \cdot 10^8$ cells/mL, which corresponds to ~7-8 cell divisions (**Equation 2**), we repeated the transfer of ~$5 \cdot 10^5$ cells/mL from the non-selective liquid mineral medium to non-selective conditions twice. This resulted, in total, in ~21-28 cell divisions under non-selective conditions. We calculated the number of cell divisions according to **Equation 2**:

$$n = \frac{log(N_t) - log(N_0)}{\log(2)} \quad \textbf{(Equation 2)}$$

where **n** is the number of generations (cell divisions), $\mathbf{N_t}$ is the cell concentration at the end of the incubation period, and $\mathbf{N_0}$ is the cell concentration in the beginning of the incubation period.

We spread-plated cells from the first selective transfer to selective solidified media plates, and from all three non-selective transfers to non-selective solidified media plates, respectively. We analyzed 16 individual clonal populations each from the selective plate (plated from selective liquid transfer) and non-selective plates (plated from all non-selective liquid transfers) *via* site-specific PCR. We found that all analyzed individual clonal populations still contained the shuttle vector construct, independent of the presence of a selection pressure (**Figure 21**).

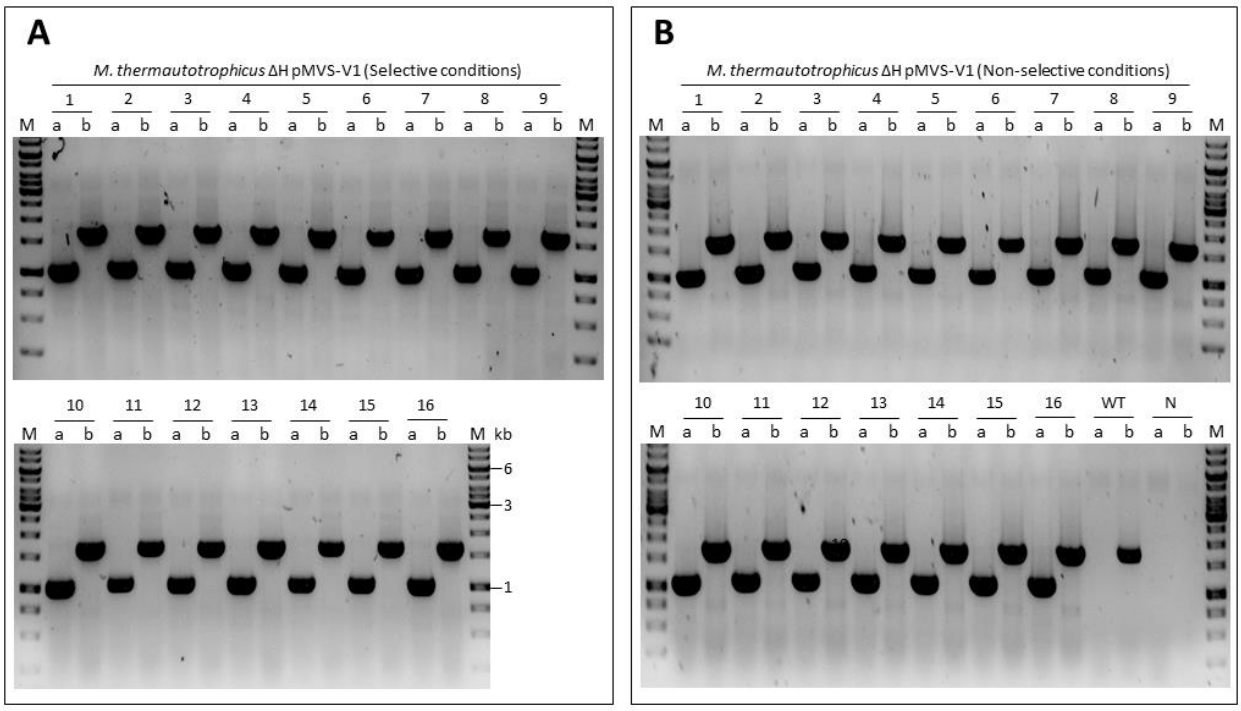

Figure 21. A) PCR analysis of individual clonal populations from selective solidified media plates after one selective transfer of pMVS-V1-carrying *M. thermautotrophicus* ΔH in liquid mineral medium. **B)** PCR analysis of individual clonal populations from non-selective solidified media plates after **three** non-selective transfers (~21-28 cell divisions) in liquid mineral medium (PCR analysis of the first and second transfer is not shown but gave the same results). A 1-kilobase fragment results from the specific primer pair for the pME2001 replicon for *M. thermautotrophicus* ΔH **(a)** and a 1.5-kilobase fragment from the specific primer pair for *M. thermautotrophicus* ΔH genomic DNA **(b)**. All 16 individual clonal populations each result in positive PCR for both primer combinations. Wild-type *M. thermautotrophicus* ΔH **(WT)** does not result in PCR signal for pMVS-V1, and water as negative control **(N)** does not result in any PCR signal. **M**, GeneRuler 1 kb DNA Ladder (Thermo Scientific, Waltham MA, USA).

3. The modular pMVS design (plasmid *Methanothermobacter* Vector System) acts as a replicative shuttle vector in *E. coli* and *M. thermautotrophicus* ΔH

To facilitate exchangeability of genetic elements in shuttle-vector constructs, and to allow fast adaptation to new findings, we decided for a modular shuttle vector design from the beginning. Inspired by the pSEVA system for Gram-negative bacteria (Martinez-Garcia *et al.* 2015), and the pMTL80000 system for Clostridia (Heap *et al.* 2009), we established the plasmid *Methanothermobacter* Vector System (pMVS) design.

The pMVS design consists of five modules, which are separated by rare eight base-pair recognition sequences for the restriction enzymes *Pme*I, *AsiS*I, *Fse*I, *Asc*I, and *Pac*I (**Figure 22**). To follow the pMVS design, these rare restriction enzyme-recognition sequences need to stay unique to grant exchangeability of the modules by restriction/ligation cloning. The five modules are (restriction enzyme boundaries are given in parenthesis): **1)** the replicon for *E. coli* (*AsiS*I, *Pme*I); **2)** the selectable marker for *E. coli* (*Pme*I, *Fse*I); **3)** the replicon for *M.*

thermautotrophicus ΔH (*Asi*SI, *Pac*I); **4)** the selectable marker for *M. thermautotrophicus* ΔH (*Asc*I, *Fse*I); and **5)** an application module that can be used to include any genetic cargo such as a reporter gene or another gene of interest (*Pac*I, *Asc*I) (**Figure 22**).

The nomenclature for the pMVS design is realized by adding a four-digit code after pMVS for the definition of the first four modules, which defines the plasmid backbone with basic functions for replication and selection in *E. coli* (module 1 and 2) and *M. thermautotrophicus* ΔH (module 3 and 4). Additional large capital letters can be amended to each digit to define differences, such as varying promoter sequences, in a given module. For the fifth (application) module, a descriptive name is added after the four-digit code, which allows to stay as flexible as possible with the used genetic cargo (without a limitation to nine digits), while staying within the pMVS design boundaries.

Based on the first shuttle vector (pMVS-V1) that led to successful DNA transfer and selection protocols, as described in **IV.2.**, we defined pMVS-V1 as our archetype shuttle vector, which does not contain a *Pac*I site or genetic cargo (**Figure 22A**). We selected the pMTL83151 plasmid from the pMTL80000 system (Heap *et al.* 2009) as the source for the backbone for *E. coli* in pMVS-V1, because this plasmid contains the *tra*-region including Ori-T from RK2 (for mobilization of the plasmid) in addition to the ColE1 replicon. Furthermore, this plasmid already brings a chloramphenicol-selectable marker (Cam^r) for selection in *E. coli*, which is separated from the replicon by a *Pme*I-recognition sequence, due to the modularity of the pMTL80000 system (Heap *et al.* 2009). As the replicon for *M. thermautotrophicus* ΔH, we chose the cryptic plasmid pME2001 from *M. marburgensis* (Bokranz *et al.* 1990). This plasmid has been studied to some extent and is the smallest plasmid, which is known in *Methanothermobacter* spp. (Meile and Reeve 1985, Meile *et al.* 1988, Luo *et al.* 2001). The plasmid contains five open-reading frames (*ORF1-5*) with barely any annotated functions. Additionally, in a ~1-kilobase section on pME2001, no open-reading frames have been annotated, but instead this section contains five sites of inserted fragments (IFs), which are different in pME2001 when compared to the similar cryptic plasmid pME2200 from *M. thermautotrophicus* ZH3, whereas IF5 only occurs in pME2001 (Luo *et al.* 2001). Previous attempts to create *E. coli-M. thermautotrophicus* ΔH shuttle vectors relied on the availability of restriction enzyme-recognition sequences in pME2001 (Meile and Reeve 1985). To not interrupt one of the open-reading frames and simultaneously to not intersect the region of a potential origin of replication for which the exact location is not known in pME2001 and pME2200, we decided to fuse the pME2001 replicon to

the other components of the shuttle vector at the position of IF5 *via* Gibson® Assembly (**See III.4.1.**), and to use the entire plasmid pME2001 as the replicon for *M. thermautotrophicus* ΔH.

We chose the thermostable neomycin-selectable marker (Neo^r) from pMU131 for positive selection in *M. thermautotrophicus* ΔH (Shaw *et al.* 2010). As a promoter, we selected a sequence published by Santangelo *et al.* (2008), which we designate P_{synth} (but which is called P_{hmtB} in Santangelo *et al.* (2008), **Figure 30A**), because the commonly used promoter $P_{mcrB(M.v.)}$ from *M. voltae* (Gernhardt *et al.* 1990) did not result in genetically modified *M. thermautotrophicus* ΔH in combination with Neo^r in our hands. The promoter sequence from Santangelo *et al.* (2008) has similarity to the upstream region of a histone-binding protein (HmtB)-encoding gene from *M. thermautotrophicus* ΔH. However, several modifications had been introduced in P_{synth} compared to the native P_{hmtB} sequence (Tabassum *et al.* 1992). The native P_{hmtB} sequence was demonstrated to initiate *in-vitro* transcription, and thus the generation of mRNA was proven when using purified native *M. thermautotrophicus* ΔH RNA polymerase (Darcy *et al.* 1999). Additionally, the P_{synth} promoter was shown to initiate gene expression in *T. kodakarensis* (Santangelo *et al.* 2008). As the terminator sequence for the selectable marker, we implemented the T_{mcr} terminator sequence of the methyl-coenzyme M reductase (*mcr*) operon from *M. voltae*, which is commonly used in constructs for genetic modification of *Methanococcus* spp. and *Methanosarcina* spp. (Sarmiento *et al.* 2011).

After we had demonstrated the functionality of pMVS-V1, our first complete shuttle vector, pMVS1111A-P_{synth}-*bgaB*, was then constructed based on this archetype shuttle vector. pMVS1111A-P_{synth}-*bgaB* contains a thermostable β-galactosidase-encoding gene *bgaB* (**See IV.5.**) as a reporter gene for *M. thermautotrophicus* ΔH and an additional *Pac*I restriction enzyme recognition site, which completes the application module. The directionality of the *bgaB* gene was such that the T_{mcr} terminator sequence from the selectable marker module is also terminating transcription of the *bgaB* gene (**Figure 22B)**.

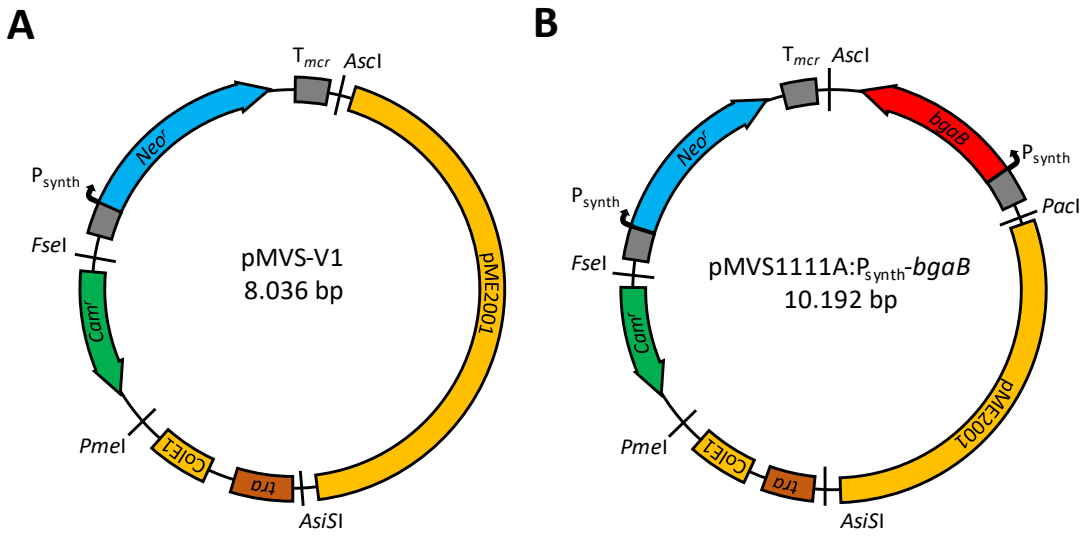

Figure 22. Plasmid maps of the *Methanothermobacter* vector system (pMVS). **A)** pMVS-V1 (8,036 bp) consists of four modules, which are intersected by the eight base-pair restriction enzyme recognition sites ***Asc*I**, ***Fse*I**, ***Pme*I**, and ***AsiS*I**. The four modules are the replicon for *E. coli* (**ColE1**, ***tra***), the selectable marker for *E. coli* (**Cam^r**), the replicon for *M. thermautotrophicus* ΔH (**pME2001**), and the selectable marker for *M. thermautotrophicus* ΔH (**Neo^r**). **B)** pMVS1111A:P$_{synth}$-*bgaB* (10,192 bp) consists of five modules, which are intersected by the eight base-pair restriction enzyme recognition sites ***Asc*I, *Fse*I**, ***Pme*I**, ***AsiS*I**, and ***Pac*I**. The five modules are as in pMVS-V1 with following differences: the replicon for *M. thermautotrophicus* ΔH is flanked by *AsiS*I and *Pac*I, and the shuttle vector contains the ***bgaB*** gene in the application module, which is flanked by *Pac*I and *Asc*I. **P$_{synth}$**, synthetic promoter sequence, which is based on P$_{hmtB}$; **T$_{mcr}$**, terminator sequence from the *mcr* operon of *M. voltae*.

4. Suicide-vector constructs facilitate genome integration in *M. thermautotrophicus* ΔH

The functional shuttle vector system enables us for expression of homologous and heterologous genes, and therefore for addition of genetic cargo to *M. thermautotrophicus* ΔH. To enable deletions, substitutions, and thus integration of genes into genomic DNA of *M. thermautotrophicus* ΔH, we expanded the pMVS design further. One way of accomplishing genomic DNA integrations is the use of suicide vectors without a replicon for *M. thermautotrophicus* ΔH. The genome integration mechanism of suicide-vector constructs relies on homologous recombination events with the genomic DNA of the host microbe. For this purpose, we constructed suicide-vector constructs with the formate dehydrogenase operon of *M. thermautotrophicus* Z-245 (fdh$_{Z-245}$) (Nölling and Reeve 1997), and the neomycin resistance gene (Neo^r) as selectable markers, which were flanked by 1-kb homologous regions up- and downstream of the target gene (**Figure 23, see III.4.2**). As a proof of principle, we chose the Mth60-fimbriae operons (*mth58-mth61*/ MTH_RS00275-290) (Thoma *et al.* 2008, Sarbu 2013) for substitution with the selectable marker, which is likely not to cause a lethal deletion in *M. thermautotrophicus* ΔH.

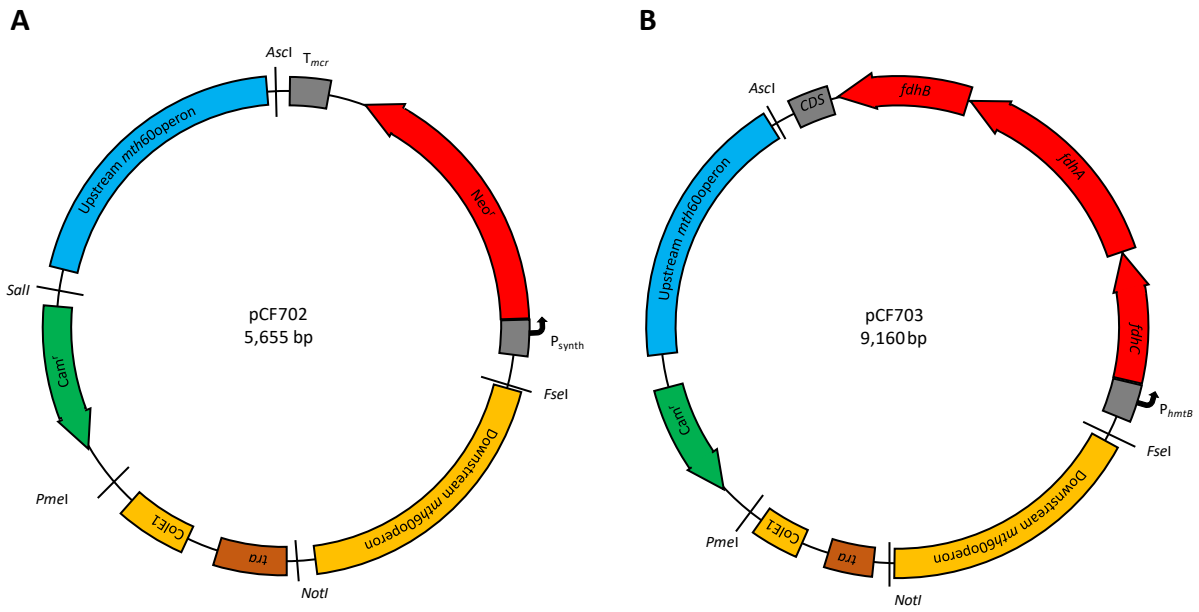

Figure 23. Suicide-vector constructs pCF702 and pCF703 for genome integration at the *mth*60-fimbriae operons site in genomic DNA of *M. thermautotrophicus* ΔH. A) pCF702 (5,655 bp) consists of five parts, which are intersected by unique restriction enzyme recognition sites in brackets, the chloramphenicol resistance (**Cam^r**) [*Pme*I, *Sal*I] and the replicon (**ColE1**) including *tra*J and OriT (***tra***) for mobilization in *E. coli* S17-1 [*Pme*I, *Not*I], the downstream homologous flanking region (1 kb) of the Mth60-fimbriae operons [*Not*I, *Fse*I], the thermostable neomycin resistance (**Neo^r**) with promoter **P$_{synth}$** and terminator **T$_{mcr}$** [*Fse*I, *Asc*I], and the upstream homologous flanking region (0.8 kb) of the Mth60-fimbriae operons [*Asc*I, *Sal*I]. B) pCF703 (9,160 bp) consists of the same parts as pCF702 except for the modular exchange of Neo^r to the formate dehydrogenase operon *fdh*$_{Z-245}$ of *M. thermautotrophicus* Z-245 (***fdhC-fdhB*, *CDS***) with the **P$_{hmtB}$** promoter [*Fse*I, *Asc*I]. With this exchange the *Sal*I restriction enzyme recognition site between Cam^r and the upstream homologous flanking region did not stay unique, anymore.

4.1 Site-specific PCR and Nanopore sequencing analysis confirm genome integration in *M. thermautotrophicus* ΔH

We performed interdomain conjugation (**See III.5.1.**) with wild-type *M. thermautotrophicus* ΔH and *E. coli* S-17, containing pCF702 and pCF703, with the aim for substitution of the Mth60-fimbriae operons *via* double homologous recombination with the formate dehydrogenase cassette (fdh$_{Z-245}$) and the neomycin resistance (Neo^r) as selectable marker, respectively (**Figure 23**). The *M. thermautotrophicus* ΔH cell recovery procedure of the conjugation protocol was adjusted as stated in **III.1.** to grow on formate or neomycin as the selectable marker. After pour-plating (formate) and spread-plating (neomycin) of the respective recovery cultures of *M. thermautotrophicus* ΔH, individual clonal populations were obtained. After enrichment of the *M. thermautotrophicus* ΔH clonal populations in selective liquid mineral medium, we extracted genomic DNA as template for PCR analysis, because the higher purity allows for the amplification of larger fragment sizes compared to boiled crude extract. We did not expect false positive PCR signals in selective liquid cultures that are derived from enriched clonal

populations, because *E. coli* DNA is sufficiently diluted at this stage (**Supplement S3**). We chose four site-specific primer combinations for the PCR analysis regarding genome integration of pCF702 and pCF703 (**Table 1**): 1) a primer combination inside of the Mth60-fimbriae operons as a control for their presence (S); 2) a primer combination inside the up- and downstream homologous flanking regions that binds in wild-type *M. thermautotrophicus* ΔH and strains with integrated selectable marker and which results in differing fragment sizes (M); 3) a primer combination that binds outside to outside of the homologous flanking regions in wild-type, single homologous recombination, and double homologous recombination and results in differing fragment sizes (L); and 4) a primer combination with one primer inside the upstream flanking region and the other in the chloramphenicol resistance gene of the *E. coli* vector backbone (V). This combination provides exclusive insights into the presence of single homologous recombined suicide-vector constructs in genomic DNA samples. Furthermore, the PCR analysis of site-specific genomic DNA integration of selectable markers was accompanied by the PCR independent whole-genome sequencing with MinIon Nanopore (**See III.5.6.**) to investigate site-specific integration with a third approach, in addition to phenotypical and PCR characterization.

4.2.1 DNA transfer of pCF703 generates site-specific integration of $fdh_{Z\text{-}245}$ in *M. thermautotrophicus* ΔH

To acquire first phenotypical evidence for a successful genome integration, we measured the formate content (*via* HPLC; the measurement was performed by Christian Klask according to the method described in Klask *et al.* (2020)) of the mixotrophic recovery culture of the conjugation experiment with pCF703 (hydrogen/carbon dioxide and 170 mM formate) and of the first enrichment culture in selective liquid mineral medium (nitrogen/carbon dioxide and 170 mM formate) with formate as the sole energy source. We compared the formate concentration of these cultures to non-inoculated blank medium. In the recovery culture, 20 mM of formate was consumed after 48 h of incubation (**Figure 24**). Due to high initial cell densities after spot-mating and hydrogen/carbon dioxide in the medium, no difference in optical density could be measured between negative control and formate recovery culture. In the first enrichment culture of *M. thermautotrophicus* ΔH Δ*mth*60 operon:$fdh_{Z\text{-}245}$, approximately 120 mM of formate were consumed after 48 h of incubation (**Figure 24**), and optical density raised from OD_{600}~0.05 to OD_{600}~0.25 (data not shown). Because the suicide vector is not replicative in *M. thermautotrophicus* ΔH, formate consumption accompanied by growth of *M. thermautotrophicus* ΔH provided evidence for successful DNA transfer, genomic-DNA integration, and functioning of the $fdh_{Z\text{-}245}$ in *M. thermautotrophicus* ΔH.

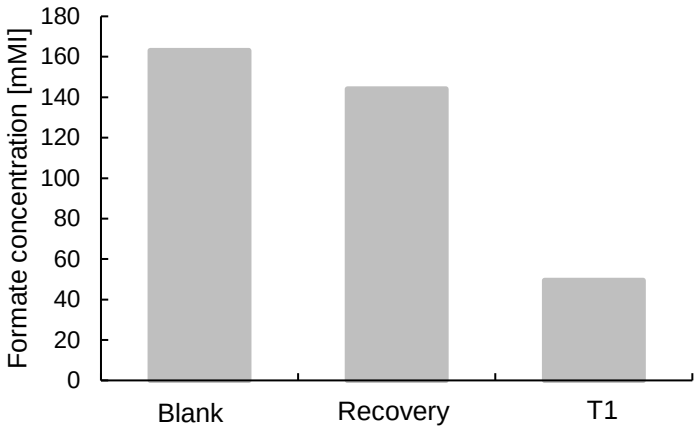

Figure 24. HPLC measurement of formate concentration in liquid mineral medium with 170 mM formate before inoculation with *M. thermautotrophicus* ΔH (**Blank**), the mixotrophic *M. thermautotrophicus* ΔH recovery culture of the conjugation experiment with pCF703 after 48 h of incubation (**Recovery**), and the first liquid enrichment culture (**T1**) from the recovery culture after 48 h of incubation. Measurement was performed quantitatively with *N*=1. Therefore, no standard deviation is given.

To add another layer of evidence, we screened for site-specific integration of the selectable marker $fdh_{Z\text{-}245}$ *via* PCR analysis. We analyzed four individual clonal populations from selective solidified mineral medium derived from pour-plated recovery culture. All four clonal populations indicated site-specific integration of $fdh_{Z\text{-}245}$, while the integration mechanism remained unclear. However, homologous recombination appeared to be most plausible. Therefore, we investigated three possible events that can result from homologous recombination. Three of four individual clonal populations provided signals with primer combination L (**See IV.4.1**) for wild-type (4.4 kb), double homologous recombination (~7 kb), and single homologous recombination (~12 kb) (**Figure 25A**). Only the clonal population #2 showed a stronger signal for double homologous integration than for wild-type, and no signal for single homologous recombination (**Figure 25A**). All clonal populations still contained the Mth60-fimbriae operons as observed with primer combination S (~1.5 kb) and M (~2.8 kb) (**See IV.4.1**) when compared to the wild-type control. In all samples of M (**See IV.4.1**) also the band for site-specific integration of $fdh_{Z\text{-}245}$ was present (~5.8 kb), which was not observed in the wild-type control (**Figure 25A**). Therefore, the enrichment culture from clonal population #2 was transferred to selective liquid mineral medium and analyzed *via* PCR (**Figure 27C**) and Nanopore whole genome sequencing (**Figure 26**). The PCR analysis of the liquid enrichment culture resulted in the same pattern as with the clonal population (**Figure 25A**), and all chromosomal integration possibilities were still present. Therefore, we pour-plated this culture for an additional purification, and we again screened four individual clonal populations from the pour-plate. These four clonal populations revealed exactly the same pattern as it was already shown for the first four clonal populations. This indicates that the community in the culture still consists of wild-type, single homologous recombined, and double homologous recombined genomic

DNA, although we transferred twice from respective individual clonal populations (**Figure 25B**). The presence of all three possible combinations of integration and non-integration suggests a broad diversity of genotypes in the individual clonal population. This could be linked to the diploid characteristic and genome distribution of *M. thermautotrophicus* ΔH (Majernik *et al.* 2005, Hildenbrand *et al.* 2011) in combination with the non-bactericidal prototrophic selectable marker *fdh*$_{Z\text{-}245}$.

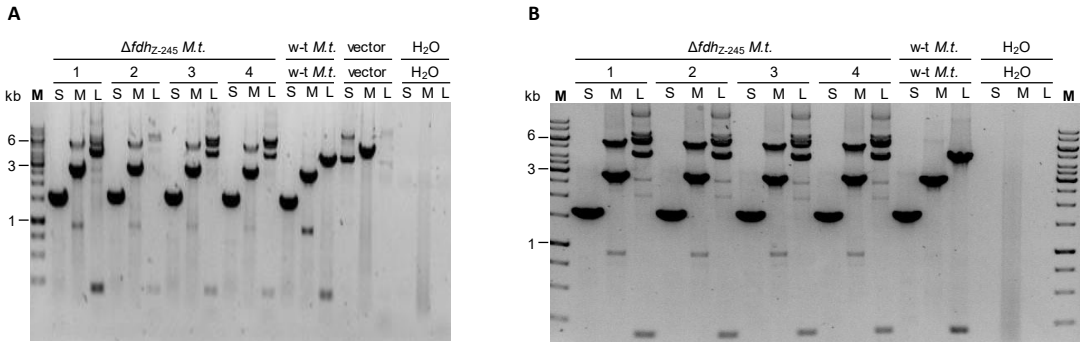

Figure 25. Site-specific PCR analysis with three primer combinations (**S**, **M**, and **L**) of genomic DNA extraction of enriched *M. thermautotrophicus* ΔH Δ*mth*60 operon:*fdh*$_{Z\text{-}245}$ (**Δ*fdh*$_{Z\text{-}245}$ *M.t*.) individual clonal populations **A**) Individual clonal populations obtained after plating of the recovery culture. **B**) Individual clonal populations after two transfers of population #2 from A. Arabic numbers represent the individual clonal population samples, Wild-type *M. thermautotrophicus* ΔH DNA was analyzed as positive control and reference (**w-t *M.t*.**), pCF703 DNA as positive control for combination M and negative control for wild-type signal (**vector**), and water as negative control (**H_2O**). **M** represents GeneRuler 1 kb DNA Ladder (Thermo Scientific, Waltham MA, USA).

The results of Nanopore whole genome sequencing backed the results of the PCR analysis. When we aligned the *M. thermautotrophicus* ΔH Δ*mth58-61*:*fdh*$_{Z\text{-}245}$ DNA reads to wild-type *M. thermautotrophicus* ΔH and double homologous recombined *fdh*$_{Z\text{-}245}$, we found that both loci are present in the DNA reads (**Figure 26A, B**), while no wild-type *M. thermautotrophicus* ΔH DNA reads aligned with the *fdh*$_{Z\text{-}245}$ (**Supplement S4**). The interfaces between the flanking homologous regions and the Mth60-fimbriae operons or the *fdh*$_{Z\text{-}245}$, respectively, and the genomic DNA regions outside of the homologous flanks were obvious by abrupt interruptions in the alignments (**Figure 26A, B, black arrows**). The number of DNA reads for the section with the best coverage in the downstream flanking homologous region was twice as high (120 reads) in *M. thermautotrophicus* ΔH Δ*mth58-61*:*fdh*$_{Z\text{-}245}$ compared to the wild-type *M. thermautotrophicus* ΔH (56 reads), when extrapolated to 200,000 DNA reads in total (**Supplement S4, Figure 26B**). This strongly indicates that the homologous region is present more than once in the sample, and therefore suggests single homologous recombination event being prevalent in the sample. Furthermore, the number of reads for the Mth60-fimbriae operons were very similar for *M. thermautotrophicus* ΔH Δ*mth58-61*:*fdh*$_{Z\text{-}245}$ and wild-type *M. thermautotrophicus* ΔH with 40-50 in the second peak (**Supplement S4**, **Figure 26A**). This

adds another layer of evidence, that the Mth60-fimbriae operons were present in this sample with the same frequency as in the wild-type sample, which was only possible when both, wild-type and single homologous recombined DNA, were present. This suggestion is also supported by the alignment of the DNA reads to a single homologous recombined DNA template where the presence of the vector could be clearly detected with DNA reads covering the entire range of the vector and strong emphasis on the chloramphenicol resistance gene (**Figure 26C, D**). Precise frequencies of wild-type, single homologous, or double homologous recombined genomic DNA in the sample were not calculatable due to the low coverage of the nanopore sequencing run.

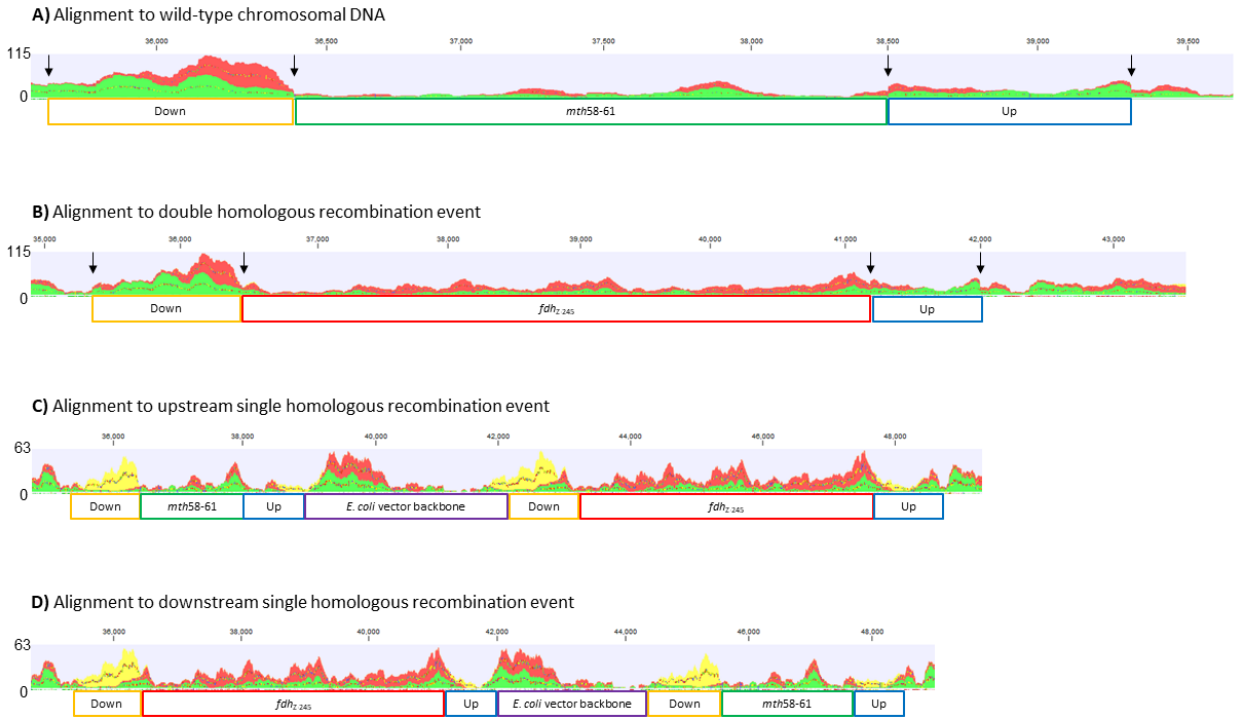

Figure 26. Sequence alignment of *M. thermautotrophicus* ΔH Δ*mth58-61*:*fdh*$_{Z\text{-}245}$ Nanopore sequencing DNA reads to *in-silico* generated reference genomes of *M. thermautotrophicus* ΔH at the locus of the Mth60-fimbriae operons and wild-type genomic DNA (**A**), double homologous recombined genomic DNA with pCF703 (**B**), upstream single homologous recombined genomic DNA with pCF703 (**C**). and downstream single homologous recombined genomic DNA with pCF702 (**D**). The black arrows in A + B indicate the interface between the homologous flanking region and the Mth60-fimbriae operons or the *fdh*$_{Z\text{-}245}$ operon on the inside and to the genomic DNA of *M. thermautotrophicus* ΔH to the outside. The numbers on the Y-axis represent the number of reads extrapolated to 200,000 DNA reads. Down (**yellow**) represents the downstream homologous region of the Mth60-fimbriae operons, *mth*58-61 (**green**) the Mth60-fimbriae operons, *fdh*$_{Z\text{-}245}$(**red**) the formate dehydrogenase operon of *M. thermautotrophicus* Z-245, *E. coli* vector backbone (**purple**), and up (**blue**) the upstream flanking region of the Mth60-fimbriae operons. The numbers left of the individual figure parts represent the number of DNA-reads gathered from Nanopore sequencing.

4.2.2 DNA transfer of pCF702 generates *M. thermautotrophicus* ΔH Δ*mth58-61*:Neo^{r}

We transferred the recovery culture of the conjugation experiment with pCF702 to selective liquid media containing 100 µg/mL of neomycin. The enrichment culture was subsequently

transferred again to liquid selective mineral medium and spread-plated on selective solidified media plates with 100 µg/mL of neomycin. We performed PCR analysis from the selective liquid transfer and from four individual clonal populations from selective solidified media plates. Although, in the liquid sample the Mth60-fimbriae operons signal was present with the primer combinations S (1.5 kb), M (2.8 kb), and L (4.4 kb) (**See IV.4.1**), the signal for site-specific integration *via* single- or double homologous recombination was also present in M (1.8 kb) and L (single homologous recombination ~ 9kb, double homologous recombination 3.5 kb), whereas the signal for double homologous recombination was most prevalent in L compared to single homologous recombination and wild-type (**Figure 27A**). Additionally, a fragment of the vector backbone to the upstream homologous flanking region (V) was amplified (2.9 kb). This confirms the presence of single homologous recombined genomic DNA in the sample (**Figure 27A**). In contrast, the four individual clonal populations showed distinct signals. While all had the same outcome for the primer combinations S and M (**See IV.4.1**), which indicated that the Mth60-fimbriae operons and Neo^r were present in the sample, in L all four clonal populations showed different patterns. In #1, four bands were present with Neo^r double homologous recombination, Mth60-fimbriae operons wild-type, a potential unspecific band at 6 kb, and the single homologous recombination signal (**Figure 27B**). In #3 and #4, the signal for double homologous recombination was not present (**Figure27B**). Since population #2 only showed the band for double homologous recombination and the potential unspecific band, we proceeded with clonal population #2 (**Figure 27B**). We transferred clonal population #2 to selective liquid media. Afterwards, PCR analysis of this transferred culture confirmed the results from transfer 1. The 6-kb band was not present anymore, and in L, the only signal was for double homologous recombination. However, in S and M the signal for the Mth60-fimbriae operons was still present (**Figure 27C**). This culture was prepared for whole genome Nanopore sequencing (**Figure 28**) and further spread-plated on selective mineral medium to screen for pure double homologous recombined individual clonal populations. Three individual clonal populations were PCR analyzed. While two showed the patter of all possible events (wild-type, single-, and double homologous recombination including the band at ~6 kb), population #1 had no more wild-type signal in S and M. Additionally, in L there was only minimal background signal for wild-type DNA (**Figure 27D**). This indicated a pure culture of double homologous recombined Neo^r, and therefore deletion of the Mth60-fimbriae operons. With this clonal population, we assumed that the Mth60-fimbriae operons deletion is not lethal for *M. thermautotrophicus* ΔH.

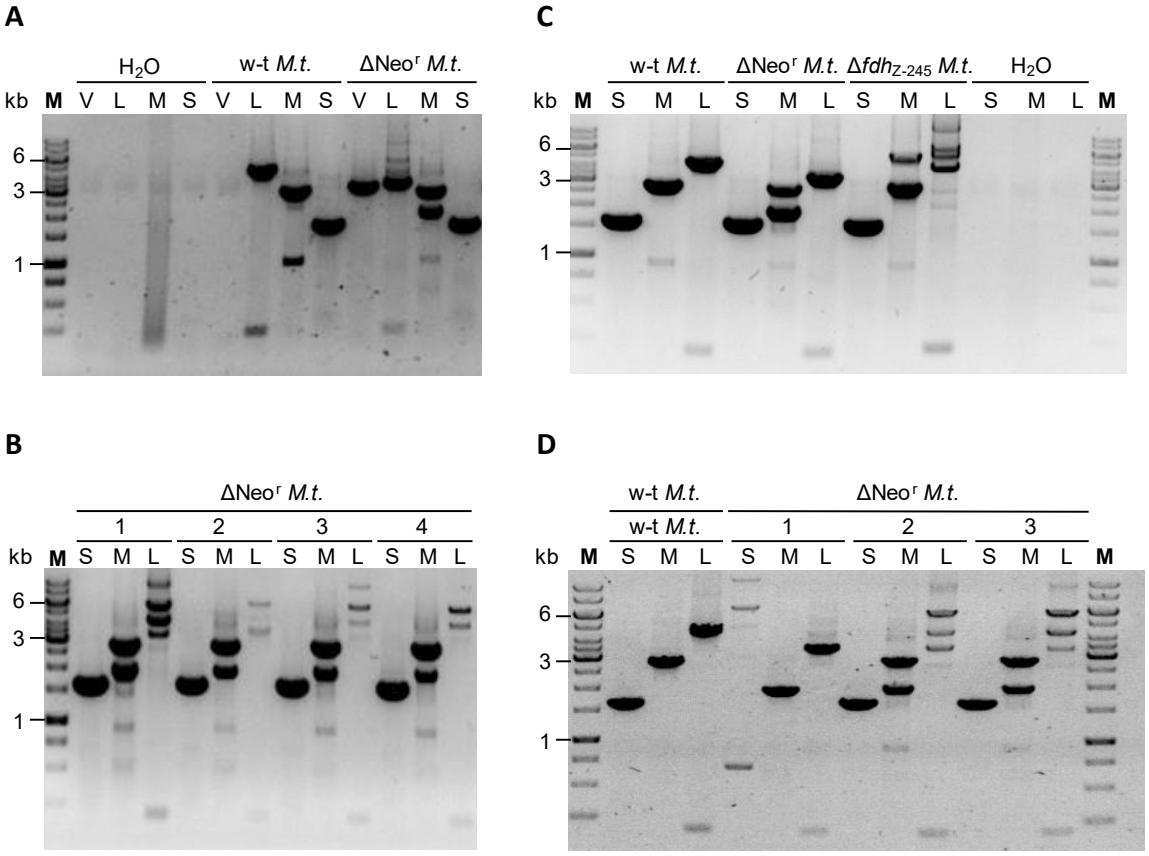

Figure 27. Site-specific PCR analysis of genomic DNA extractions from *M. thermautotrophicus* ΔH Δ*mth58-61*:Neo^r (**ΔNeo^r *M.t.*)** enrichment cultures with three primer combinations (**S**, **M**, and **L**) and combination **V** for *E. coli* vector backbone integration in A. **A**) Analysis of second selective liquid transfer after recovery of *M. thermautotrophicus* ΔH Δ*mth58-61*:Neo^r. **B**) Analysis of four Individual clonal populations derived from the first selective liquid transfer. **C**) Analysis of liquid selective transfer of clonal population #2 from B and from clonal population #2 of **Figure 25A**. Wild-type *M. thermautotrophicus* ΔH and the two enriched clonal populations were Nanopore whole genome sequenced. **D**) Analysis of three individual clonal populations of spread-plated clonal population #2 from C. **Arabic numbers** represent the individual clonal population samples, Wild-type *M. thermautotrophicus* ΔH DNA was analyzed as positive control and reference (**w-t *M.t.***), and water as negative control (**H_2O**). **M** represents GeneRuler 1 kb DNA Ladder (Thermo Scientific, Waltham MA, USA).

The results of Nanopore whole genome sequencing backed the results of the PCR analysis of **Figure 27C**. When we aligned the *M. thermautotrophicus* ΔH Δ*mth58-61*:Neo^r DNA reads to wild-type *M. thermautotrophicus* ΔH and double homologous recombined Neo^r, we found that both loci are present in the DNA reads (**Figure 28A, B**). The interfaces between the flanking homologous regions and the *mth58-61* and the Neo^r, respectively, as well as between homologous flanks and the outside genomic DNA regions can be easily detected by abrupt interruptions in the sequencing reads (**Figure 28A, B, black arrows**). The interruption in the interface between wild-type Mth60-fimbriae operons and downstream homologous flanking region was more pronounced than for Neo^r. Additionally, the number of downstream homologous flanking region DNA reads (peak) was not twice as high (102) as in the wild-type

genomic DNA (60) compared to the *fdh*$_{Z\text{-}245}$ integration sample (120) (**Supplement S4, Figure 28B**). Furthermore, the number of *mth58-61* reads (18) were lower relatively to *fdh*$_{Z\text{-}245}$ integration sample reads (40) (**Figure 26A, Figure28A)** and wild-type (50) (**Supplement S4, Figure S11A**) at the second peak of the operon. These three observations confirm the presence of double homologous recombined chromosomes in the Neo^{r} sample in higher frequencies than in the *fdh*$_{Z\text{-}245}$ integration sample (**See IV.4.2.1**). Single homologous recombination was also present, but Cam^{r} reads (highest peak in *E. coli* vector backbone) have a lower number of reads (30) (**Figure 28C, D**) compared to *fdh*$_{Z\text{-}245}$ integration (60) (**Figure 26C**). The shift towards double homologous recombination could be linked to the bactericidal activity of neomycin, which excludes wild-type *M. thermautotrophicus* ΔH cells to stay viable without the resistance gene. Additionally, the deletion of the Mth60-fimbriae operons together with the substitution to the neomycin resistance could provide an advantage regarding growth rate due to less expression burden in double homologous recombined *M. thermautotrophicus* ΔH compared to single homologous recombined *M. thermautotrophicus* ΔH.

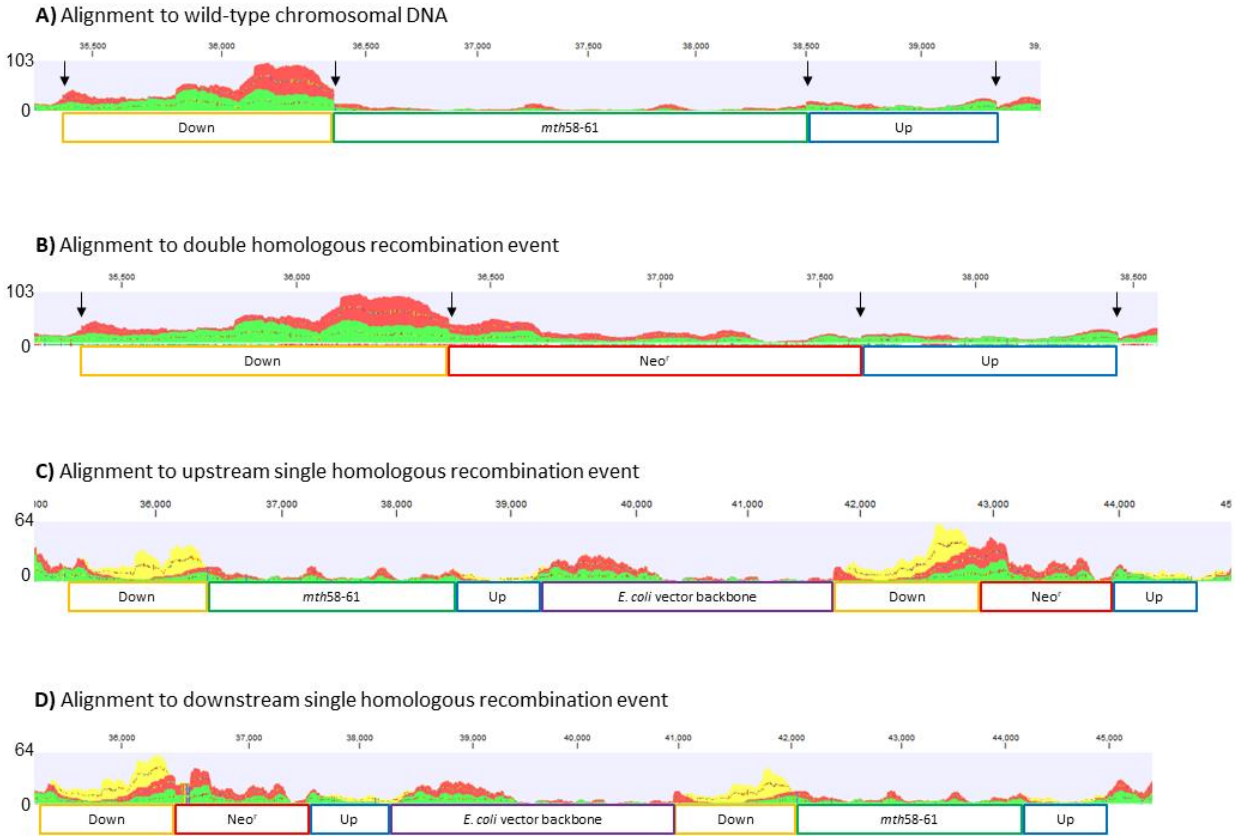

Figure 28. Sequence alignment of *M. thermautotrophicus* ΔH Δ*mth58-61*:Neo^r Nanopore sequencing DNA reads to *in-silico* generated reference genomes of *M. thermautotrophicus* ΔH at the locus of the Mth60-fimbriae operons; wild-type genomic DNA (**A**), double homologous recombined genomic DNA with pCF702 (**B**), upstream single homologous recombined genomic DNA with pCF702 (**C**), and downstream single homologous recombined genomic DNA with pCF702 (**D**). The **black arrows** in A + B indicate the interface between the homologous flanking region and the Mth60-fimbriae operons or Neo^r on the inside and to the genomic DNA of *M. thermautotrophicus* ΔH to the outside. The numbers on the Y-axis represent the number of reads extrapolated to 200,000 DNA reads. Down (**yellow**) represents the downstream homologous region of the Mth60-fimbriae operons, *mth*58-61 (**green**) the Mth60-fimbriae operons, Neo^r (**red**) the thermostable neomycin resistance gene, *E. coli* vector backbone (**purple**), and up (**blue**) the upstream flanking region of the Mth60-fimbriae operons. The numbers left of the individual figure parts represent the number of DNA-reads gathered from Nanopore sequencing.

5. A thermostable ß-galactosidase (BgaB) from *Geobacillus stearothermophilus* is a functional reporter to investigate promoter sequences in *M. thermautotrophicus* ΔH

With a DNA-transfer protocol and a functional shuttle vector, we proceeded with adding a genetic cargo (*i.e.*, gene of interest) to the application module of the archetype pMVS-V1 shuttle vector (**Figure 22**). To enable the analysis of the effects from different promoter sequences on gene expression in *M. thermautotrophicus* ΔH, we decided to implement a reporter gene as our first gene of interest. We chose the thermostable β-galactosidase encoding *bgaB* gene from *Geobacillus stearothermophilus* (Jensen *et al.* 2017). We placed a codon-optimized version of the *bgaB* gene under the control of the non-native P_{synth} promoter

(**See III.4.1**). We transferred the resulting shuttle vector pMVS1111A:P_{synth}-*bgaB* (**Figure 22B**) into *M. thermautotrophicus* ΔH *via* conjugation. In a qualitative preliminary experiment with cell lysate from pMVS1111A:P_{synth}-*bgaB*-carrying *M. thermautotrophicus* ΔH cells (and pMVS-V1-carrying cells as an empty vector negative control), we found that, indeed, the β-galactosidase BgaB is produced by *M. thermautotrophicus* ΔH and results in a color reaction in an enzyme assay with 3,4-cyclohexenoesculetin-β-D-galactopyranoside (S-Gal) only in the presence of the *bgaB* gene (**Figure 30B**).

This result sparked us to establish a quantitative β-galactosidase enzyme activity assay with o-nitrophenyl-β-D-galactopyranoside (ONPG) as the chromogenic substrate for the β-galactosidase, which allowed us to investigate promoter sequences for their relative *in-vivo* effect on gene expression in *M. thermautotrophicus* ΔH during a growth experiment (**Figure 29**). While we did not intend to perform an exhaustive promoter study, we first selected three promoters that represent a subset of promoter sequences with distinctive features. The first promoter, P_{synth}, is a synthetic promoter, which was based on the promoter sequence of the HmtB-encoding gene from *M. thermautotrophicus* ΔH (P_{hmtB}) (Tabassum *et al.* 1992), but with several sequence modifications between the start-codon and the TATA-box sequence (**Figure 30A**) (Santangelo *et al.* 2008). This P_{synth} promoter was shown to be functional in *T. kodakarensis* (Santangelo *et al.* 2008), and we had successfully used P_{synth} to drive our neomycin-selectable marker (**Figure 22**). In addition, as the second promoter, we used the promoter sequence upstream of the *hmtB*-gene from *M. thermautotrophicus* ΔH to include the native version of the promoter (Tabassum *et al.* 1992) on which P_{synth} was based on (**Figure 30A).** As a third promoter, we included the promoter sequence from upstream of one of the two isoforms for the methyl-coenzyme M reductase operons from *M. thermautotrophicus* ΔH the $P_{mrt(M.t.)}$ promoter (**Figure 30A**). The $P_{mrt(M.t.)}$ promoter does not contain the typical BRE and TATA-box sequences of archaeal promoters, but instead palindromic sequences that consist exclusively of thymine and adenine bases (Shinzato *et al.* 2008) (**Figure 30A**).

To implement the β-galactosidase enzyme activity assay for *M. thermautotrophicus* ΔH, we determined the β-galactosidase activity in different genetically modified *M. thermautotrophicus* ΔH strains after different incubation periods over the course of a growth experiment (**Figure 29**). Samples to assess β-galactosidase activity were taken after four different incubation periods during the growth experiment (subscript number gives time of incubation period in hours): $\mathbf{t_{15}}$, mid-exponential growth phase; $\mathbf{t_{19}}$, late-exponential growth phase; $\mathbf{t_{23}}$, early stationary growth phase; and $\mathbf{t_{36}}$, late-stationary growth/death phase (**Figure 29**). We determined the β-galactosidase activity after these various incubation periods for four different genetically modified *M. thermautotrophicus* ΔH strains, which carry the empty vector pMVS-V1 as negative control, the pMVS1111A:P_{synth}-*bgaB*, or one of two shuttle vectors,

pMVS1111A:P_{hmtB}-*bgaB* and pMVS1111A:$P_{mrt(M.t.)}$-*bgaB*, which have the P_{synth} promoter exchanged for the P_{hmtB} or the $P_{mrt(M.t.)}$ promoter, respectively. We found similar growth behaviors, with similar maximum OD_{600} values of ~0.4, for all four strains, and only the empty vector pMVS-V1-carrying strain reached the late-exponential growth phase already after 19 h, instead of after 23 h for the other three strains (**Figure 29A-D**). The β-galactosidase activity, given as Miller Units ($Absorbance_{420}$/(Incubation time [h]·OD_{600} ·volume [L])), was low, with 15±5 and 18±5 Miller Units for the empty vector control (pMVS-V1) and for the pMVS1111A:$P_{mrt(M.t.)}$-*bgaB*-carrying strain after all incubation periods (**Figure 29E**), respectively. For the pMVS1111A:P_{synth}-*bgaB*-carrying strain, the activity increased over the course of the growth experiment to 125±15 Miller Units after 36 h of incubation (**Figure 29E**). The pMVS1111A:$P_{hmtB(M.t.)}$-*bgaB*-carrying strain showed the highest β-galactosidase activity with 270±20 Miller Units, while already after 19 h of incubation, no further increase in the enzyme activity was observed (**Figure 29E**).

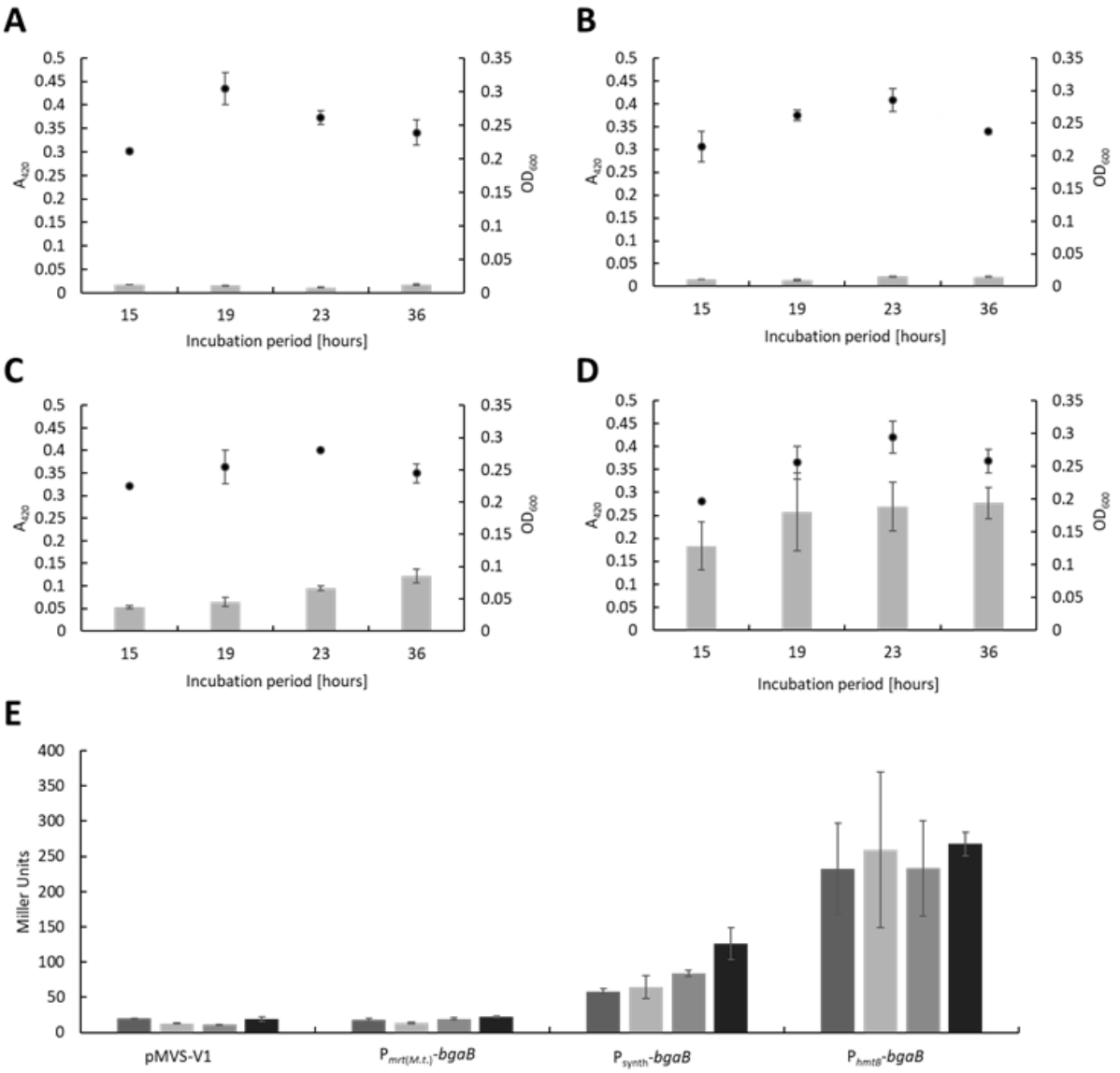

Figure 29. **A-D)** The measurements of absorbance at 420 nm **(A_{420})** of the enzyme activity assay **(bars)** and optical density at 600 nm **(OD_{600})** of the corresponding genetically engineered *M. thermautotrophicus* ΔH strain **(dots)** after different incubation periods (*M. thermautotrophicus* ΔH with **A**, pMVS-V1; **B,** pMVS1111A:$P_{mrt(M.t.)}$-*bgaB*; **C,** pMVS1111A:P_{synth}-*bgaB*; **D,** pMVS1111A:P_{hmtB}-*bgaB*). **E)** The resulting Miller Units from A-D for the four different *M. thermautotrophicus* ΔH strains is given for the incubation periods 15 h, 19 h, 24 h, and 36 h for each strain from left to right. Average (pMVS-V1 (*N*=2), pMVS1111A:$P_{mrt(M.t.)}$-*bgaB* (*N*=3), pMVS1111A:P_{synth}-*bgaB* (*N*=2), and pMVS1111A:P_{hmtB}-*bgaB* (*N*=3)) with error bars indicating standard deviation. The Miller Units in this experiment are lower compared to the experiment in **Figure 30C** because of differences in the experimental parameters (**see III.6.**).

However, after this first quantitative promoter assay, we realized that we had misinterpreted the annotation of the P_{synth} promoter in Santangelo *et al.* (2008), and our P_{synth} promoter did not contain the transcription factor B recognition element (BRE) sequence of archaeal promoters (Allers and Mevarech 2005). Therefore, we implemented an additional promoter by adding the BRE sequence to the P_{synth} promoter sequence to generate the $P_{synth(BRE)}$ promoter

sequence, but left all modifications from Santangelo *et al.* (2008) intact (**Figure 30A**). With these four distinct promoter sequences (P_{synth}, $P_{synth(BRE)}$, P_{hmtB}, and $P_{mrt(M.t.)}$) based on our previous results and the peer-reviewed literature, we compared the effects of the promoters on gene expression with the optimized enzyme assay (**Figure 29**). We found that the P_{synth} promoter, without a transcription factor B recognition element (BRE) sequence, resulted in a significantly higher β-galactosidase enzyme activity (510±50 Miller Units), when compared to the empty vector control (46±5 Miller Units; $P<0.01$; **Figure 30C**). However, significantly lower enzyme activity was measured with this promoter, when compared to the $P_{synth(BRE)}$ (1350±140 Miller Units; $P<0.05$) and the P_{hmtB} (5000±100 Miller Units; $P<0.01$; **Figure 30C**) promoters, which both contained a BRE sequence (**Figure 30A**). The $P_{mrt(M.t.)}$ promoter only resulted in a β-galactosidase activity (65±5 Miller Units) that was comparable and not significantly different to the empty vector negative control in the enzyme assay (45±5 Miller Units; **Figure 30C**). Therefore, this promoter has to be considered inactive under the tested conditions (**Figure 30C**). We did not include the commonly used $P_{mcrB(M.v.)}$ promoter for methanogen genetic systems in this comparison, because we already had found that this promoter is not functional in driving the neomycin-selectable marker.

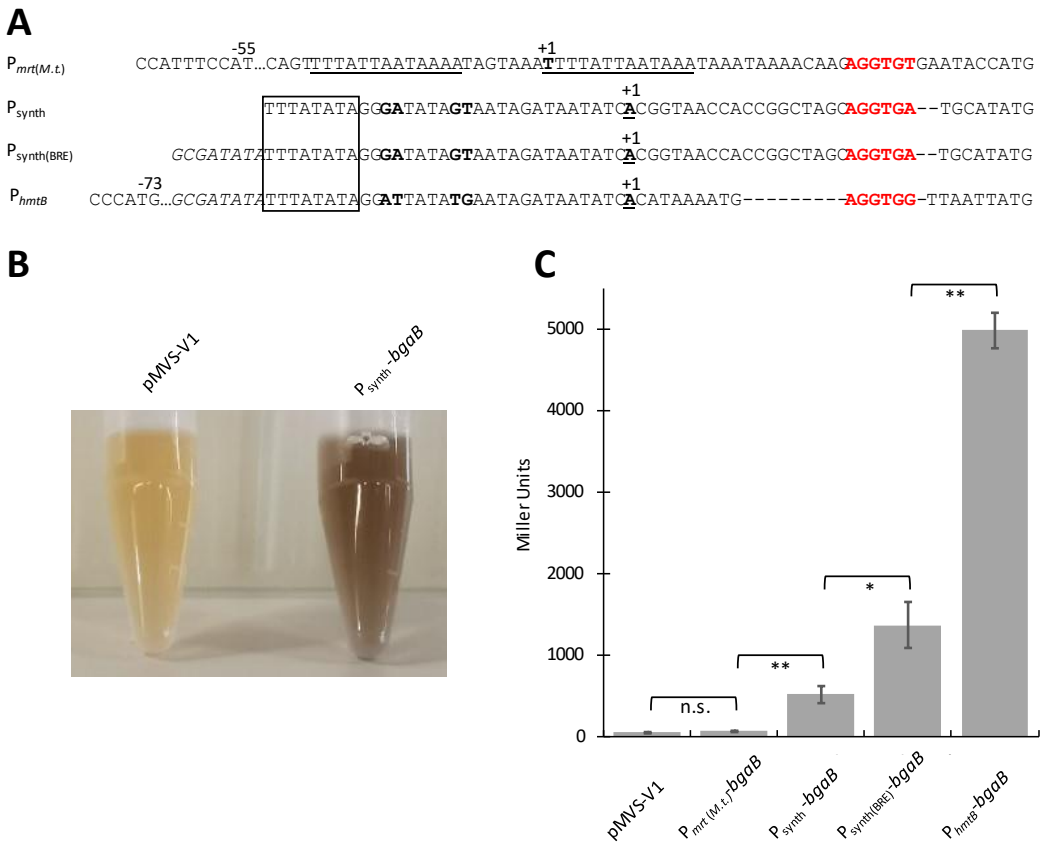

Figure 30. Enzyme activity assays with *M. thermautotrophicus* ΔH strains that carry a thermostable β-galactosidase (BgaB)-encoding gene under the control of four distinct promoter sequences. **A**) Sequence alignment of distinct putative promoter sequences that we analyzed for activity to drive the expression of a thermostable β-galactosidase (*bgaB*) gene. Sequence inverted repeats in $P_{mrt(M.t.)}$ are underlined. The transcription start site is indicated by "**+1**", highlighted in bold, and underlined. TATA-box sequences of P_{synth}, $P_{synth(BRE)}$, and P_{hmtB} are surrounded by a box. BRE sequences are highlighted in italics and ribosome-binding sites in red. Dashes are used as spacers, while dots indicate additional base pairs, which are left out here for visualization. Differences of P_{synth}, $P_{synth(BRE)}$, and P_{hmtB} between the TATA-box sequence and transcription start site are highlighted in bold. **B**) Qualitative analysis of BgaB activity with S-Gal as chromogenic substance in an in-vitro assay with cell lysate of empty vector-carrying *M. thermautotrophicus* ΔH (**pMVS-V1**) or pMVS1111A:P_{synth}-*bgaB*-carrying *M. thermautotrophicus* ΔH (**P_{synth}-*bgaB***) cells. **C**) Quantitative analysis of BgaB activity with ONPG as chromogenic substance in an *in-vitro* assay with cell lysate of *M. thermautotrophicus* ΔH strains that carry plasmids with the *bgaB* gene under the control of the four distinct promoters (**pMVS-V1**, empty vector control; **$P_{mrt(M.t.)}$-*bgaB***, pMVS1111A:$P_{mrt(M.t.)}$-*bgaB*; **P_{synth}-*bgaB***, pMVS1111A:P_{synth}-*bgaB*; **$P_{synth(BRE)}$-*bgaB***, pMVS1111A:$P_{synth(BRE)}$-*bgaB*; **P_{hmtB}-*bgaB*** pMVS1111A:P_{hmtB}-*bgaB*). Average (N=3) with error bars indicating standard deviation. Significance was tested with Student's t-test (two-tailed): *****, significant difference (P<0.05); ******, highly significant difference (P<0.01); **n.s**., no significant difference (P>0.05).

V. Discussion

Here, we report a robust method for genetic modification of *M. thermautotrophicus* ΔH based on interdomain conjugation of *E. coli* S17-1 and *M. thermautotrophicus* ΔH (**Figure 17**). For heterologous gene expression and generation of deletion mutants in *M. thermautotrophicus* ΔH, we developed the modular shuttle vector system (pMVS) as a replicative vector, and suicide vectors for genome integration in *M. thermautotrophicus* ΔH. With these systems, we demonstrated functionality of two selectable markers for positive selection. A thermostable neomycin resistance (Neo^r) conferred resistance to neomycin. A formate dehydrogenase-encoding operon ($fdh_{Z\text{-}245}$) from *M. thermautotrophicus* Z-245 enabled prototrophy in *M. thermautotrophicus* ΔH for growth on formate as the sole growth substrate (Nölling and Reeve 1997). Additionally, we showed heterologous gene expression with a thermostable β-galactosidase-encoding gene (*bgaB*) from *G. stearothermophilus* as a reporter to study gene expression (Jensen *et al.* 2017).

To achieve genetic modification of *M. thermautotrophicus* ΔH, in a first step, we investigated existing protocols to obtain individual clonal populations on solidified media plates by using different plating techniques. While we realized plating efficiencies of up to 100%, the plating conditions, such as humidity of the gas phase, growth phase of the microbial culture, and plating technique, considerably influenced the outcome over a range of three orders of magnitude (**Figure 12**). In several experiments, we observed plating efficiencies of more than 100%. *Methanothermobacter* spp., including *M. thermautotrophicus* ΔH, form filaments of cells and/or show aggregation of cells depending on the growth phase and culture conditions, as it has been reported before (Kiener and Leisinger 1983, Majernik *et al.* 2005). This complicates cell counting in the Petroff-counting chamber and can result in an underestimation of the initial number of cells for plating, which leads to calculated plating efficiencies of more than 100%. The number of individual clonal populations on solidified media plates was further dependent on factors, such as the position of the plate within the stainless-steel jar for anaerobic cultivation (**Figure 11**). In a typical experiment, up to ten plates were incubated in one jar, and even with plates that were prepared from the same media batch, and with the same liquid *M. thermautotrophicus* ΔH culture, we observed large variations in the number of individual clonal populations. Furthermore, we found considerably decreased plating efficiencies, when solidified media plates were not sufficiently dry to absorb the *M. thermautotrophicus* ΔH culture completely during the plating procedure. The accumulation of too much water can result from the formation of metabolic water during hydrogenotrophic methanogenesis ($4\,H_2 + \,CO_2 -> \,CH_4 + \,2\,H_2O$) (Lyu *et al.* 2018), but also due to incomplete drying of media plates after pouring hot media inside the anaerobic chamber (**See III.1.**). Therefore, a drying step was crucial, while

this drying step should not exceed 2 h in our experimental set-up, to avoid loss of carbon dioxide from the carbonate buffer system in the solidified media plates (because we used a nitrogen atmosphere in our anaerobic chamber; **See III.1.**). While this was sufficient as long as the humidity of the anaerobic chamber was sufficiently low, with accumulation of moisture inside the chamber, a 2 h-drying step still resulted in accumulation of water in the plates. Thus, we had implemented paper clips as spacers for the petri dishes (**Figure 12E**), which helped to overcome this issue, especially when the humidity in the anaerobic chamber was high. These paper clips ensured efficient gas-solid mass transfer of hydrogen and carbon dioxide. We observed a considerable increase in spread-plating efficiency of one-order of magnitude, when we added 0.1 volume% of hydrogen sulfide to the gas-phase of the anaerobic jar (**Figure 12D**). Hydrogen sulfide works as a sulfur source in *M. thermautotrophicus* ΔH and as a reducing agent that lowers the redox potential, which is required for cultivation of methanogenic archaea (King 2013, Martin *et al.* 2013). The sulfur source is not the limiting factor in liquid cultivations, because we were able to supply additional hydrogen and carbon dioxide several times with continuing growth in a fed batch cultivation. Thus, hydrogen and carbon dioxide are limiting factors before the sulfur source is depleted (data not shown). Therefore, it is more likely that the characteristic of hydrogen sulfide as a reducing agent leads to a lower redox potential on the surface of solidified media plates. This most likely resulted in beneficial growth conditions and in higher spread-plating efficiencies.

However, highest plating efficiencies of up to 100% were observed with the pour-plating technique. Individual clonal populations within the solidified medium of the top agar had a reduced diameter compared to populations that formed on the surface of the solidified medium (**Figure 12B, C**). One possible reason for larger clonal population diameter on the surface could be the larger contact area that is accessible to *M. thermautotrophicus* ΔH cells between the solidified media plate and the gas headspace, therefore, leading to better gas-liquid mass transfer of hydrogen and carbon dioxide when compared to cells within the solidified media plates, especially with elevated temperatures. This larger surface is also one of the key advantages for anaerobic trickle-bed reactors (Thema *et al.* 2021). A second reason could be quorum-sensing in *M. thermautotrophicus* ΔH for which a specific number of cells need to be in close vicinity to initiate the formation of individual populations. Regulation of cell assembly with acyl-homoserine-lactone-based quorum-sensing was found in methanogenic archaea (Zhang *et al.* 2012), and in the context of biofilm formation quorum-sensing is widespread with bacterial species, such as *Vibrio cholerae*, *Streptococcus* spp., or *Staphylococcus* spp. (Cvitkovitch *et al.* 2003, Hammer and Bassler 2003, Kong *et al.* 2006). The formation of individual populations is considered as the initiation step of biofilm formation (Jamal *et al.* 2018). Therefore, a quorum-sensing regulation might explain the discrepancy in colony

diameter on the surface of solidified media plates, but also between plating efficiencies with pour- and spread-plating. Another reason for the discrepancy in the number of individual clonal populations could be a more evenly distributed cell-culture during the pour-plating in comparison to the spread-plating procedure, which might lead to a better accessibility for *M. thermautotrophicus* ΔH to media components, or more stable pH conditions.

Thus, for specific purposes the plating technique has to be carefully considered to avoid misleading results such as false interpretations of successful or non-successful DNA-transfer events into *M. thermautotrophicus* ΔH. We found for colony PCR experiments with individual population samples from inside the solidified media plates, that high concentrations of agar contaminations are likely inhibiting or decreasing the DNA amplification *via* PCR. This goes along with previous studies on PCR inhibition by agar contaminations (Gibb and Wong 1998). Additionally, DNA residues from lysed *E. coli* or non-viable *M. thermautotrophicus* ΔH cells are more likely to be still present in samples from inside the solidified media plates than from the surface. This could lead to false positive PCR signals with shuttle-vector constructs or suicide-vector constructs for genome integration (**Supplement S3**). Therefore, sampling of individual clonal populations for PCR analysis is more reliable from spread-plated than from pour-plated populations. Furthermore, with a too high plating efficiency, spontaneous-antibiotic-resistant cells might overgrow genetically modified *M. thermautotrophicus* ΔH, because timing is of utmost importance for successful experiments as further discussed below.

With the detailed studies on plating efficiency of *M. thermautotrophicus* ΔH, we performed preliminary experiments to plate *M. thermautotrophicus* Z-245 with hydrogen and carbon dioxide or with formate. We found that *M. thermautotrophicus* Z-245 is forming individual clonal population with pour- and spread-plating when cultivated with hydrogen and carbon dioxide as energy and carbon source with the same media conditions than *M. thermautotrophicus* ΔH. When *M. thermautotrophicus* Z-245 was cultivated on solidified media plates with formate and nitrogen/carbon dioxide gas phase, colony formation could only be observed with pour-plating. One possible reason could be the reduced formate accessibility on the surface of the plate, or fast-changing pH conditions during the consumption of formate with production of carbon dioxide. A second possibility is the absence of hydrogen sulfide as reducing agent in the headspace of the stainless-steel jar to further reduce the redox potential on the surface of the solidified media plate, which was required to allow efficient growth of *M. thermautotrophicus* ΔH with spread-plating. While plating efficiencies for *M. thermautotrophicus* Z-245 need to be further optimized, we observed a relevant issue that also needs to be addressed. The formate dehydrogenase enzyme reaction produces one mole of carbon dioxide and one mole of reduced cofactor F_{420} from one mole of formate (Maia *et al.* 2015, Pan *et al.* 2016). Four moles

of reduced cofactor F_{420} and one mole of carbon dioxide are required for the production of one mole of methane. This leads to a large excess of carbon dioxide during the cultivation of *M. thermautotrophicus* Z-245 on formate. Therefore, we observed production of gas bubbles, which intersect the solidified media plates and render picking of individual clonal populations almost impossible (**Figure 13B**). Therefore, it is important to plate low numbers of *M. thermautotrophicus* Z-245 cells (<10,000/plate) and transfer small individual populations after 48-60 h of incubation. The same implies for genetically modified *M. thermautotrophicus* ΔH strains enabled for formate utilization described below. However, in *Methanococcus* spp. spread-plating on formate-containing solidified medium with the Hungate technique resulted in formation of individual populations (Long *et al.* 2017). Therefore, further adaptions to growth on formate-containing solidified media plates, such as reducing agent in headspace or media composition, can result in practicable spread-plating approaches.

The optimized plating efficiencies with hydrogen and carbon dioxide enabled us to test growth inhibition of *M. thermautotrophicus* ΔH with antibiotic substances on solidified media plates. We tested three antibiotic substances with existing corresponding selectable marker genes for positive selection in genetic systems for methanogenic archaea. We found puromycin to inhibit growth of *M. thermautotrophicus* ΔH starting from 40 µg/mL on solidified media plates and with an inhibiting concentration from 50 µg/mL in liquid mineral medium. This is a higher inhibiting concentration that is required when compared to *Methanosarcina* spp. with 1 µg/mL, and *Methanococcus* spp. with 2.5 µg/mL (Gernhardt *et al.* 1990, Metcalf *et al.* 1997). To confer resistance to puromycin in *Methanosarcina* spp. and *Methanococcus* spp. the puromycin acetyltransferase (Pac) was applied. Although Pac was shown to be temperature stable *in-vitro* at 70°C for 10 min (Paik *et al.* 1985), it has never been implemented in thermophilic genetic systems, so far. With the ability of cultivating *M. thermautotrophicus* ΔH under mesophilic conditions, which is possible with our established protocol (data not shown), an approach analog to the temperature adaption of the thermostable neomycin resistance could be performed (Hoseki *et al.* 1999). This would allow *pac* to become a powerful selectable marker for *M. thermautotrophicus* ΔH.

Lovastatin, which is preferably used for growth inhibition of *M. jannaschii*, did not inhibit growth of *M. thermautotrophicus* ΔH. For the derivate simvastatin, the inhibiting concentration started from 50 µM (21.5 µg/mL) (**Figure 15A**). This is a 5-10 times higher concentration compared to the inhibiting concentrations that were reported to be required for *P. furiosus* or *M. jannaschii* (10-20 µM or 4-8 µg/mL), respectively (Waege *et al.* 2010, Susanti *et al.* 2019). Resistance towards simvastatin is conferred through an overproduction of the Hmg-CoA reductase, which is an essential enzyme in the cell membrane biosynthesis in archaea. The Hmg-CoA reductase

is inactivated when binding simvastatin. The overproduction buffers the simvastatin toxicity. Therefore, Hmg-CoA reductase needs to be constitutively produced to maintain the buffer and its actual function (Hileman and Santangelo 2012). According to this resistance mechanisms, it is important to find the suitable simvastatin concentration and promoter strength of the Hmg-CoA reductase-encoding gene for a balanced system of sufficiently expressed Hmg-CoA reductase, but also inhibitory simvastatin concentration towards wild-type *M. thermautotrophicus* ΔH. Additionally, the use of a heterologous Hmg-CoA reductase-encoding gene is favorable to avoid off-target homologous recombination events, and therefore integration of the shuttle or suicide vectors at the native Hmg-CoA reductase locus. Thus, for *Thermococcus kodakarensis*, the Hmg-CoA reductase-encoding gene from *P. furiosus* was implemented and *vice versa* (Waege *et al.* 2010, Hileman and Santangelo 2012). The implementation of a Hmg-CoA reductase from a closely related *Methanothermobacter* spp. could be considered for *M. thermautotrophicus* ΔH. For neomycin, the *M. thermautotrophicus* ΔH growth inhibiting concentration was 250 µg/mL (**Figure 15B**), which is lower compared to *Methanococcus* spp. where 500 µg/mL are commonly applied for DNA-transfer experiments (Sarmiento *et al.* 2011). Neomycin acts as a bactericidal antibiotic substance, and therefore efficiently reduces the wild-type background in DNA-transfer experiments (Garrett and Won 1973).

In general, it was noticeable that spontaneous-resistant *M. thermautotrophicus* ΔH cells appeared readily with puromycin, simvastatin, and neomycin. Once those spontaneous-resistant mutant strains appeared, they were not inhibited or delayed in growth with subsequent transfers in liquid media as well as on solidified media plates. This had been already reported with neomycin for *M. thermautotrophicus* ΔH (Majernik *et al.* 2003), *M. maripaludis*, and *Methanococcus vanielli* (Argyle *et al.* 1996). However, in comparison to *M. maripaludis* for which spontaneous neomycin-resistant individual clonal populations appeared to be smaller than genetically modified populations (which were found to carry a neomycin-selectable marker) (Jones *et al.* 1983), we cannot see this difference in population size, potentially due to apparently faster growth rates of *M. thermautotrophicus* ΔH on solidified media plates.

Besides selectable markers for positive selection, we tested substances that are commonly used for negative selection in regard to potential future application in marker-less mutagenesis or plasmid curing systems. The antibiotic substance 5-fluoroorotic-acid (5-FOA) inhibited growth with concentrations of 0.5 mg/mL. Together with a deletion of the unique *pyrF* gene of *M. thermautotrophicus* ΔH (Smith *et al.* 1997), we had anticipated to develop this into a negative selectable marker for *M. thermautotrophicus* ΔH. However, since the *pyrF* deletion

leads to uracil auxotrophy in *Thermoanaerobacter* spp. (Basen *et al.* 2018), we tested how uracil supplementation acts on the efficiency of 5-FOA inhibition of *M. thermautotrophicus* ΔH. With this, we found that the affinity towards uracil is higher than for 5-FOA resulting in a complete reversal of the inhibition (**Supplement S2.3.**). These results go along with growth-inhibition experiments using 5-Fluoro-uracil (5-FU), which is a direct metabolite of 5-FOA with similar effects on PyrF on *M. marburgensis* (Teal and Nagle 1986, Nagle *et al.* 1987). This renders screening for deletion mutants of *pyrF* with 5-FOA impossible. A *M. thermautotrophicus* ΔH *pyrF* deletion strain, which might be obtained with CRISPR-Cas tools, however, could still be used as an auxotrophic marker towards uracil, as it was shown for *Sulfolobus* spp. (Wagner *et al.* 2012).

Furthermore, we tested the toxic base analogs 8-aza-hypoxanthine and 6-aza-uracil. The inhibiting concentrations for the toxic base analogs with *M. thermautotrophicus* ΔH were 50 µg/mL for 6-azauracil and 100 µg/mL for 8-azahypoxanthine, respectively (**Figure 16**). Compared to 1 mg/mL of 8-aza-hypoxanthine in *Methanococcus* spp. (Sarmiento *et al.* 2011) and 20 µg/mL of 8-Aza-2,4 diaminopurine (8-ADP) in *Methanosarcina* spp., the inhibiting concentrations for *M. thermautotrophicus* ΔH were lower or equal to the aforementioned species. Resistance towards the toxic base analogs is conferred by deletion of the hypoxanthine phosphoribosyl transferase gene (*hpt*) for 8-aza-hypoxanthine, and deletion of the uracil phosphoribosyl transferase gene (*upt*) for 6-aza-uracil (Enzmann *et al.* 2018). Both genes are annotated as unique in the genome of *M. thermautotrophicus* ΔH (Smith *et al.* 1997). However, both genes are located in operonal genomic structures in which deletions or substitution with a selectable marker could cause lethal polar effects on the surrounding genes. Whereas *hpt* is the first gene of the operon, where a substitution with a selectable marker could interrupt a proper read-over to the following gene, the *upt* gene is the last gene in its operon and would, therefore be the first choice for a gene deletion.

This set of reactive antibiotic substances against *M. thermautotrophicus* ΔH and corresponding resistance mechanisms provided us the ability for testing selectable markers in *M. thermautotrophicus* ΔH with a broad variety of approaches. The first successfully implemented selectable marker was the thermostable neomycin resistance conferring resistance against neomycin. The high rate of spontaneous resistant mutants as mentioned above forced us to implement a selective-enrichment step in liquid media. This provides enough time for growth of the genetically modified *M. thermautotrophicus* ΔH, while at the same time excludes the onset of growth of the spontaneous-resistant cells by substrate limitation in the gas phase, because those cells appear only after a longer incubation period. After the selective-enrichment step, the genetically modified *M. thermautotrophicus* ΔH cells outcompeted the

spontaneous-resistant cells sufficiently to obtain and select genetically modified individual clonal populations on selective solidified media plates.

With a slightly modified protocol without the selective-enrichment step and with a prolonged non-selective recovery, we observed conjugation frequencies ranging from $4 \cdot 10^{-9}$ to $6 \cdot 10^{-6}$, which was only approximately three to ten individual clonal populations in absolute numbers per solidified media plate in various experiments under the utilized experimental conditions (**Table 15**). In our standard protocol for conjugational DNA transfer, which includes the selective-enrichment step, we found many more individual clonal populations, which makes the transfer of a shuttle vector construct efficient and reliable. However, these individual clonal populations do not represent independent genetically modified *M. thermautotrophicus* ΔH cells, but represent a population, which is derived from only a few transconjugant cells.

To further enhance the conjugation protocol of *E. coli* S17-1 and *M. thermautotrophicus* ΔH cells, spot-mating on filter membrane might lead to higher conjugation frequencies (Smith and Guild 1980, Tominaga *et al.* 2016). In addition, spot-mating on a filter membrane would facilitate and would optimize the wash-off process after the mating step. This method would provide solid data on the number of viable recovered *M. thermautotrophicus* ΔH cells after mating and further define the calculations on conjugation efficiencies (**Table 15**). With the standard protocol for conjugation of *M. thermautotrophicus* ΔH with *E. coli* S17-1, we were using stationary cultures. Other studies on conjugation used late exponential *E. coli* cultures for the mating process, which could provide better DNA-transfer frequencies (Tominaga *et al.* 2016). Also, the ratio of *E. coli* to *M. thermautotrophicus* ΔH cells can be further investigated, as well as other parameters, such as the growth conditions during the mating process or different conjugative *E. coli* strains.

An additional important factor for conjugation efficiency is the state of methylation of heterologous DNA for the DNA transfer. Conjugation frequencies could be higher when a conjugative *E. coli* strain is applied that lacks the *dcm* and *dam* methyltransferases. The genomic DNA methylation state of *M. thermautotrophicus* ΔH basically consists of one prevalent pattern (deduced from Pacific Biosciencieces sequencing results in the Environmental Biotechnology Group, PhD thesis work of Isabella Casini), which indicates for a type I restriction methylation system (Loenen *et al.* 2014). In *M. thermautotrophicus* ΔH there is only one type I restriction/methylation complex annotated with the putative methyltransferase MTH_TS04455 (Annotation as multispecies N-6 DNA methylase from *Methanothermobacter* spp. in BLASTp of NCBI). Since, plasmid DNA that contains the respective methylation pattern was linearized with *M. thermautotrophicus* ΔH crude extract at optimal growth temperature (**Supplement S5**), the responsible methyltransferase gene of this type I complex could be

used in a helper plasmid in *E. coli* to imitate the methylation state of *M. thermautotrophicus* ΔH, and therefore enhance the DNA-transfer efficiencies. Helper plasmids or genome integrated methyltransferase are commonly applied in DNA-transfer protocols for other microbes, such as *Clostridium* spp. *Staphylococcus aureus*, or *Bacillus* spp. (Mermelstein and Papoutsakis 1993, Groot *et al.* 2008, Monk *et al.* 2012, Zhang *et al.* 2012).

A further possibility to enhance DNA-transfer frequencies besides the optimization of the protocols for DNA transfer, is the adaption of the shuttle- or integration vector constructs by reduction in size. It is known that small constructs are taken up with higher frequencies than larger ones, such as shown for the *M. maripaludis* shuttle vector pURB500 for which a size reduction led to elevated DNA-transfer frequencies (Walters *et al.* 2011). The reduction of the *M. thermautotrophicus* ΔH replicon size in shuttle-vector constructs can be performed targeted or randomized. A targeted fashion would imply deletions of the annotated open reading frames on pME2001, and subsequent tests whether DNA transfer and replication is still functional (Luo *et al.* 2001). This could also elucidate the functions of the open reading frames further. However, it requires more time and deeper insights. The faster method would be random deletion of parts of the replicon combined with a screening approach. The most applicable approach is probably an initial screening with the deletion of several open reading frames, followed by the deeper investigation of the individual function.

Furthermore, shuttle-vector modules with the same function could be determined to reduce the size of the shuttle-vector construct. We could demonstrate that the neomycin-selectable marker module also works for mesophilic selection in *E. coli* with kanamycin (Pers. comm. Dr. Sebastian Beblawy). Thus, it would be possible to select for *M. thermautotrophicus* ΔH and *E. coli* with the same selectable marker module. Thus, the chloramphenicol resistance as selectable marker module for *E. coli* would be redundant and might be removed from the shuttle vector constructs. A similar approach was followed in the pMTL80000 system with the chloramphenicol module as selectable marker in *E. coli* and *Clostridium* spp. (Heap *et al.* 2009). To implement these changes, the modularity of the pMVS design with its five modules can be used. If the chloramphenicol selectable marker would be exchanged to a spacer of ~0.1-kb non-sense DNA with the modular restriction enzyme recognition sites *Pme*I and *Fse*I, the shuttle-vector construct size would be decreased by 0.7 kb (**Figure 22**).

An exchange of the replicon module for *M. thermautotrophicus* ΔH to a spacer with deletion of the *Not*I restriction enzyme recognition site, and therefore the adaption of the pMVS design to suicide-vector constructs for genomic DNA would provide a more versatile spectrum of tools with the pMVS design. The adaption additionally requires homologous flanking regions in the pMVS vector constructs to enable homologous recombination events with genomic DNA. By

the use of the proof-of-principle suicide-vector construct with the unique *Sal*I and *Not*I restriction enzyme recognition sites, flanking the homologous regions (**Figure 23**), two further modules can be implemented in the pMVS design (**Figure 31**). With 132 loci for *Sal*I and 4 loci for *Not*I the restriction enzyme recognition sites are not very frequent in the genomic DNA of *M. thermautotrophicus* ΔH. *M. thermautotrophicus* ΔH contains 1855 open reading frames (Smith *et al.* 1997). With 136 restriction enzyme recognition sites, the uniqueness would affect less than 10% of all deletion approaches with suicide vector constructs. If the flanking homologous regions can be shorter than one kb, as it is known for genetic systems in yeast with 50-100 bp (Hua *et al.* 1997, Verbeke *et al.* 2013), the prevalence of the restriction enzyme recognition sites would be even less likely to affect the cloning approach using the modular restriction enzyme recognition sites.

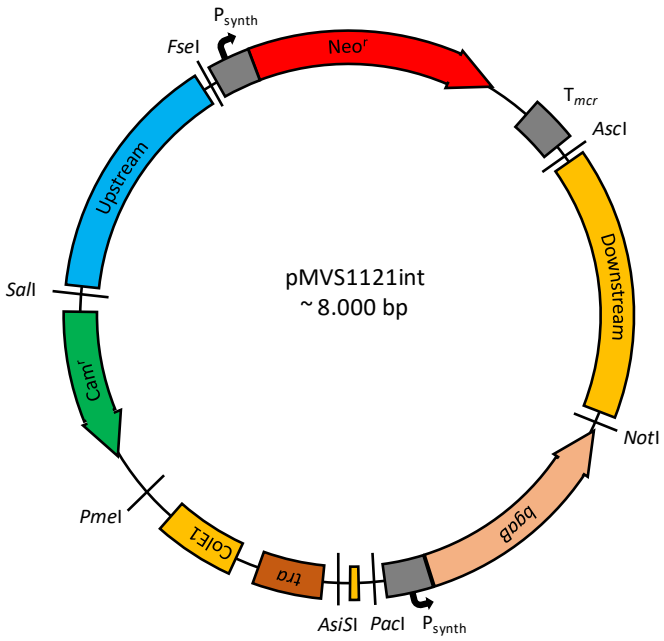

Figure 31. Vector map of a putative integration vector construct following the pMVS design (**pMVS1121int**) with modular restriction enzyme recognition sites in brackets. The selectable marker modules for *M. thermautotrophicus* ΔH (**Neo**^{r}) [***Asc*I**, ***Fse*I**] and *E. coli* (**Cam**^{r}) [***Sal*I**, ***Pme*I**], the *E. coli* replicon with **ColE1** and ***tra*** [***Pme*I**, ***Asi*SI**], as well as the application module remain the same as in pMVS1111:P$_{synth}$-*bga* [***Pac*I**, ***Not*I**] (**Figure 22**). The *M. thermautotrophicus* ΔH replicon will be exchanged to a non-sense DNA spacer of 100 bp [***Asi*SI**, ***Pac*I**]. Additionally, two more modules will be implemented, the **upstream**- [***Fse*I**, ***Sal*I**] and **downstream** [***Not*I**, ***Asc*I**] homologous flanking regions for gene deletion *via* homologous recombination.

Before implementing these adaptions to the pMVS design towards suicide-vector constructs, we attempted a proof-of-principle whether genome integration into *M. thermautotrophicus* ΔH genomic DNA *via* homologous recombination was indeed possible. Therefore, we generated a construct with 1-kb homologous flanking regions of the Mth60-fimbriae operons (*mth*58-*mth*61/MTH_RS00275-290) (Sarbu 2013), because the deletion of the Mth60-fimbriae operons was not likely to cause a lethal deletion in *M. thermautotrophicus* ΔH. Additionally, the *E. coli*

vector backbone (module 1 + 2) of the pMVS design and two selectable markers between the flanking regions were implemented (**Figure 23**). With the standard conjugation protocol for DNA transfer, we successfully integrated the selectable markers *fdh*$_{Z\text{-}245}$ and Neo^{r} site-specifically into the genome of *M. thermautotrophicus* ΔH. However, the site-specific integration did not necessarily result in double homologous recombination events, which would substitute the gene of interest with the selectable marker, and therefore lead to a deletion of the gene of interest. Instead, we also observed site-specific single homologous recombination events that resulted in the integration of the entire suicide-vector construct including *E. coli* backbone and duplication of the homologous flanking regions into the genomic DNA. With single homologous recombination, the wild-type gene of interest stays intact. In conjugational DNA transfer, DNA is transferred as single strand linearized DNA. Linear DNA can only integrate *via* double homologous recombination into the host genomic DNA apart from less apparent integration mechanisms, such as non-homologous-end-joining (NHEJ) or micro-homology-mediated-end-joining (MMEJ) (Smith 1988, Nayak and Metcalf 2017, Perez-Arnaiz *et al.* 2020). We knew, however, that the linearized transferred vector DNA needs to be re-circularized in *M. thermautotrophicus* ΔH otherwise the shuttle vector constructs could not be replicated. Therefore, the occurrence of single homologous recombination events was not surprising. A comparison to a second method of DNA transfer with circular DNA, such as electroporation could provide solid data whether double homologous recombination occurs more frequently with conjugation (linear DNA) as with electroporation (circular or linear DNA).

While we were able to suppress the wild-type PCR signal with neomycin selection (**Figure 27**), we found the wild-type being present in all samples of individual clonal populations with formate prototrophy for at least 8 transfers (2x individual clonal population from plate) (**Figure 25**). Since neomycin is a bactericidal antibiotic substance, the remaining wild-type *M. thermautotrophicus* ΔH was lysed and the wild-type signal disappeared. The prototrophic marker which enables for formate usage, however, does not have toxic effects on wild-type *M. thermautotrophicus* ΔH. Thus, there is the possibility of a single homologous recombined population to switch to double homologous recombination and wild-type in between the same clonal population, while the main-share remains single homologously recombined. A possible explanation for the remaining wild-type PCR signal could be heterozygosity of the diploid characteristic of *M. thermautotrophicus* ΔH. With the neomycin selective pressure, it is beneficial for *M. thermautotrophicus* ΔH to inherit the neomycin resistance gene to both chromosomes which favors the generation of homozygous chromosomes. If the *fdh*$_{Z\text{-}245}$ activity is limited by availability of cofactor F_{420} (Crable *et al.* 2011), it could be beneficial to keep only one *fdh*$_{Z\text{-}245}$ with a constitutive promoter and the second chromosome as wild-type. It is known that *M. thermautotrophicus* ΔH is diploid at all times (Majernik *et al.* 2005). Therefore, the

heterozygous chromosomes could be either transferred to daughter cells together, which would not change the state of homologous recombination, or individually, which would require a duplication before transfer. One possibility to find double homologous recombined *M. thermautotrophicus* ΔH would be a large screening approach with individual clonal populations directly after conjugation.

Nanopore sequencing analysis also revealed that both individual clonal populations (Neo^r and *fdh*$_{Z\text{-}245}$) consisted of a mixed genotype. However, with these Nanopore sequencing reads it was not possible to directly distinguish between wild-type and single homologous recombination events, because the read-length was not long enough to range from outside to outside of the homologous flanking regions on genomic DNA of *M. thermautotrophicus* ΔH. The same applies for the analysis of double- or single homologous recombination events. However, by comparison of the read-count of wild-type, *fdh*$_{Z\text{-}245}$ and Neo^r at specific positions of the Mth60-fimbriae operons, that were extrapolated to 200,000 total reads, we observed, that *fdh*$_{Z\text{-}245}$ and wild-type shared roughly the same count, while the Neo^r read count was decreased. Additionally, the read-count for a specific position in the downstream homologous flank *fdh*$_{Z\text{-}245}$ was exceeding wild-type exactly twice (**Figure 26, Supplement S4**), which derived from duplication of the flanking regions during the single homologous recombination event. The read-count of Neo^r only exceeded the wild-type read-counts by 1.5 times (**Figure 28, Supplement S4**). As a third specific position we compared the reads of the Cam^r in the *E. coli* backbone in *fdh*$_{Z\text{-}245}$ and Neo^r and found a largely higher count in *fdh*$_{Z\text{-}245}$. Taking these three comparisons into account, we reached the conclusion that *fdh*$_{Z\text{-}245}$ consisted of mostly single homologous recombined chromosomes, while Neo^r had to inhabit double homologous recombined chromosomes in the sample but still contained low amount of single homologous recombined chromosomes (**Figure 28**). This went along with the PCR results of Neo^r for which no wild-type and single homologous recombined genomic DNA was detected in L, while in M and S the Mth60-fimbriae operons signal was still present (**Figure 27C**). This could be due to the smaller fragment size from double homologous recombined genomic DNA, which is favored in the PCR reaction over the larger fragment sizes from wild-type and single homologous recombined genomic DNA. With the PCR signals and the Nanopore sequencing results, it was very likely that the double homologous recombined *M. thermautotrophicus* ΔH strain was present in the sample. After one additional isolation step on solidified media plates, we were able to enrich a double homologous recombined clonal population that proved the previous results (**Figure 27D**). With this clonal population, it is possible to analyze the absence of the Mth60-fimbriae operons by probing the protein production in future experiments. Specific polyclonal antibodies against Mth58, Mth59, Mth60, and Mth61, in addition to antibodies against fimbriae extractions, are available. With these specific antibodies, protein crude extract

of wild-type *M. thermautotrophicus* ΔH and *M. thermautotrophicus* ΔH Δ*Mth58-61*:Neo^r can be analyzed towards the presence or absence of the corresponding proteins of the Mth60-fimbriae operons and the specific genes *via* western blot and fluorescence microscopy. This analysis can further confirm, that the deletion of the Mth60-fimbriae operons is not lethal to *M. thermautotrophicus* ΔH, and the strains can be phenotypically analyzed in further experiments (**See VI.2.1.**).

With a system for genome integration and stable replication in *M. thermautotrophicus* ΔH, we are able to perform homologous or heterologous (over)-expression of genes in *M. thermautotrophicus* ΔH. Therefore, it is beneficial to possess a range of constitutive promoters to initially predict the level of expression. With the thermostable β-galactosidase (*bgaB)* as a reporter gene*,* we tested a set of four distinct promoters ($P_{mrt(M.t.)}$, P_{synth}, $P_{synth(BRE)}$, and P_{hmtB}). While also a thermostable variant of a native β-glucuronidase (*gusB*) was proven to be a functional reporter gene in *Sulfolobus solfataricus* Δ*gusB* Δ*lacZ* (Honarbakhsh *et al.* 2012), we chose the codon-optimized *bgaB* for *M. thermautotrophicus* ΔH as genetic cargo (Jensen *et al.* 2017). One reason is the availability of an oxygen-independent screening method *via* S-Gal with β-galactosidase (Heuermann and Cosgrove 2001, Jensen *et al.* 2017), which is not possible with β-glucuronidase under anaerobic conditions. However, X-Gluc was already demonstrated to result in color change through β-glucuronidase activity for qualitative analysis in *M. acetivorans* replica patching of clonal populations on oxidized plates (Pritchett *et al.* 2004). Additionally, qualitative analysis of mesophilic β-galactosidase functionality was shown with *M. maripaludis via* spraying of X-Gal solution on oxidized plates, which resulted in a color change of clonal populations (Lie and Leigh 2007). To avoid unnecessary oxygen exposure of genetically modified *M. thermautotrophicus* ΔH strains for qualitative initial screening, we proved conversion of S-Gal under anaerobic conditions with a *bgaB*-containing construct with P_{synth} as promoter (Heuermann and Cosgrove 2001) (**Figure 30B**).

To further compare the level of expression with the different promoters, we established an 2-Nitrophenyl β-D-galactopyranoside (ONPG) assay for quantitative analysis in *M. thermautotrophicus* ΔH based on Jensen *et al.* (2017). The promoter region upstream of the *mrt* gene of *M. thermautotrophicus* ΔH ($P_{mrt(M.t.)}$) did not lead to production of a functional BgaB. This is consistent with transcription assays with the *mrt* gene from Darcy *et al.* (1999), where no *in-vitro*-transcription activity with $P_{mrt(M.t.)}$ could be observed. We found evidence in the peer-reviewed literature that this might be because of regulatory effects based on the availability of hydrogen, which might in turn influence the gene expression from the $P_{mrt(M.t.)}$ promoter (Shinzato *et al.* 2008). In contrast, with the promoters P_{synth}, $P_{synth(BRE)}$, and P_{hmtB}, which are all based on the promoter region upstream of the *hmtB* gene of *M. thermautotrophicus* ΔH, we

found significant differences in the β-galactosidase enzyme activity when compared to pMVS-V1 without the *bgaB* gene (**Figure 30C**). The BRE sequence upstream of the P_{synth} sequence, which we had implemented in $P_{synth(BRE)}$, influenced the promoter strength significantly. Similar observations were made with archaeal promoters in *S. solfataricus* and *Haloferax volcanii*, respectively, where promoter strength was influenced by the presence or absence of a BRE sequence (Gregor and Pfeifer 2005, Ao *et al.* 2013). Fine tuning promoter studies with *M. acetivorans* found that especially the positions 4 and 5 of the BRE sequence were strongly influencing the transcription initiation rates (Karim *et al.* 2018). Nevertheless, the enzyme activity with the native P_{hmtB} was enhanced significantly when compared to both P_{synth} and $P_{synth(BRE)}$ (**Figure 30C**). This is potentially due to modifications in the transcription-initiation region in the promoter sequence, which was also shown to influence the strength of gene expression in *Sulfolobus acidocaldarius* and *S. solfataricus* (Peng *et al.* 2009, Ao *et al.* 2013). Further *in-vivo* promoter studies will elucidate more details on the promoter structures of *M. thermautotrophicus* ΔH. For this, the thermostable β-galactosidase as a reporter provides an adequate basis. These results are a cornerstone for heterologous and homologous (over)-expression of genes in *M. thermautotrophicus* ΔH to study many hypotheses from four decades of research on a genetic level.

For further studies of using genetically modified *M. thermautotrophicus* ΔH in bioreactors and experiments regarding plasmid curing systems, we found high segregational stability with shuttle-vector constructs in *M. thermautotrophicus* ΔH for more than 20 generations without selective pressure of neomycin. This stability is favorable during bioreactor operations due to lowering the cost for antibiotic substances. However, for plasmid curing we need to develop further techniques such as negative selection *via* the *hpt* gene complementation (Nayak and Metcalf 2017).

We believe that the most important parameters for the successful implementation of genetic tools for *M. thermautotrophicus* ΔH, when compared to previous attempts during the last four decades, were: 1) the adaptations to the conjugation protocol, specifically the applied temperature, media, and headspace gas conditions during the spot-mating procedure, in combination with the selective-enrichment step with limited gas supply that facilitated the selection for genetically modified cells over spontaneous-resistant cells; 2) the utilization of a constitutive native promoter sequence, which was demonstrated to be functional *in-vitro* and in other thermophilic archaea, because the classical $P_{mcrB(M.v.)}$ promoter turned out to be inactive in *M. thermautotrophicus* ΔH; and 3) the construction of the shuttle vector with restriction/ligation-independent cloning to fuse the pME2001 replicon with the other modules

precisely at the IF5 sequence, to not interrupt any open reading frame or potential sequence of the origin of replication.

VI. Outlook

1. Expanding the tool-box for genetic engineering of *M. thermautotrophicus* ΔH

We established a basic system for genetic modification of *M. thermautotrophicus* ΔH with a replicating shuttle-vector system (pMVS) and suicide-vector constructs for integration in genomic DNA. On this basis, further improvements will be made to expand the genetic engineering tool-box and also the module range within the pMVS design. One first step will be the adoption of additional selectable markers for positive- and negative selection. For positive selection, a Hmg-CoA reductase conferring simvastatin resistance will be functionalized. We already fused a native Hmg-CoA reductase gene of a spontaneous simvastatin resistant mutant of *M. thermautotrophicus* ΔH, which inhabits three point-mutations that could have led to an enhanced binding capacity towards simvastatin (**Supplement S2.2.**). Similar results were reported with mutations in the Hmg-CoA reductase of *T. kodakarensis* leading to enhanced resistance towards simvastatin (Hileman and Santangelo 2012). Besides the approach with the optimized native Hmg-CoA reductase gene, a *T. kodakarensis* hmg-CoA reductase gene is already present in suicide-vector constructs and can be adapted with functional promoters and *E. coli* backbone for mobilization. Together with the constitutive P_{hmtB} promoter and adjusted simvastatin concentrations in the recovery and the enrichment cultures on solidified media plates or liquid medium, it could serve as a second selectable marker with potentially better efficiencies due to lower frequencies in spontaneous resistant mutant generation of *M. thermautotrophicus* ΔH (**Figure 15A**) than with neomycin (**Figure 15B**). The same procedure could be applied for the puromycin acetyl transferase gene (*pac*). Since we are able to cultivate *M. thermautotrophicus* ΔH under mesophilic conditions, the codon-optimized mesophilic *pac* could be fused and tested with three promoter strengths of P_{synth}, $P_{synth(BRE)}$, and P_{hmtB}. After successful application of the resistance with mesophilic conditions, the protein stability with thermophilic conditions could be adapted throughout several transfers as it was shown for the generation of a thermostable kanamycin resistance gene (Hoseki *et al.* 1999). An additional approach could be splitting of the $fdh_{Z\text{-}245}$ operon into two parts (*fdhC* and *fdhA*+*B*). With a genome integration of *fdhA*+*B* at the residual native site in *M. thermautotrophicus* ΔH compared to *M. thermautotrophicus* Z-245 (Nölling and Reeve 1997), we could amend *M. thermautotrophicus* ΔH to formate utilization with only the small *fdhC* subunit, and therefore reduce the size of the selectable marker $fdh_{Z\text{-}245}$ tremendously. With these potential four selectable markers for positive selection, it will be possible to generate multiple deletion mutants of *M. thermautotrophicus* ΔH and its complementations.

However, the expression of resistance genes always adds energetic burden to the microbe, and therefore changes the energetic parameters for the analysis of deletion mutants compared to the wild-type strain. Therefore, we are also looking into the possibility to generate marker-

less deletion mutants. This could be accomplished by the *hpt* and *upt* deletion and complementation mentioned above. We confirmed that the corresponding toxic base analogs are inhibiting *M. thermautotrophicus* ΔH (**Figure 16A, B**). When these deletion mutants of *M. thermautotrophicus* ΔH are present, we are enabled to use the *upt* or *hpt* gene on shuttle vector constructs for plasmid curing or for counterselection in genome integration to select for double homologous recombination events. Plasmid curing is especially important when we look into more sophisticated and even more efficient methods for generation of deletion mutants such as with CRISPR-Cas9. A thermostable Cas9 variant was proven to be active after heterologous expression in thermophilic microbes (Mougiakos *et al.* 2017). Thus, we could implement the *thermoCas9* gene with repair template (homologous flanking regions), and guide RNA to further enhance the efficiency of marker-less gene deletion. We already generated constructs for *mth60* gene deletions with the *thermoCas9* (**Supplement S6**). An exchange of the *E. coli* vector backbone from pUC to the suicide vector backbone (**See III.4.2**) enables the vector to be mobilizable, and could be used to investigate the deletion efficiencies of this construct in comparison to a suicide vector without the *thermoCas9* to proof the Cas9 functionality. Additionally, a vector construct with only *thermoCas9* and guide RNA without repair template should result in no positive individual clonal populations after conjugation as a control experiment. With these techniques for marker-less deletion mutants, we would be able to implement even more selectable markers for positive selection using auxotrophic markers. Therefore, we could delete *pyrF* (unique compared to *pyrE* in *M. thermautotrophicus* ΔH), which leads to uracil auxotrophy (Basen *et al.* 2018), and complement the auxotrophy with *pyrF* on the shuttle-vector constructs *M. thermautotrophicus* ΔH. Besides auxotrophy towards nucleobases, also amino acid auxotrophies are considered, such as deletion of (parts of-) the tryptophan operon (Meile *et al.* 1991, Xie and Reeve 2005).

Conjugation is our established method for DNA transfer, so far. Since natural competence for circular DNA is apparently not occurring (**Figure 20A**), it would be possible to test further DNA-transfer methods for *M. thermautotrophicus* ΔH, which could result in higher DNA-transfer efficiencies such as electroporation or sonoporation (Kolek *et al.* 2016). In electroporation, an electric shock causes pore formation in the cell-wall of microbes and enables DNA transfer into the microbe (Fiedler and Wirth 1988). In sonoporation, the same result is generated through ultra-sonification. While we do not have an established protocol for sonoporation, for electroporation the Environmental Biotechnology group has a lot of experience with *Clostridium* spp. that share similarities in cell-wall composition with *M. thermautotrophicus* ΔH (pseudomurein). We tested electroporation with *M. thermautotrophicus* ΔH (**Supplement S1.2.**), and confirmed that cells are viable after the electroporation treatment. However, these tests were performed with vector constructs that were not successfully transferred, replicated,

or integrated with the established conjugation protocol either. Therefore, electroporation has to be investigated with vector constructs that are confirmed to be functional.

The conjugation protocol for DNA transfer together with suicide vector constructs enable us to generate gene deletions in *M. thermautotrophicus* ΔH. However, the generation of double homologous recombined deletion mutants was accompanied by a large screening effort due to single homologous integration events that did not result in gene deletion but only in addition of the selectable marker and the *E. coli* vector backbone (**Figure 25-28**). As a fast applicable technique until marker-less mutagenesis or CRISPR techniques are established, we could implement the functional β-galactosidase into the *E. coli* vector backbone of suicide-vector constructs (**Figure 31**). Qualitative screening of individual clonal populations with a rapid ONPG testing would allow us to discard single homologous recombined clonal populations without further PCR testing effort, and therefore reduce the workload. With optimized patching of clonal population on X-gal in an oxidized state or generating a color change of clonal populations with S-gal directly on the plate, which would result in blue- or black color change (**Figure 30B**, **Supplement S7**), respectively, could reduce the screening workload even more.

With the aforementioned methods and techniques, we would facilitate and optimize genetic engineering of *M. thermautotrophicus* ΔH. A major reason to perform genetic engineering, however, is to test the genetic cargo for heterologous or homologous (over)-expression in *M. thermautotrophicus* ΔH. Since expression of genetic cargo could have toxic effects to the host microbe, a constitutive promoter without regulation could result in low expression or lower the viability. Thus, inducible promoter systems are of utmost importance for heterologous gene expression systems. Furthermore, inducible promoters facilitate the comparison of the wild-type microbe to genetically modified strains.

In a first approach, the established tetracycline inducible promoter system from *M. acetivorans* was amended for use in *M. thermautotrophicus* ΔH (Berens and Hillen 2004, Guss *et al.* 2008). Tetracycline is not toxic to *M. thermautotrophicus* ΔH in low concentrations (Hilpert *et al.* 1981). However, the tetracycline stability needs to be tested with elevated temperatures for stable activation. Moreover, different hydrogen concentrations change the expression levels of mRNA transcripts (Kato *et al.* 2008). Therefore, hydrogen induced promoter systems must be present in *M. thermautotrophicus* ΔH. With the amendment of growth on formate the influence of higher hydrogen concentrations on *M. thermautotrophicus* ΔH can be tested *via* quantitative real-time PCR. Afterwards, putative promoter regions of upregulated genes could be tested with the β-galactosidase reporter gene in the established ONPG assay. Further targets for inducible promoters could be temperature induced promoters (Liu *et al.* 2019), or the tryptophan operon regulation system of *M. thermautotrophicus* ΔH (Xie and Reeve 2005).

Inducible promoter systems allow initiation of expression in a targeted fashion. After this step, when protein biosynthesis occurs, we can switch the analysis from genomics and transcriptomics to proteomics and metabolomics techniques. In this field it is important to gather methods for protein purification, *in-vitro* analyses, or pull-down experiments for complex analysis. Common affinity tag systems can be tested for protein purification and pull-down experiments, such as histidine-tag, strep-tag, or maltose-binding protein (mbp)-tag. Additionally, epitope tag systems for western blotting or immunofluorescence analysis such as myc-tag or spot-tag can be considered (Young *et al.* 2012). Possible targets are the subunits of Mth60-fimbriae operons for pull-down experiments or western blots as described below.
These genetic tools enable us to modify and amend the metabolism of *M. thermautotrophicus* ΔH not only on the substrate, but also on the product side. The possibility to change the product spectrum of hydrogenotrophic methanogenic archaea has been demonstrated already for *M. maripaludis* with a genetic modification that resulted in geraniol production (Lyu *et al.* 2016). Our genetic tools for heterologous gene expression enable us now to broaden the product spectrum of *M. thermautotrophicus* ΔH, and to utilize this industrially relevant and robust microbe for power-to-chemicals (power-to-x) applications.

2. Broaden the basic knowledge of adherence mechanisms and energy metabolism of *M. thermautotrophicus* ΔH

2.1. Deletion of Mth60-fimbriae operons potentially leads to loss of adherence ability

The genetic tools described in this study enable us to gather more specific insights into the lifestyle of the *M. thermautotrophicus* ΔH. The operon deletion of the Mth60-fimbriae genes (*mth58-61*/MTH_RS00275-290) provides the possibility to elucidate the loss of fimbriae, and therefore a potential loss of adherence ability. On the basis of Thoma *et al.* (2008) and Sarbu (2013), it is possible to analyze the differences in the wild-type *M. thermautotrophicus* ΔH phenotype compared to the deletion mutant. Since attachment of wild-type *M. thermautotrophicus* ΔH on several surfaces, such as glass, metal, wood, or chitin, was reported, cultivation of *M. thermautotrophicus* ΔH in the presence of these substances can be used for this purpose (Thoma *et al.* 2008). Wild-type and mutant *M. thermautotrophicus* ΔH can be analyzed *via* light microscopy, electron microscopy, and in western blots with the available antibodies.

Fimbriae deletion mutants that lack the ability of adherence to surfaces could also be deficient in biofilm formation. This could facilitate cultivation of *M. thermautotrophicus* ΔH in bioreactor

systems, and therefore enhance methane production efficiency or prevent the system from clogging through biofilm production.

2.2. ATP availability could be enhanced with an optimized adenine deiminase pathway (ADI)

Arginine serves as an energy conservation substance for microbes *via* the arginine deiminase pathway (ADI) (**Figure 32**). Since *M. thermautotrophicus* ΔH lacks genes for the entire pathway, the genome must be complemented with heterologous genes. Two additional genes for structural enzymes and an ornithine-arginine antiporter need to be heterologously expressed in the microbe. If the constitutively expressed genes complete the ADI, arginine should be metabolized to ornithine *via* citrulline, generating one ATP for each reaction. Thus, there should be a significantly higher level of ornithine in the cells after supplementing the media with arginine than in cells grown in arginine supplemented media without the genetic manipulation. This would be a first proof-of-principle. In addition, it could be helpful to optimize the microbe towards energy conservation. Due to the production of one ATP trough metabolizing arginine, a supplementation of the media with arginine could lead to a reduction of the Na^+ gradient that is consumed by ATP synthases. It was already demonstrated that feeding arginine has an impact on energy levels in *Clostridium autoethanogenum* (Valgepea *et al.* 2017).

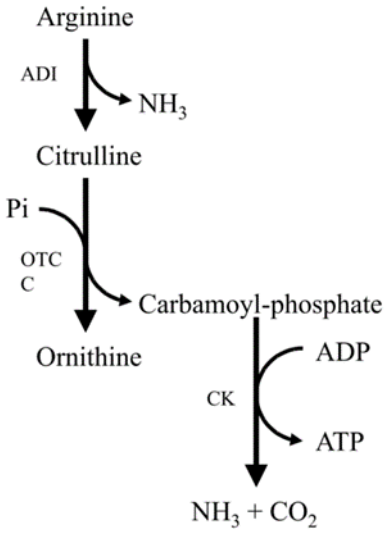

Figure 32. Scheme of the arginine deiminase pathway (ADI).

VII. Supplemental information

S1. DNA-transfer protocols with various suicide-vector constructs did not result in successful genetic modification of *M. thermautotrophicus* ΔH

Before we developed the successful DNA-transfer protocol using interdomain conjugation of *E. coli* S17-1 and *M. thermautotrophicus* ΔH, several methods for DNA-transfer were tested with various potential suicide-vector constructs for *M. thermautotrophicus* ΔH. In the following sections, the applied DNA-transfer protocols for natural DNA-uptake and electroporation are explained in more detail.

S1.1. Natural competence

We tested two protocols for genetic modification of *M. thermautotrophicus* ΔH based on natural DNA-uptake.

a) DNA-uptake during overnight cultivation

Experimental design described in main text (**See IV.2.2.**), adjusted from the protocol stated in Basen *et al.* (2018). Furthermore, we attempted the addition of 100 ng/µL genomic DNA of *M. thermautotrophicus* ΔH additionally to suicide-vector DNA to mask heterologous DNA from native *M. thermautotrophicus* ΔH restriction enzymes, which would digest incorrectly methylated heterologous DNA (**See S5**).

b) DNA-transfer with heat-shock ((Susanti *et al.* 2019), modified)

We extracted plasmid DNA of 10 mL NEB non-methylating *E. coli* overnight culture containing the suicide vector of interest with the QIAprep Spin Miniprep kit (Qiagen, Hilden, Germany) according to the manufacturer manual. The resulting DNA concentration in 50 µL elution fraction were ~0.6 µg/µL. 10 µL (6 µg of plasmid DNA) were used in a 50 µL restriction enzyme digestion with the unique cutter *Apa*I located in the *E. coli* vector backbone. After 1 h of digestion and PCR purification with QIAquick PCR Purification Kit (Qiagen, Hilden, Germany), the elution fraction contained ~0.4 µg/µL of predominantly linearized DNA (analyzed *via* agarose gel-electrophoresis).

We prepared 20 mL of a stationary wild-type *M. thermautotrophicus* ΔH overnight culture with an OD_{600} of ~0.3. After cooling the culture to room temperature, 6 mL were stepwise centrifuged anaerobically with 8500 g for 4 min at RT (MySPIN™ 12 Mini Centrifuge, Thermo Scientific Waltham MA, USA). After the stepwise centrifugation, the pelleted wild-type *M. thermautotrophicus* ΔH cells were washed once with 1.5 mL of 10 volume% glycerol solution

(centrifugation parameter as mentioned above). The washed cells were resuspended gently in 0.2 mL of 10 volume% glycerol solution.

After incubating the cell suspension for 1 h on ice, 10 µL corresponding to 4 µg of linearized plasmid DNA were added to the washed cells. Afterwards, samples were incubated on ice for another 30 min followed by a 1 min heat shock at 85°C. To cool down the cells subsequentially, the aliquot was incubated for 10 min on ice. Afterwards, the cells suspension was transferred to 5 mL recovery medium supplemented with 15 µM uracil (in case of selectable marker Hmg-CoA reductase, recovery medium was also supplemented with 30 µM simvastatin) containing 1 bar overpressure of H_2/CO_2. The recovery cultures were incubated at 65°C without shaking for 16 h.

Recovered *M. thermautotrophicus* ΔH cultures were analyzed *via* PCR for site-specific integration of the suicide vector constructs and transferred to selective solidified media plates and selective liquid medium. While most of the constructs showed the correct phenotype (growth with selective pressure) (**see S2**) and positive PCR signals for upstream- or downstream integration in the recovery culture and the first selective transfer (**see S3**), no genetically modified individual clonal population was obtained with this protocol. The tested suicide-vector constructs are given in **Table S1**.

Table S1.Suicide-vector constructs tested with the heat-shock protocol (all contain pUC57 *E. coli* vector backbone)

Target gene	Resistance gene	Promoter
pyrF (MTH_RS00570)	*hmg-CoA reductase* (*T. kodakarensis*)	$P_{mcrB(M.v.)}$
pyrF (MTH_RS00570)	*hmg-CoA reductase* (*T. kodakarensis*)	P_{hmtB}
pyrF (MTH_RS00570)	Neo^r	P_{synth}
mth60 (MTH_RS00285)	*hmg-CoA reductase (M. thermautotrophicus* ΔH)	P_{synth}
mth60 (MTH_RS00285)	fdh_{Z-245} (*M. thermautotrophicus* Z-245)	native fdh_{Z-245} promoter

S1.2. Electroporation

We tested an electroporation protocol inspired by commonly used protocols for Gram-positive bacteria (Molitor *et al.* 2016). Therefore, we extracted plasmid DNA from 10 mL NEB non-methylating *E. coli* overnight culture containing the suicide vector of interest with the QIAprep Spin Miniprep kit (Qiagen, Hilden, Germany) according to the manufacturer manual. The resulting DNA concentration in 50 µL elution fraction were ~0.6 µg/µL. Additionally, we prepared 20 mL of an exponential wild-type *M. thermautotrophicus* ΔH overnight culture with an OD_{600} of ~0.15. This culture was supplemented with ~10 ng/µL pseudomurein endoisopeptidase (PeiP) (**See III.7.**) and incubated for 30 min at 65°C. After cooling the culture to room temperature, 8 mL were stepwise centrifuged anaerobically with 8500 g for 4 min at

RT (MySPIN™ 12 Mini Centrifuge, Thermo Scientific Waltham MA, USA). The supernatant was discarded by pipetting. The resulting pellet was washed with 1.5 mL ice-cold 10 volume% glycerol solution twice and the final pellet was resuspended in 0.2 mL 10 volume% glycerol solution. 5-10 µg of suicide vector DNA was added immediately after resuspending and the cell suspension was incubated on ice for 30 min. Electroporation of 0.2 mL cell suspension was performed in 2-mm gap electroporation cuvettes with program EC3 (3 kV) (GenePulser, Biorad, Hercules (CA), USA), if not stated differently. The electroporated cell suspension was directly transferred to 5 mL liquid mineral medium supplemented with 15 µM uracil or 0.1 weight% yeast extract, depending on the applied suicide vector construct, and incubated at 65°C for ~20 h rotating with 150 rpm.

Recovered *M. thermautotrophicus* ΔH cultures were analyzed *via* PCR for site-specific integration of the suicide vector constructs and transferred to selective solidified media plates and selective liquid medium. While most of the constructs showed the correct phenotype (growth with selective pressure), the analyzed cultures from the third transfer on did not reveal positive PCR signals for integration, anymore, and therefore are considered spontaneous resistant mutants (**See S2**). The tested suicide-vector constructs including modifications to the electroporation protocol are given in **Table S2**.

Table S2. Suicide vector constructs tested with the electroporation protocol (all contain pUC57 *E. coli* vector backbone)

Target gene	Resistance gene	Promoter	Electroporation program	PeiP	Supplements in recovery medium
pyrF (MTH_RS00570)	*hmg-CoA reductase* (*T. k.*)	$P_{mcrB(M.v.)}$	EC3	yes	-
pyrF (MTH_RS00570)	*hmg-CoA reductase* (*T. k.*)	$P_{mcrB(M.v.)}$	EC3	yes	20 µM simvastatin at T_0
pyrF (MTH_RS00570)	*hmg-CoA reductase* (*T. k.*)	P_{hmtB}	EC3	no	30 µM simvastatin at T_0 or T_{8h}
pyrF (MTH_RS00570)	*hmg-CoA reductase* (*T. k.*)	P_{hmtB}	EC3	yes	30 µM simvastatin at T_0 or T_{8h}
pyrF (MTH_RS00570)	Neo^r	$P_{mcrB(M.v.)}$	EC3	yes	-
pyrF (MTH_RS00570)	Neo^r	$P_{mcrB(M.v.)}$	EC3 (2x)	yes	-

pyrF (MTH_RS00570)	Neo^r	$P_{mcrB(M.v.)}$	EC3 (3 M Sorbitol instead of 10% glycerol)	yes	-
hpt (MTH_RS06300)	*pac*	$P_{mcrB(M.v.)}$	EC3	yes	0.3 mg/mL 8-aza-hypoxanthine
hpt (MTH_RS06300)	*pac*	$P_{mcrB(M.v.)}$	EC3	yes	5x elevated concentration of Mg^{2+} and Ca^{2+}
hpt (MTH_RS06300)	*pac*	$P_{mcrB(M.v.)}$	EC3	yes	-

S2. Selective pressure with antibiotic substances leads to generation of spontaneous resistant mutants of *M. thermautotrophicus* ΔH

Within this chapter we show the generation of spontaneous antibiotic resistant mutants of *M. thermautotrophicus* ΔH with the antibiotic substances neomycin, simvastatin, and 5-fluoroorotic-acid (5-FOA). The generated spontaneous resistant mutant strains showed adaption to the antibiotic substance resulting in wild-type-like growth behavior in subsequential transfers with selective pressure. We observed *M. thermautotrophicus* ΔH to grow to high densities (OD_{600}>0.2) also with puromycin or 8-aza-hypoxanthine after several days of incubation (>80 h). This growth behavior, however, could be traced back to instability of the antibiotic substance at elevated temperatures (>60°C) since these *M. thermautotrophicus* ΔH strains did not show signs of adaption to the antibiotic substance when transferred to the same selective pressure conditions.

S2.1. Neomycin

Spontaneous resistance of *M. thermautotrophicus* ΔH towards neomycin was already reported (Šmigáň *et al.* 1997). While the isolated mutant strain in Šmigáň *et al.* (1997) was gathered with 0.1 mg/mL neomycin, we found spontaneous resistant mutants with 0.3 mg/mL neomycin on solidified media plates and liquid mineral medium within incubation periods as depicted in **Figures 14 and 15** (**Table S3**). Uracil was added due to putative uracil auxotrophy accompanied with potential *pyrF* gene deletion regarding the used suicide-vector constructs (Basen *et al.* 2018). However, uracil was not responsible for generation of spontaneous resistant mutants, since they also appeared in experiments without uracil. The analyzed spontaneous resistant mutants derived from electroporation experiments stated in **Table S2** (Neo^r). We isolated three respective neomycin resistant *M. thermautotrophicus* ΔH strains from first selective transfers after recovery, two from solidified media plates with 0.3 mg/mL

neomycin derived from 3 M sorbitol and 10 volume% glycerol in washing step of electroporation, and one from liquid mineral media enrichment with 0.3 mg/mL neomycin. Spontaneous resistant mutants showed wild-type-like growth behavior with 0.3 mg/mL neomycin compared to non-selective conditions in further selective transfers (**Table S3**, **Incubation start and stop).** PCR analysis concerning integration of the neomycin resistance gene in *M. thermautotrophicus* ΔH was performed after seven transfers (2x individual clonal population from selective solidified media plates, 5x liquid selective transfer) (**Table S3**) without any positive signals (**Figure S1**). Illumina sequencing of the three respective strains confirmed the absence of the neomycin resistance gene in the genome of *M. thermautotrophicus* ΔH when aligned to a neomycin resistance gene-containing reference genome (data not shown).

Table S3. Transfer scheme of spontaneous neomycin resistance mutants of *M. thermautotrophicus*

Culture transfer	**Incubation start [date]**	**Incubation stop [date]**	**Neo conc. [mg/ml}**	**Liquid/solid**
Recovery in MS medium + Uracil	5/23/2019	5/24/2019	-	liquid
Sample from selective liquid media	5/25/2019	5/30/2019	0.3	liquid
Sample from selective liquid media T1	5/31/2019	6/2/2019	0.3	liquid
Sample from selective liquid media T2	6/3/2019	6/4/2019	0.3	liquid
Sample from selective liquid media T3	6/4/2019	6/5/2019	0.3	liquid
Sample from selective liquid media T4	6/12/2019	6/16/2019	0.3	solid
Sample from selective liquid media T5 purity plated	6/18/2019	6/22/2019	0.3	solid
Sample from selective liquid media T6	6/24/2019	6/27/2019	0.3	liquid

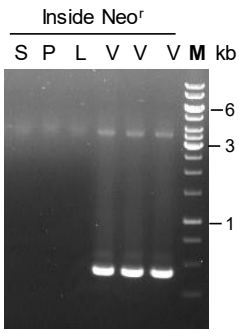

Figure S1. PCR analysis of three spontaneous neomycin resistant *M. thermautotrophicus* ΔH cultures T7 (**Table S3**) with a primer combination specific to a ~0.4 kb fragment inside the neomycin resistance gene (**Inside Neo^r**) that were subsequently prepared for Illumina sequencing. One strain derived from electroporation with a 3 M sorbitol washing step (**S**), the other two from electroporation with a 10 volume% glycerol solution washing step, where one was isolated from liquid selective media (**L**) and the other from solidified media plate (**P**). The suicide vector control was performed in triplicate (**V**) and **M** represents GeneRuler 1 kb DNA Ladder (Thermo Scientific, Waltham MA, USA).

S2.2. Simvastatin

The occurrence of spontaneous resistant mutants towards simvastatin was reported to be an issue with genetic modification of *T. kodakarensis* (Hileman and Santangelo 2012). Analysis of spontaneous simvastatin resistant *T. kodakarensis* mutants revealed that mutations in the locus of the native hmg-CoA reductase gene lead to higher susceptibility towards simvastatin in the respective mutants (Hileman and Santangelo 2012).

a) Generation of spontaneous simvastatin resistant mutants of *M. thermautotrophicus* ΔH

We obtained spontaneous simvastatin resistant *M. thermautotrophicus* ΔH mutants in the DNA-transfer experiments using the suicide-vector construct in line 1 of **Table S1**. After non-selective recovery for 20 h after the heat-shock, 1 mL of the recovery culture was anaerobically centrifuged with 8500 g for 4 min at RT (MySPIN™ 12 Mini Centrifuge, Thermo Scientific Waltham MA, USA), resuspended in 50 µL and added to 10 mL of soft-agar for pour-plating. The experiment was conducted twice, once with 30 µM simvastatin and 15 µM uracil and once with 60 µM simvastatin and 15 µM uracil in the solidified media plates. After 4 days of incubation microbial growth was visible on either of the selective solidified media plates (**Figure S2**). While 30 µM simvastatin resulted in lawn formation (**Figure S2A**), individual clonal population could be obtained from the 60 µM simvastatin plate (**Figure S2B**). Colony PCR of nine individual clonal populations and parts of the lawn did not reveal any results with our common colony PCR method (**Figure S3**) (**See III.3.6.**). Therefore, the nine individual clonal populations were transferred to a 60 µM simvastatin containing rescue plate. After 60 h of incubation growth was obtained and two respective clonal populations were enriched in liquid mineral media for further analysis. Spontaneous resistant mutants showed wild-type-like growth behavior with 60 µM simvastatin compared to non-selective conditions in further transfers.

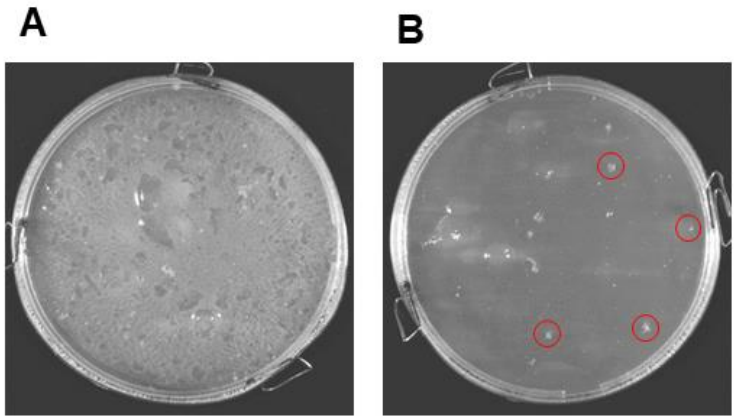

Figure S2. Formation of spontaneous simvastatin resistant *M. thermautotrophicus* ΔH strains cultivated on solidified media plates that contained 30 µM simvastatin/15 µM uracil (**A**) and 60 µM simvastatin/15 µM uracil (**B**). **Red circles** in B show exemplified the presence of individual clonal populations.

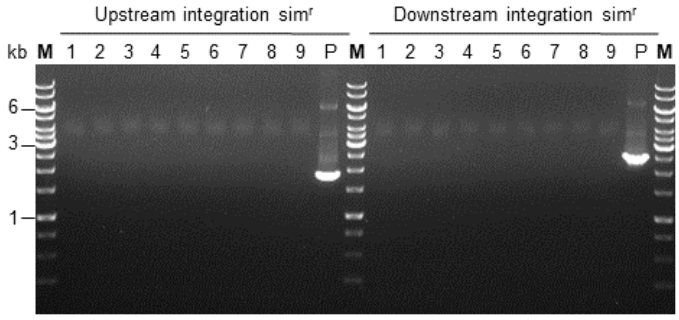

Figure S3. PCR analysis of nine individual clonal populations of spontaneous simvastatin resistant *M. thermautotrophicus* ΔH (**1-9**), re-streaked, and transferred to selective liquid media containing 60 µM simvastatin. Primer combinations for upstream integration with one primer binding in the heterologous resistance gene and the other outside the upstream homologous flanking region (**Upstream integration sim^r**) (~1.8 kb) and downstream integration with one primer binding in the heterologous resistance gene and the other outside the downstream homologous flanking region (**Downstream stream integration sim^r**) (~2.4 kb) were used. **P** represents the plasmid control that consists of subcloned fragments derived from previous experiments (**Figure S8**) and **M** the GeneRuler 1 kb DNA Ladder (Thermo Scientific, Waltham MA, USA).

b) Analysis of native hmg-CoA reductase gene of spontaneous simvastatin resistant *M. thermautotrophicus* ΔH strain

After three selective transfers (2x solidified media plates, 1x liquid medium) of spontaneous resistant *M. thermautotrophicus* ΔH mutants, we analyzed two mutant strains for single-base exchange events in the hmg-CoA reductase gene. Therefore, we PCR amplified (Q5 high-fidelity polymerase (**See III.3.1**.)) and subcloned the hmg-CoA reductase gene, including a second *ORF* within the operonal structure and the putative promoter region into pMiniT 2.0 (**see III.3.2.**). From there, the subcloned fragments were Sanger sequenced in up- and downstream direction. We found two and three single-base exchange events in the fragments,

respectively (**Figure S4, S5, blue box**) that were not present in the wild-type gene (**Figure S6**). The downstream single-base exchange from G to A at position +845 (counted from the 'A' of the start codon) appeared to be the same in both fragments and causes an amino acid exchange from glycine to aspartic acid. There were no single-base exchanges in the promoter regions (**Figure S4, S5, grey box**).

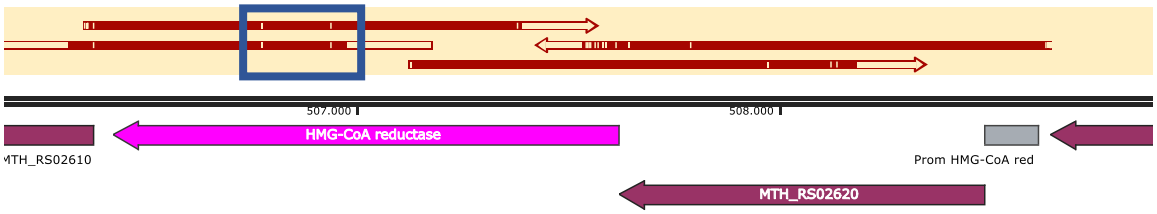

Figure S4. Results of Sanger sequencing of clonal *E. coli* population A and alignment to wild-type *M. thermautotrophicus* ΔH genomic DNA (Smith *et al.* 1997). Red arrows indicate the sequence and its direction. The blue box indicates the region with single-base exchanges (white interruption of red arrow).

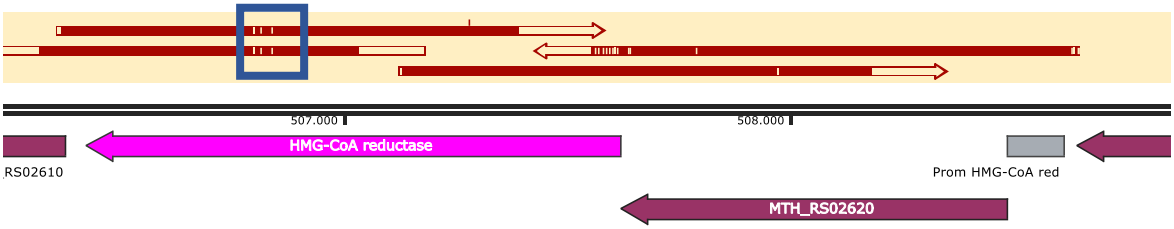

Figure S5. Results of Sanger sequencing of clonal *E. coli* population B and alignment to wild-type *M. thermautotrophicus* ΔH genomic DNA (Smith *et al.* 1997). Red arrows indicate the sequence and its direction. The blue box indicates the region with single-base exchanges (white interruption of red arrow).

The hmg-CoA reductase gene (Sim^r native, optimized) from mutant strain (**Figure S4**) and the wild-type *M. thermautotrophicus* ΔH hmg-CoA reductase gene (Sim^r native) with the native P_{hmtB} promoter were fused with a pUC57-containing suicide-vector construct with *pyrF* as a target gene (**Figure S6, S7**). Since P_{hmtB} was proven to be a functional constitutive promoter in *M. thermautotrophicus* ΔH (**See IV.5.**), exchange of the *E. coli* vector backbone from pUC57 to the mobilizable *E. coli* vector backbone from the pMVS would enable conjugational DNA transfer and could lead to simvastatin resistance in *M. thermautotrophicus* ΔH.

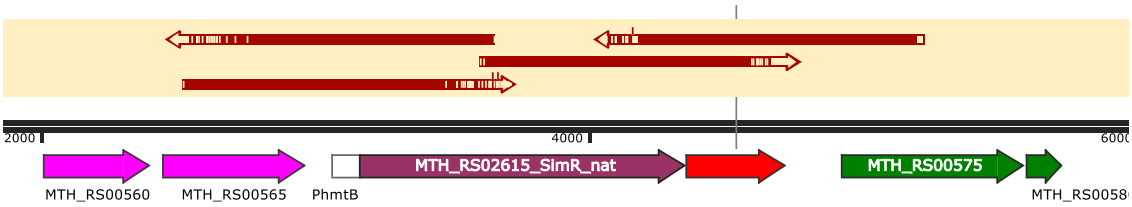

Figure S6. Results of Sanger sequencing of a clonal *E. coli* population containing a suicide-vector construct with the native hmg-CoA reductase gene from *M. thermautotrophicus* ΔH (**dark red**) with promoter P_{hmtB} (**white**) and *pyrF* homologous flanking regions (**green + pink**). And the Terminator $T_{mcr(M.v.)}$ (**red**). Red arrows indicate the sequence and its direction.

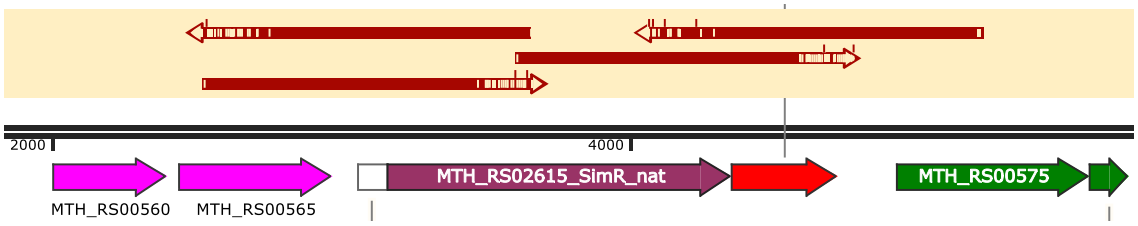

Figure S7. Results of Sanger sequencing of a clonal *E. coli* population containing a suicide-vector construct with the native hmg-CoA reductase gene from *M. thermautotrophicus* ΔH including two single base exchanges (**Figure S4)** (**dark red**) with promoter P_{hmtB} (**white**) and *pyrF* homologous flanking regions (**green + pink**). And the Terminator $T_{mcr(M.v.)}$ (**red**). Red arrows indicate the sequence and its direction.

S2.3. 5-Fluoroorotic-acid (5-FOA)

It was shown that deletion of the orotidine-5'-phosphate decarboxylase (*pyrF*) gene leads to auxotrophy for uracil and resistance to 5-FOA in thermophilic bacteria, such as *Thermoanaerobacter kivui* (Basen *et al.* 2018). Since *M. thermautotrophicus* ΔH has a unique *pyrF* gene, a single gene deletion event could allow for 5-FOA resistance. We tested concentrations of 5-FOA (dissolved in dimethyl-sulfoxide (DMSO)) ranging from 0.1 mg/mL to 1 mg/mL on solidified media plates (N=1) and found complete inhibition of growth for at least 100 h of incubation at 65°C. Wild-type *M. thermautotrophicus* ΔH grew well without 5-FOA and in presence of the highest DMSO concentration used in 1 mg/mL 5-FOA with 0.66 volume% (**Table S4**). However, when the 0.5 mg/mL of 5-FOA was applied to wild-type *M. thermautotrophicus* ΔH on solidified media plates during supplementation with uracil, no growth inhibition was observed (**Table S4**). The same was observed with 5-fluoro-uracil (5-FU) and *M. thermautotrophicus* ΔH, that did not inhibit growth with uracil supplementation, anymore (Teal and Nagle 1986, Nagle *et al.* 1987).

Table S4. Growth inhibition of wild-type *M. thermautotrophicus* ΔH with different 5-FOA concentrations with or without uracil supplementation

Media condition	0.00 mg/ml	0.1 mg/ml	0.25 mg/ml	0.50 mg/ml	0.75 mg/ml	1.00 mg/ml	DMSO control (0.66 volume%)
Mineral media w/o uracil	+++	-	-	-	-	-	+++
Mineral media w/ uracil	+++	n. t.[1]	n. t.[1]	+++	n. t.[1]	n. t.[1]	n. t.[1]

[1]n.t.=not tested

S3. High residual heterologous DNA concentrations lead to false positive PCR signals for genome integration in *M. thermautotrophicus* ΔH

We gathered the first correct signals for integration of suicide vectors into the DNA of *M. thermautotrophicus* ΔH *via* site-specific PCR analysis using the Phire Plant PCR master mix (**See III.5.4**.) with primer combinations with one primer binding inside the resistance gene and one primer binding outside the flanking regions on genomic DNA. The results were achieved with the heat-shock DNA-transfer protocol for *M. thermautotrophicus* (**See S1**). To add another layer of evidence that the positive PCR signals with the correct size were no artefacts and consist of the expected fragment, we performed subcloning in pMiniT 2.0 (**See III.3.2.**) and Sanger sequenced the respective pMiniT 2.0 clonal populations that contained the PCR product. After alignment to sequences of the expected outcome that we prepared *in-silico via* SnapGene, we were sure that the PCR amplification generated the correct DNA fragment that covered the region from inside of the resistance gene to outside of the flanking region (**Figure S8**). This approach was successfully tested with several different constructs (different locus on chromosomal DNA and different resistance gene) (**Table S1**). However, depending on the antibiotic substance either no growth was obtained in selective liquid medium or on solidified media plates (8-aza-hypoxanthin, 6-azauracil) or spontaneous resistant *M. thermautotrophicus* ΔH mutants were observed that did not show the correct PCR signal after two transfers latest, anymore (simvastatin, neomycin). At this stage, we assumed that the antibiotic concentration was incorrect or that the resistance gene/promoter did not work in *M. thermautotrophicus* ΔH in our hands. Additionally, although we got inside resistance to outside flanking regions PCR signals, we never obtained signals for genetic modification with primer combinations that covered the outside to outside from the homologous flanking regions.

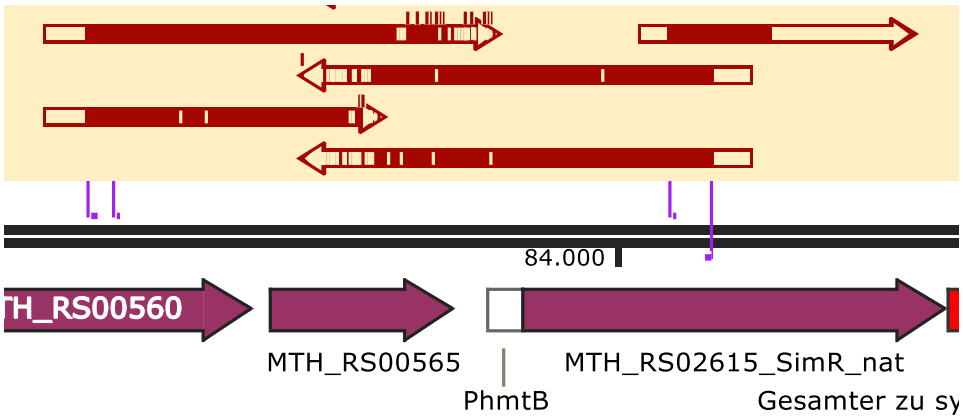

Figure S8. Results of Sanger sequencing as an example for an upstream integration PCR product subcloned in pMiniT 2.0. (hmg-CoA reductase gene with P_{hmtB} and *pyrF* as integration site). While the inner purple line on the left marks the start of the homologous flanking region, the outer left purple line is only present on the genome of *M. thermautotrophicus* ΔH, not in the suicide vector construct. The right purple lines are only present on the suicide-vector construct. Red arrows indicate the sequence and its direction.

On the basis of these distinct results, it became obvious that the PCR signals were likely the result of an artificial PCR product that was not existing on the genomic DNA of *M. thermautotrophicus* ΔH. Therefore, we imitated the PCR conditions but instead of using recovered cells from the transformation procedure we used non-transformed wild-type *M. thermautotrophicus* ΔH cells, inactivated them by boiling, and added linearized suicide vector construct DNA after the inactivation. We obtained the same PCR signal for the inside resistance gene to outside the homologous flanking region with this preparation method as with transformed *M. thermautotrophicus* ΔH cells (**Figure S9**). As controls, we tested boiled cells of wild-type *M. thermautotrophicus* ΔH, suicide vector DNA, and water as negative control (**Figure S9**). Furthermore, with every control, we tested combinations in which one primer (instead of two) or no primer was used in the PCR mix (**Figure S9**). We only obtained a PCR product with the expected fragment size (~1.5 kb) for the combination of boiled *M. thermautotrophicus* ΔH cells with suicide-vector DNA and both primers (**Figure S9C, red box**). This leads to the conclusion, that the mixture of large amount of linearized suicide vector DNA with homologous flanking regions and genomic DNA from boiled *M. thermautotrophicus* ΔH cells allows the amplification of artificial PCR products of the inside resistance gene to outside of the homologous flanking regions (**Figure S9**).

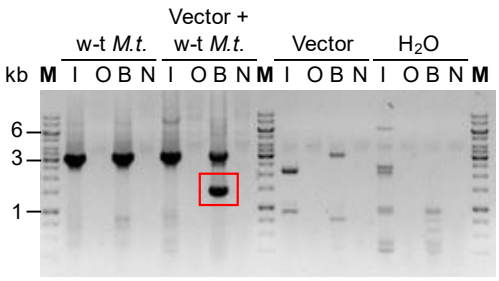

Figure S9. PCR analysis of only boiled *M. thermautotrophicus* ΔH cells (**w-t *M.t.***), boiled *M. thermautotrophicus* ΔH cells together with suicide-vector DNA (**Vector + w-t *M.t.***), only suicide vector DNA (**Vector**), and water as negative control (**H_2O**) with different primer combinations. **I**: only one primer inside the resistance gene **O**: only one primer outside the homologous flanking regions **B**: both primers in combination. **N**: no primer was added. The expected fragment with both primers in combination resulted in ~1.4 kb (**red box**). **M** represents the GeneRuler 1 kb DNA Ladder (Thermo Scientific, Waltham MA, USA).

The finding of artificial PCR products leads to the hypothesis, that homologous flanking regions on suicide-vector constructs could be used to prime the homologous DNA parts of *M. thermautotrophicus* ΔH or *vice versa* (**Figure S10A**). Without any primer involved, the polymerase fills the rest of the single-stranded DNA next to the homologous flanking parts (similar to overlap-extension PCR) (**Figure S10B**). After this occasional event (which probably increases with higher concentrations of genomic DNA), the template for an upstream- and downstream integration PCR product is available. From this step on, the primer outside the homologous flanking region and the primer in the resistance gene could prime for generation of the “correct” false positive integration signal for up- or downstream integration, respectively (**Figure S10C**). With this hypothesis, it is very unlikely that an outside-outside signal can be observed due to two homologous flanking regions that are facing in opposite directions.

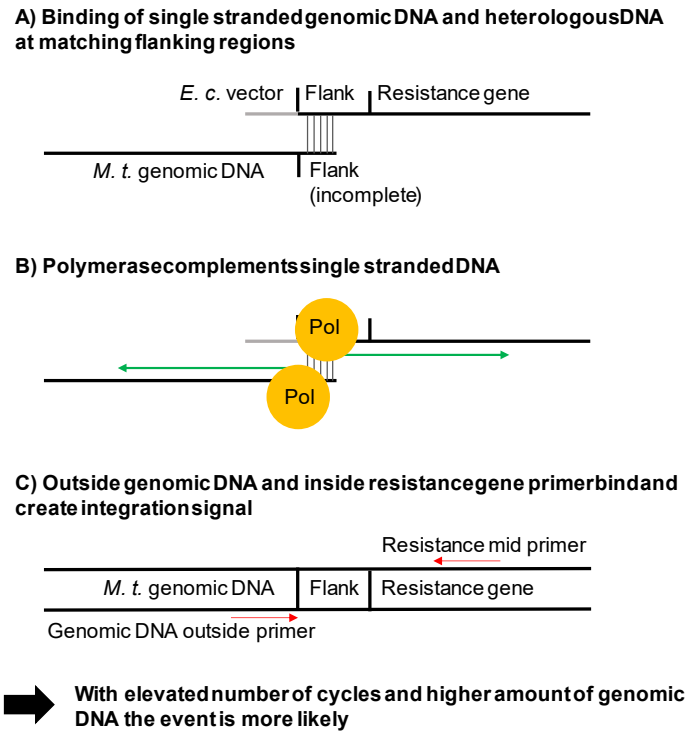

Figure S10. Hypothesis of generation of artificial PCR products as signals for genome integration. **A**) The suicide vector construct (***E. c.* vector**) including a homologous flanking region (**Flank**) acts as a primer to the corresponding region on genomic DNA of *M. thermautotrophicus* ΔH (***M.t.* genomic DNA**). **B**) The polymerase (**Pol**) complements the single stranded DNA in both directions. **C**) A primer combination of inside the resistance gene and outside the homologous flanking regions bind both to the artificial DNA from the "B" construct, which leads to amplification *via* PCR.

S4. Nanopore sequencing reads of wild-type *M. thermautotrophicus* ΔH do not align to $fdh_{Z\text{-}245}$ and Neo^r

Additional to the two genetically modified *M. thermautotrophicus* ΔH strains with the $fdh_{Z\text{-}245}$ and Neo^r (**See IV.4.**), we sequenced wild-type *M. thermautotrophicus* ΔH as a reference genome with MinIon Nanopore sequencing (**See III.5.6.**). We aligned the wild-type *M. thermautotrophicus* ΔH reads to the wild-type *M. thermautotrophicus* ΔH genome sequence (Smith *et al.* 1997) (**Figure S11A**). Furthermore, we aligned the wild-type *M. thermautotrophicus* ΔH reads to *in-silico* prepared *M. thermautotrophicus* ΔH genomes containing double homologous recombination events at the Mth60-fimbriae operon with $fdh_{Z\text{-}245}$ and Neo^r, respectively, to screen for matches (**Figures S11B, C**). No alignments with the heterologous sequences were obtained.

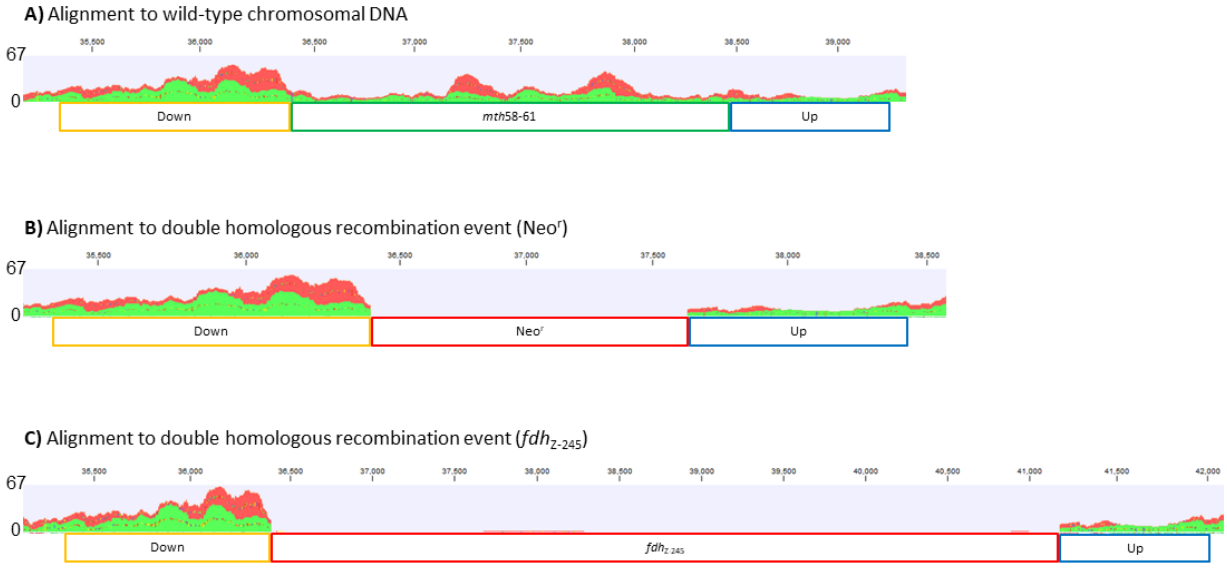

Figure S11. Sequence alignment of wild-type *M. thermautotrophicus* ΔH Nanopore sequencing DNA reads *in-silico* generated reference genomes of *M. thermautotrophicus* ΔH at the locus of the Mth60-fimbriae operon and wild-type genomic DNA (**A**), double homologous recombined genomic DNA with pCF703 (**B**), and double homologous recombined genomic DNA with pCF702. The numbers on the Y-axis represent the number of reads extrapolated to 200,000 DNA total reads. Down (**yellow**) represents the downstream homologous region of the Mth60-fimbriae operon, *mth*58-61 (**green**) the Mth60-fimbriae operon, Neo^r or *fdh*$_{Z-245}$ (**red**) the neomycin resistance gene or the formate dehydrogenase operon of *M. thermautotrophicus* Z-245, respectively, and up (**blue**) the upstream flanking region of the Mth60-fimrbiae operon. The numbers left of the individual figure parts represent the number of DNA-reads gathered from Nanopore sequencing

S5. Treatment with wild-type *M. thermautotrophicus* ΔH crude extract leads to linearization of non-methylated circular plasmid DNA

When we sequenced the wild-type *M. thermautotrophicus* ΔH genome with Pacific Biosciences Sequel I (Menlo Park (CA), USA) whole genome sequencing (PhD thesis Isabella Casini, unpublished), besides the genome sequence, we also obtained the methylation motives of wild-type *M. thermautotrophicus* ΔH genomic DNA (**Table S5**). The prevalent motive ACA-N$_6$-TGG is typical for Type I restriction/methylation systems (Bilcock *et al.* 1999). In *M. thermautotrophicus* ΔH the only annotated restriction/methylation system is a putative Type I restriction/methylation system.

Table S5. Methylation motives, type, and frequencies

Methylation motive	Modification type	N (genome)
ACANNNNNNNTGG	m6A	991
CCANNNNNNNTGT	m6A	991
GBNTGAACRT	modified_base	98
HGGGATGNTY	modified_base	136

Therefore, we tested whether non-methylated suicide-vector DNA that contained three ACA-N_6-TGG loci was digested by the native *M. thermautotrophicus* ΔH restriction enzyme. For that, we prepared *M. thermautotrophicus* ΔH crude extract *via* PeiP digestion (**See III.3.6.**) and treated 50 µL (20 ng/µL) of the aforementioned suicide-vector DNA, as linearized and circular DNA, with the crude extract at 65°C for 1 h with shaking. While linearized suicide-vector DNA did not show any differences before and after the treatment with the crude extract (**Figure S12A, B**), circular (supercoiled) suicide-vector DNA led to linearization with the crude extract (**Figure S12C, red box**).

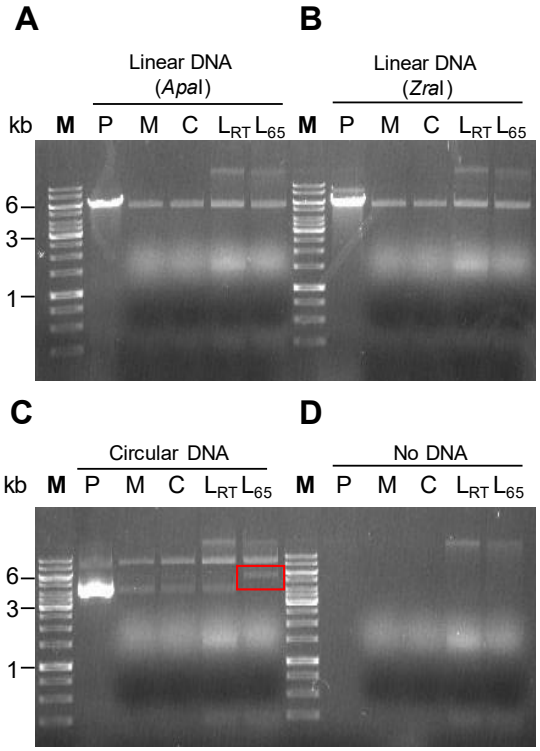

Figure S12. Test for digestion of suicide-vector DNA with *M. thermautotrophicus* ΔH crude extract. Suicide-vector DNA was tested linearized with the unique restriction enzyme *Apa*I (**linear DNA (*Apa*I**)) (**A**) and with the unique restriction enzyme *Zra*I (**linear DNA (*Zra*I**)) (**B**). Further, we tested circular DNA (**C**) and no DNA (**D**), in addition. The differently prepared DNA and the control without DNA was tested untreated (**P**), incubated with blank medium at 65°C (**M**), incubated with non-lysed *M. thermautotrophicus* ΔH cell suspension at 65°C (**C**), incubated with *M. thermautotrophicus* ΔH crude extract at room-temperature (**L_{RT}**), and incubated with *M. thermautotrophicus* ΔH crude extract at 65°C (**L_{65}**), the red box marks the different fragment that we observed in sample C). **M** represents the GeneRuler 1 kb DNA Ladder (Thermo Scientific, Waltham MA, USA).

S6. Preliminary suicide-vector fusion with *thermoCas9* and guideRNA for gene deletion in *M. thermautotrophicus* ΔH

To optimize genome integration and gene deletion in *M. thermautotrophicus* ΔH, we fused suicide vector constructs for transient expression of ThermoCas9 with specific guideRNAs

causing a potential double strand break in *pyrF* (**Figure S13**) and *mth60* (data not shown) based on (Mougiakos *et al.* 2017).

ThermoCas9 was cloned under the control of the native P_{mrt} promoter of *M. thermautotrophicus* ΔH, the guideRNA was placed under the control of the P_{hmtB} promoter, and the native T_{mcr} terminator of *M. thermautotrophicus* ΔH was fused between *thermoCas9* and guide RNA. The PAM (protospacer adjacent motive) was obtained from Mougiakos et al. 2017: CAGCCAAA. We identified exactly one sequence that meets the PAM sequence requirements in the *pyrF* gene of *M. thermautotrophicus* ΔH. The 20 bp upstream of the PAM sequence were used as the protospacer. The rest of the guideRNA scaffold was copied from the plasmid map of the tCAS9 plasmid (Mougiakos *et al.* 2017). The resulting plasmid also contained the *T. kodakarensis* hmg-CoA reductase gene with $P_{mcrB(M.v.)}$ between the *pyrF* repair template homologous regions to potentially confer resistance to simvastatin (**Figure S6**). The same plasmid, but with *mth60* repair template was also fused. Since $P_{mcrB(M.v.)}$ is not initiating gene expression in our hands, these plasmids cannot be functional for simvastatin selection in *M. thermautotrophicus* ΔH. However, with slight optimizations towards the use of Neo^r with P_{synth}, and exchange of the *E. coli* vector backbone to the mobilizable vector backbone, they could be used for further experiments regarding the functioning of ThermoCas9 in *M. thermautotrophicus* ΔH.

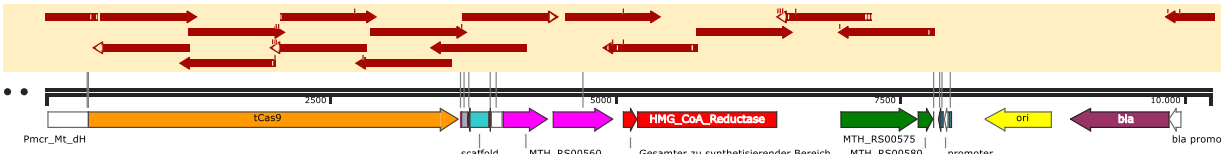

Figure S13. Results of Sanger sequencing of a clonal *E. coli* population containing a suicide vector construct with the native hmg-CoA reductase gene from *M. thermautotrophicus* ΔH (**dark red**) with promoter P_{hmtB} (**white**) and *pyrF* homologous flanking regions (**green + pink**). Furthermore, a *thermoCas9* (**orange**) and the guideRNA scaffold (**blue**) was added. Red arrows indicate the sequence and its direction.

S7. Addition of S-Gal and ammonium-iron-citrate to solidified medium plates results in color change with functional β-galactosidase BgaB in *M. thermautotrophicus* ΔH

We found the thermostable β-galactosidase BgaB to be functional as a reporter in *M. thermautotrophicus* ΔH (**See IV.5.**). For a rapid screening process of individual clonal populations containing the *bgaB* gene, we tested the addition of S-Gal and ammonium-iron-citrate to solidified media plates. Because a color change by the generation of a black chromophore of S-Gal and Iron (Fe^{3+}) only occurs in oxidized conditions, the plates were exposed to air for 5 h after cultivation (Heuermann and Cosgrove 2001). For better

visualization, we left out the redox indicator resazurin to maintain the color-less characteristic of the plates. With this experimental setting, we were able to demonstrate a color change from yellowish to black with pMVS1111:P_{hmtB}-*bgaB*, while this was not possible with pMVS-V1 without the *bgaB* gene (**Figure S14**). The color change, however, was not visible with spread-plating approaches. Potentially this was the case due to the small size of the individual clonal populations compared to the re-streaked biofilm in **Figure S14B**.

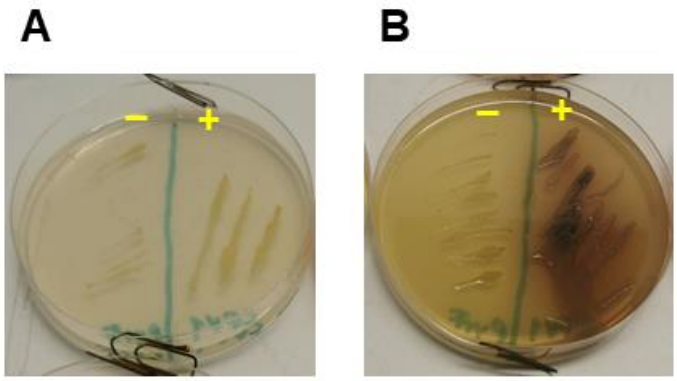

Figure S14. Comparison of growth and color change with *M. thermautotrophicus* ΔH containing pMVS-V1 (**-**) and pMVS1111:P_{hmtB}-*bgaB* (**+**) on solidified media plates without (**A**) or with (**B**) S-Gal and ammonium-iron-citrate. Both solidified media plates are in oxidized condition after 5 h exposure to air and do not contain resazurin as redox indicator.

S8. Plasmid list supplement

Table S6. List of plasmids used in the supplement

Name	Function	Reference
pCF413	pUC_Sim^r(*T.k.*)_$P_{mcrB(M.v.)}$_*pyrF*	this study
pCF415	pUC_Sim^r(*T.k.*)_P_{hmtB}_*pyrF*	this study
pCF601	pUC_CRISP2_Sim^r(*T.k.*)_ $P_{mcrB(M.v.)}$_pyrF	this study
pCF610	pUC_CRISP2_Sim^r(*M.t.*)_P_{hmtB}_*mth60*	this study
pCF611	pUC_CRISP2_$fdh_{Z\text{-}245}$_*mth60*	this study
pCF612	pUC_CRISP2_Neo^r_P_{hmtB}_*mth60*	this study
pSB1	pUC_Neo^r_P_{hmtB}_*pyrF*	this study
pCF407	pUC_Neo^r_ $P_{mcrB(M.v.)}$_*pyrF*	this study
pCF400	pUC_*pac*_ $P_{mcrB(M.v.)}$_*hpt*	this study

VIII. Bibliography

Adam, P. S., G. Borrel, C. Brochier-Armanet and S. Gribaldo (2017). "The growing tree of archaea: New perspectives on their diversity, evolution and ecology." ISME J **11**(11): 2407-2425.

Aldridge, J., S. Carr, K. A. Weber and N. R. Buan (2021). "Anaerobic production of isoprene by engineered *Methanosarcina* species archaea." Appl Environ Microbiol **87**(6).

Allers, T. and M. Mevarech (2005). "Archaeal genetics - the third way." Nat Rev Genet **6**(1): 58-73.

Ao, X., Y. Li, F. Wang, M. Feng, Y. Lin, S. Zhao, Y. Liang and N. Peng (2013). "The *Sulfolobus* initiator element is an important contributor to promoter strength." J Bacteriol **195**(22): 5216-5222.

Argyle, J. L., D. L. Tumbula and J. A. Leigh (1996). "Neomycin resistance as a selectable marker in *Methanococcus maripaludis*." Appl Environ Microbiol **62**(11): 4233-4237.

Balch, W., G. Fox, L. Magrum, C. Woese and R. Wolfe (1979). "Methanogens: Reevaluation of a unique biological group." Microbiol Rev **43**(2): 260-296.

Basen, M., I. Geiger, L. Henke and V. Müller (2018). "A genetic system for the thermophilic acetogenic bacterium *Thermoanaerobacter kivui*." Appl Environ Microbiol **84**(3).

Berens, C. and W. Hillen (2004). Gene regulation by tetracyclines. Genetic engineering: principles and methods, Springer**:** 255-277.

Bilcock, D. T., L. E. Daniels, A. J. Bath and S. E. Halford (1999). "Reactions of type II restriction endonucleases with 8-base pair recognition sites." J Biol Chem **274**(51): 36379-36386.

Boccazzi, P., J. K. Zhang and W. W. Metcalf (2000). "Generation of dominant selectable markers for resistance to pseudomonic acid by cloning and mutagenesis of the *ileS* gene from the archaeon *Methanosarcina barkeri* fusaro." J Bacteriol **182**(9): 2611-2618.

Bokranz, M., A. Klein and L. Meile (1990). "Complete nucleotide sequence of plasmid pME2001 of *Methanobacterium thermoautotrophicum* (Marburg)." Nucleic Acids Res **18**(2): 363.

Burkhardt, M., T. Koschack and G. Busch (2015). "Biocatalytic methanation of hydrogen and carbon dioxide in an anaerobic three-phase system." Bioresour Technol **178**: 330-333.

Costa, K. C., T. J. Lie, M. A. Jacobs and J. A. Leigh (2013). "H_2-independent growth of the hydrogenotrophic methanogen *Methanococcus maripaludis*." MBio **4**(2).

Crable, B. R., C. M. Plugge, M. J. McInerney and A. J. Stams (2011). "Formate formation and formate conversion in biological fuels production." Enzyme Res **2011**: 532536.

Cvitkovitch, D. G., Y.-H. Li and R. P. Ellen (2003). "Quorum sensing and biofilm formation in streptococcal infections." J Clin Investig **112**(11): 1626-1632.

Darcy, T. J., W. Hausner, D. E. Awery, A. M. Edwards, M. Thomm and J. N. Reeve (1999). "*Methanobacterium thermoautotrophicum* RNA polymerase and transcription *in vitro*." J Bacteriol **181**(14): 4424-4429.

Darken, M. A. (1964). "Puromycin inhibition of protein synthesis." Pharmacological Rev **16**: 223-243.

de Macario, E. C., M. Guerrini, C. B. Dugan and A. J. Macario (1996). "Integration of foreign DNA in an intergenic region of the archaeon *Methanosarcina mazei* without effect on transcription of adjacent genes." J Mol Biol **262**(1): 12-20.

Deobald, D., L. Adrian, C. Schone, M. Rother and G. Layer (2018). "Identification of a unique radical SAM methyltransferase required for the sp^3-C-methylation of an arginine residue of methyl-coenzyme M reductase." Sci Rep **8**(1): 7404.

Dodsworth, J. A., L. Li, S. Wei, B. P. Hedlund, J. A. Leigh and P. de Figueiredo (2010). "Interdomain conjugal transfer of DNA from bacteria to archaea." Appl Environ Microbiol **76**(16): 5644-5647.

Doney, S. C., V. J. Fabry, R. A. Feely and J. A. Kleypas (2009). "Ocean acidification: The other CO_2 problem." Ann Rev Mar Sci **1**: 169-192.

Drevland, R. M., Y. Jia, D. R. Palmer and D. E. Graham (2008). "Methanogen homoaconitase catalyzes both hydrolyase reactions in coenzyme B biosynthesis." J Biol Chem **283**(43): 28888-28896.
Ellermann, J., R. Hedderich, R. Böcher and R. K. Thauer (1988). "The final step in methane formation: Investigations with highly purified methyl-CoM reductase (component C) from *Methanobacterium thermoautotrophicum* (strain Marburg)." Eur J Biochem **172**(3): 669-677.
Enkerlin, A. M. (2020). Construction of a modular shuttle vector system and investigation of interdomain conjugation for the genetic manipulation of Methanothermobacter thermautotrophicus ΔH. Bachelor, University of Tuebingen.
Enzmann, F., F. Mayer, M. Rother and D. Holtmann (2018). "Methanogens: Biochemical background and biotechnological applications." AMB Express **8**(1): 1.
Esquivel-Elizondo, S., C. Bağcı, M. Temovska, B. S. Jeon, I. Bessarab, R. B. Williams, D. H. Huson and L. T. Angenent (2021). "The isolate *Caproiciproducens* sp. 7D4C2 produces n-caproate at mildly acidic conditions from hexoses: genome and rBOX comparison with related strains and chain-elongating bacteria." Front Microbiol **11**: 3335.
Farley, K. R. and W. W. Metcalf (2019). "The streptothricin acetyltransferase (*sat*) gene as a positive selectable marker for methanogenic archaea." FEMS Microbiol Lett **366**(17): fnz216.
Fiedler, S. and R. Wirth (1988). "Transformation of bacteria with plasmid DNA by electroporation." Anal Biochem **170**(1): 38-44.
Fink, C., S. Beblawy, A. M. Enkerlin, L. Mühling, L. T. Angenent and B. Molitor (2021). "A shuttle-vector system allows heterologous gene expression in the thermophilic methanogen *Methanothermobacter thermautotrophicus* ΔH." bioRxiv.
Fonseca, D. R., M. F. A. Halim, M. P. Holten and K. C. Costa (2020). "Type IV-like pili facilitate transformation in naturally competent archaea." J Bacteriol **202**(21): e00355-00320.
Fox, G. E., L. J. Magrum, W. E. Balch, R. S. Wolfe and C. R. Woese (1977). "Classification of methanogenic bacteria by 16S ribosomal RNA characterization." Proc Natl Acad Sci U S A **74**(10): 4537-4541.
Gardner, W. L. and W. B. Whitman (1999). "Expression vectors for *Methanococcus maripaludis*: Overexpression of acetohydroxyacid synthase and β-galactosidase." Genetics **152**(4): 1439-1447.
Garrett, E. R. and C. M. Won (1973). "Kinetics and mechanisms of drug action on microorganisms XVII: Bactericidal effects of penicillin, kanamycin, and rifampin with and without organism pretreatment with bacteriostatic chloramphenicol, tetracycline, and novobiocin." J Pharm Sci **62**(10): 1666-1673.
Gernhardt, P., O. Possot, M. Foglino, L. Sibold and A. Klein (1990). "Construction of an integration vector for use in the archaebacterium *Methanococcus voltae* and expression of a eubacterial resistance gene." Mol Gen Genet **221**(2): 273-279.
Gibb, A. P. and S. Wong (1998). "Inhibition of PCR by agar from bacteriological transport media." J Clin Microbiol **36**(1): 275-276.
Goldberg, G. W. and L. A. Marraffini (2015). "Resistance and tolerance to foreign elements by prokaryotic immune systems - curating the genome." Nat Rev Immunol **15**(11): 717-724.
Götz, M., J. Lefebvre, F. Mörs, A. McDaniel Koch, F. Graf, S. Bajohr, R. Reimert and T. Kolb (2016). "Renewable Power-to-Gas: A technological and economic review." Renew Energ **85**: 1371-1390.
Gregor, D. and F. Pfeifer (2005). "*In vivo* analyses of constitutive and regulated promoters in halophilic archaea." Microbiology **151**(1): 25-33.
Groot, M. N., F. Nieboer and T. Abee (2008). "Enhanced transformation efficiency of recalcitrant *Bacillus cereus* and *Bacillus weihenstephanensis* isolates upon *in-vitro* methylation of plasmid DNA." Appl Environ Microbiol **74**(24): 7817-7820.
Guss, A. M., M. Rother, J. K. Zhang, G. Kulkkarni and W. W. Metcalf (2008). "New methods for tightly regulated gene expression and highly efficient chromosomal integration of cloned genes for *Methanosarcina* species." Archaea **2**(3): 193-203.
Hammer, B. K. and B. L. Bassler (2003). "Quorum sensing controls biofilm formation in *Vibrio cholerae*." Mol Microbiol **50**(1): 101-104.

Hartmann, T., N. Schwanhold and S. Leimkühler (2015). "Assembly and catalysis of molybdenum or tungsten-containing formate dehydrogenases from bacteria." Biochim Biophys Acta **1854**(9): 1090-1100.
Heap, J. T., O. J. Pennington, S. T. Cartman and N. P. Minton (2009). "A modular system for *Clostridium* shuttle plasmids." J Microbiol Methods **78**(1): 79-85.
Henning, H.-M. and A. Palzer (2014). "A comprehensive model for the German electricity and heat sector in a future energy system with a dominant contribution from renewable energy technologies—Part I: Methodology." J Renew Sustain Ener **30**: 1003-1018.
Heuermann, K. and J. Cosgrove (2001). "S-Gal™: An autoclavable dye for color selection of cloned DNA inserts." Biotechniques **30**(5): 1142-1147.
Hildenbrand, C., T. Stock, C. Lange, M. Rother and J. Soppa (2011). "Genome copy numbers and gene conversion in methanogenic archaea." J Bacteriol **193**(3): 734-743.
Hileman, T. H. and T. J. Santangelo (2012). "Genetics techniques for *Thermococcus kodakarensis*." Front Microbiol **3**: 195.
Hilpert, R., J. Winter, W. Hammes and O. Kandler (1981). "The sensitivity of archaebacteria to antibiotics." Zb1. Bakt. Hyg., 1. Abt. Orig. C **2**: 11-20.
Honarbakhsh, M., A. A. Villafane, I. Ruhl, D. Sannino and E. Bini (2012). "Development of a thermostable β-glucuronidase-based reporter system for monitoring gene expression in hyperthermophiles." Biotechnol Bioeng **109**(7): 1881-1886.
Hoseki, J., T. Yano, Y. Koyama, S. Kuramitsu and H. Kagamiyama (1999). "Directed evolution of thermostable kanamycin-resistance gene: A convenient selection marker for *Thermus thermophilus*." J Biochem **126**(5): 951-956.
Hua, S.-b., M. Qiu, E. Chan, L. Zhu and Y. Luo (1997). "Minimum length of sequence homology required for in-vivo cloning by homologous recombination in yeast." Plasmid **38**(2): 91-96.
Jamal, M., W. Ahmad, S. Andleeb, F. Jalil, M. Imran, M. A. Nawaz, T. Hussain, M. Ali, M. Rafiq and M. A. Kamil (2018). "Bacterial biofilm and associated infections." Chin Med J **81**(1): 7-11.
Jenal, U., T. Rechsteiner, P.-Y. Tan, E. Bühlmann, L. Meile and T. Leisinger (1991). "Isoleucyl-tRNA synthetase of *Methanobacterium thermoautotrophicum* Marburg. Cloning of the gene, nucleotide sequence, and localization of a base change conferring resistance to pseudomonic acid." J Biol Chem **266**(16): 10570-10577.
Jensen, T. O., I. Pogrebnyakov, K. B. Falkenberg, S. Redl and A. T. Nielsen (2017). "Application of the thermostable β-galactosidase, BgaB, from *Geobacillus stearothermophilus* as a versatile reporter under anaerobic and aerobic conditions." AMB Express **7**(1): 169-179.
Jentsch, M., T. Trost and M. Sterner (2014). "Optimal use of Power-to-Gas energy storage systems in an 85% renewable energy scenario." Energy Procedia **46**: 254-261.
Jones, W. J., W. B. Whitman, R. D. Fields and R. S. Wolfe (1983). "Growth and plating efficiency of *Methanococci* on agar media." Appl Environ Microbiol **46**(1): 220-226.
Kandler, O. and H. König (1998). "Cell wall polymers in archaea (archaebacteria)." Cell Mol Life Sci **54**(4): 305-308.
Karim, A. A., D. R. Gestaut, M. Fincker, J. C. Ruth, E. C. Holmes, W. Sheu and A. M. Spormann (2018). "Fine-tuned protein production in *Methanosarcina acetivorans* C2A." ACS Synth Biol **7**(8): 1874-1885.
Kaster, A. K., M. Goenrich, H. Seedorf, H. Liesegang, A. Wollherr, G. Gottschalk and R. K. Thauer (2011). "More than 200 genes required for methane formation from H_2 and CO_2 and energy conservation are present in *Methanothermobacter marburgensis* and *Methanothermobacter thermautotrophicus*." Archaea: 973848.
Kato, S., T. Kosaka and K. Watanabe (2008). "Comparative transcriptome analysis of responses of *Methanothermobacter thermautotrophicus* to different environmental stimuli." Environ Microbiol **10**(4): 893-905.
Kiener, A., H. König, J. Winter and T. Leisinger (1987). "Purification and use of *Methanobacterium wolfei* pseudomurein endopeptidase for lysis of *Methanobacterium thermoautotrophicum*." J Bacteriol **169**(3): 1010-1016.

Kiener, A. and T. Leisinger (1983). "Oxygen sensitivity of methanogenic bacteria." Syst Appl Microbiol **4**(3): 305-312.
Kiener, A., W. H. Orme-Johnson and C. T. Walsh (1988). "Reversible conversion of coenzyme F_{420} to the 8-OH-AMP and 8-OH-GMP esters, F_{390}-A and F_{390}-G, on oxygen exposure and reestablishment of anaerobiosis in *Methanobacterium thermoautotrophicum*." Arch Microbiol **150**(3): 249-253.
King, S. B. (2013). "Potential biological chemistry of hydrogen sulfide (H_2S) with the nitrogen oxides." Free Radic Biol Med **55**: 1-7.
Klask, C.-M., N. Kliem-Kuster, B. Molitor and L. T. Angenent (2020). "Nitrate feed improves growth and ethanol production of *Clostridium ljungdahlii* with CO_2 and H_2, but results in stochastic inhibition events." Frontiers in microbiology **11**: 724.
Kolek, J., K. Sedlar, I. Provaznik and P. Patakova (2016). "Dam and Dcm methylations prevent gene transfer into *Clostridium pasteurianum* NRRL B-598: development of methods for electrotransformation, conjugation, and sonoporation." Biotechnol Biofuels **9**: 14.
Kong, K.-F., C. Vuong and M. Otto (2006). "*Staphylococcus* quorum sensing in biofilm formation and infection." Int J Med Microbiol Suppl **296**(2-3): 133-139.
Kovach, M. E., P. H. Elzer, D. S. Hill, G. T. Robertson, M. A. Farris, R. M. Roop II and K. M. Peterson (1995). "Four new derivatives of the broad-host-range cloning vector pBBR1MCS, carrying different antibiotic-resistance cassettes." Gene **166**(1): 175-176.
Lacalle, R. A., D. Pulido, J. Vara, M. Zaiacaín and A. Jiménez (1989). "Molecular analysis of the *pac* gene encoding a puromycin N-acetyl transferase from *Streptomyces alboniger*." Gene **79**(2): 375-380.
Leigh, J. A., S. V. Albers, H. Atomi and T. Allers (2011). "Model organisms for genetics in the domain archaea: Methanogens, Halophiles, Thermococcales and Sulfolobales." FEMS Microbiol Rev **35**(4): 577-608.
Leisinger, T. and L. Meile (1993). Plasmids, phages, and gene transfer in methanogenic bacteria. Genetics and Molecular Biology of Anaerobic Bacteria, Springer**:** 1-12.
Lie, T. J. and J. A. Leigh (2002). "Regulatory response of *Methanococcus maripaludis* to alanine, an intermediate nitrogen source." J Bacteriol **184**(19): 5301-5306.
Lie, T. J. and J. A. Leigh (2007). "Genetic screen for regulatory mutations in *Methanococcus maripaludis* and its use in identification of induction-deficient mutants of the euryarchaeal repressor NrpR." Appl Environ Microbiol **73**(20): 6595-6600.
Lie, T. J., G. E. Wood and J. A. Leigh (2005). "Regulation of *nif* expression in *Methanococcus maripaludis*: Roles of the euryarchaeal repressor NrpR, 2-oxoglutarate, and two operators." J Biol Chem **280**(7): 5236-5241.
Liu, C., L. Mao, X. Zheng, J. Yuan, B. Hu, Y. Cai, H. Xie, X. Peng and X. Ding (2019). "Comparative proteomic analysis of *Methanothermobacter thermautotrophicus* reveals methane formation from H_2 and CO_2 under different temperature conditions." MicrobiologyOpen **8**(5): e00715.
Loenen, W. A., D. T. Dryden, E. A. Raleigh and G. G. Wilson (2014). "Type I restriction enzymes and their relatives." Nucleic Acids Res **42**(1): 20-44.
Long, F., L. Wang, B. Lupa and W. B. Whitman (2017). "A flexible system for cultivation of *Methanococcus* and other formate-utilizing methanogens." Archaea **2017**: 7046026.
Luo, Y., T. Leisinger and A. Wasserfallen (2001). "Comparative sequence analysis of plasmids pME2001 and pME2200 of *Methanothermobacter marburgensis* strains Marburg and ZH3." Plasmid **45**: 18-30.
Luo, Y., P. Pfister, T. Leisinger and A. Wasserfallen (2002). "Pseudomurein endoisopeptidases PeiW and PeiP, two moderately related members of a novel family of proteases produced in *Methanothermobacter* strains." FEMS Microbiol Lett **208**(1): 47-51.
Luton, P. E., J. M. Wayne, R. J. Sharp and P. W. Riley (2002). "The *mcrA* gene as an alternative to 16S rRNA in the phylogenetic analysis of methanogen populations in landfill." Microbiology **148**(11): 3521-3530.
Lyu, Z., R. Jain, P. Smith, T. Fetchko, Y. Yan and W. B. Whitman (2016). "Engineering the autotroph *Methanococcus maripaludis* for geraniol production." ACS Synth Biol **5**(7): 577-581.

Lyu, Z., N. Shao, T. Akinyemi and W. B. Whitman (2018). "Methanogenesis." Curr Biol **28**(13): R727-R732.
Lyu, Z. and W. B. Whitman (2019). "Transplanting the pathway engineering toolbox to methanogens." Curr Opin Biotechnol **59**: 46-54.
Madigan, M. T., J. M. Martinko and J. Parker (1997). Brock biology of microorganisms, Prentice hall Upper Saddle River, NJ.
Maia, L. B., J. J. Moura and I. Moura (2015). "Molybdenum and tungsten-dependent formate dehydrogenases." J Biol Inorg Chem **20**(2): 287-309.
Majernik, A., L. u. Cubonova, P. Polak, P. Smigan and M. Greksak (2003). "Biochemical analysis of neomycin-resistance in the methanoarchaeon *Methanothermobacter thermautotrophicus* and some implications for energetic processes in this strain." Anaerobe **9**: 31-38.
Majernik, A. I., M. Lundgren, P. McDermott, R. Bernander and J. P. Chong (2005). "DNA content and nucleoid distribution in *Methanothermobacter thermautotrophicus*." J Bacteriol **187**(5): 1856-1858.
Malone Rubright, S. L., L. L. Pearce and J. Peterson (2017). "Environmental toxicology of hydrogen sulfide." Nitric Oxide **71**: 1-13.
Marinus, M. G. (1987). "DNA methylation in *Escherichia coli*." Annu Rev Genet **21**(1): 113-131.
Marinus, M. G. and N. R. Morris (1973). "Isolation of deoxyribonucleic acid methylase mutants of *Escherichia coli* K-12." J Bacteriol **114**(3): 1143-1150.
Martin, M. R., J. J. Fornero, R. Stark, L. Mets and L. T. Angenent (2013). "A single-culture bioprocess of *Methanothermobacter thermautotrophicus* to upgrade digester biogas by CO_2-to-CH_4 conversion with H_2." Archaea **2013**: 157529.
Martinez-Garcia, E., T. Aparicio, A. Goni-Moreno, S. Fraile and V. de Lorenzo (2015). "SEVA 2.0: An update of the Standard European Vector Architecture for de-/re-construction of bacterial functionalities." Nucleic Acids Res **43**(D1183–D1189).
Meile, L., P. Abendschein and T. Leisinger (1990). "Transduction in the archaebacterium *Methanobacterium thermoautotrophicum* Marburg." J Bacteriol **172**(6): 3507-3508.
Meile, L., J. Madon and T. Leisinger (1988). "Identification of a transcript and its promoter region on the archaebacterial plasmid pME2001." J Bacteriol **170**(1): 478-481.
Meile, L. and J. N. Reeve (1985). "Potential shuttle vectors based on the methanogen plasmid pME2001." Nature Biotechnol **3**(1): 69-72.
Meile, L., R. Stettler, R. Banholzer, M. Kotik and T. Leisinger (1991). "Tryptophan gene cluster of *Methanobacterium thermoautotrophicum* Marburg: Molecular cloning and nucleotide sequence of a putative *trpEGCFBAD* operon." J Bacteriol **173**(16): 5017-5023.
Mermelstein, L. and E. Papoutsakis (1993). "*In-vivo* methylation in *Escherichia coli* by the *Bacillus subtilis* phage phi3T I methyltransferase to protect plasmids from restriction upon transformation of *Clostridium acetobutylicum* ATCC 824." Appl Environ Microbiol **59**(4): 1077-1081.
Metcalf, W. W., W. Jiang and B. L. Wanner (1994). "Use of the *rep* technique for allele replacement to construct new *Escherichia coli* hosts for maintenance of R6Kλ origin plasmids at different copy numbers." Gene **138**(1): 1-7.
Metcalf, W. W., J. K. Zhang, E. Apolinario, K. R. Sowers and R. S. Wolfe (1997). "A genetic system for archaea of the genus *Methanosarcina*: Liposome-mediated transformation and construction of shuttle vectors." Proc Natl Acad Sci U S A **94**(6): 2626-2631.
Mets, L. (2016). *Methanothermobacter thermautotrophicus* strain and variants thereof. U. o. Chicago. U.S.A.
Micheletti, P. A., K. A. Sment and J. Konisky (1991). "Isolation of a coenzyme M-auxotrophic mutant and transformation by electroporation in *Methanococcus voltae*." J Bacteriol **173**(11): 3414-3418.
Molitor, B., K. Kirchner, A. W. Henrich, S. Schmitz and M. A. Rosenbaum (2016). "Expanding the molecular toolkit for the homoacetogen *Clostridium ljungdahlii*." Sci Rep **6**: 31518.

Mondorf, S., U. Deppenmeier and C. Welte (2012). "A novel inducible protein production system and neomycin resistance as selection marker for Methanosarcina mazei." Archaea **2012**: 973743.
Monk, I. R., I. M. Shah, M. Xu, M. W. Tan and T. J. Foster (2012). "Transforming the untransformable: Application of direct transformation to manipulate genetically *Staphylococcus aureus* and *Staphylococcus epidermidis*." mBio **3**(2).
Moore, B. C. and J. A. Leigh (2005). "Markerless mutagenesis in *Methanococcus maripaludis* demonstrates roles for alanine dehydrogenase, alanine racemase, and alanine permease." J Bacteriol **187**(3): 972-979.
Mougiakos, I., P. Mohanraju, E. F. Bosma, V. Vrouwe, M. Finger Bou, M. I. S. Naduthodi, A. Gussak, R. B. L. Brinkman, R. van Kranenburg and J. van der Oost (2017). "Characterizing a thermostable Cas9 for bacterial genome editing and silencing." Nat Commun **8**(1): 1647.
Nagle, D., R. Teal and A. Eisenbraun (1987). "5-Fluorouracil-resistant strain of *Methanobacterium thermoautotrophicum*." J Bacteriol **169**(9): 4119-4123.
Nayak, D. D. and W. W. Metcalf (2017). "Cas9-mediated genome editing in the methanogenic archaeon *Methanosarcina acetivorans*." Proc Natl Acad Sci U S A **114**(11): 2976-2981.
Nölling, J., M. Frijlink and W. M. de Vos (1991). "Isolation and characterization of plasmids from different strains of *Methanobacterium thermoformicicum*." Microbiology **137**(8): 1981-1986.
Nölling, J. and J. N. Reeve (1997). "Growth-and substrate-dependent transcription of the formate dehydrogenase (*fdhCAB)* operon in *Methanobacterium thermoformicicum* Z-245." J Bacteriol **179**(3): 899-908.
Paik, S.-Y., M. Sugiyama and R. Nomi (1985). "Isolation and properties of a puromycin acetyltransferase from puromycin-producing *Streptomyces alboniger*." J Antibiot **38**(12): 1761-1766.
Pan, X., I. Angelidaki, M. Alvarado-Morales, H. Liu, Y. Liu, X. Huang and G. Zhu (2016). "Methane production from formate, acetate and H_2/CO_2; focusing on kinetics and microbial characterization." Bioresour Technol **218**: 796-806.
Patel, G. B., J. H. Nash, B. J. Agnew and G. D. Sprott (1994). "Natural and electroporation-mediated transformation of *Methanococcus voltae* protoplasts." Appl Environ Microbiol **60**(3): 903-907.
Peng, N., Q. Xia, Z. Chen, Y. X. Liang and Q. She (2009). "An upstream activation element exerting differential transcriptional activation on an archaeal promoter." Mol Microbiol **74**(4): 928-939.
Perez-Arnaiz, P., A. Dattani, V. Smith and T. Allers (2020). "*Haloferax volcanii*-a model archaeon for studying DNA replication and repair." Open Biol **10**(12): 200293.
Perona, J. J., B. J. Rauch and C. M. Driggers (2018). Sulfur assimilation and trafficking in methanogens. Molecular Mechanisms of Microbial Evolution, Springer**:** 371-408.
Pfeifer, K., İ. Ergal, M. Koller, M. Basen, B. Schuster and K.-M. R. Simon (2020). "Archaea biotechnology." Biotechnol Adv: 107668.
Pozzi, R., M. Coles, D. Linke, A. Kulik, M. Nega, W. Wohlleben and E. Stegmann (2016). "Distinct mechanisms contribute to immunity in the lantibiotic NAI-107 producer strain *Microbispora* ATCC PTA-5024." Environ Microbiol **18**(1): 118-132.
Pritchett, M. A., J. K. Zhang and W. W. Metcalf (2004). "Development of a markerless genetic exchange method for *Methanosarcina acetivorans* C2A and its use in construction of new genetic tools for methanogenic archaea." Appl Environ Microbiol **70**(3): 1425-1433.
Ragsdale, S. W. and E. Pierce (2008). "Acetogenesis and the Wood–Ljungdahl pathway of CO_2 fixation." Biochim Biophys Acta **1784**(12): 1873-1898.
Riahi, K., D. P. van Vuuren, E. Kriegler, J. Edmonds, B. C. O'Neill, S. Fujimori, N. Bauer, K. Calvin, R. Dellink, O. Fricko, W. Lutz, A. Popp, J. C. Cuaresma, S. Kc, M. Leimbach, L. Jiang, T. Kram, S. Rao, J. Emmerling, K. Ebi, T. Hasegawa, P. Havlik, F. Humpenöder, L. A. Da Silva, S. Smith, E. Stehfest, V. Bosetti, J. Eom, D. Gernaat, T. Masui, J. Rogelj, J. Strefler, L. Drouet, V. Krey, G. Luderer, M. Harmsen, K. Takahashi, L. Baumstark, J. C. Doelman, M. Kainuma, Z. Klimont, G. Marangoni, H. Lotze-Campen, M. Obersteiner, A.

Tabeau and M. Tavoni (2017). "The shared socioeconomic pathways and their energy, land use, and greenhouse gas emissions implications: An overview." Glob Environ Change **42**: 153-168.
Rospert, S., D. Linder, J. Ellermann and R. K. Thauer (1990). "Two genetically distinct methyl-coenzyme M reductases in *Methanobacterium thermoautotrophicum* strain Marburg and ΔH." Eur J Biochem **194**(3): 871-877.
Rother, M. and W. W. Metcalf (2005). "Genetic technologies for archaea." Curr Opin Microbiol **8**(6): 745-751.
Sambrook, J., E. F. Fritsch and T. Maniatis (1989). Molecular Cloning: A Laboratory Manual, Cold spring harbor laboratory press.
Santangelo, T. J., L. Cubonova, R. Matsumi, H. Atomi, T. Imanaka and J. N. Reeve (2008). "Polarity in archaeal operon transcription in *Thermococcus kodakaraensis*." J Bacteriol **190**(6): 2244-2248.
Santangelo, T. J., L. Cubonova and J. N. Reeve (2010). "*Thermococcus kodakarensis* genetics: TK1827-encoded β-glycosidase, new positive-selection protocol, and targeted and repetitive deletion technology." Appl Environ Microbiol **76**(4): 1044-1052.
Sarbu, C. (2013). Untersuchung der Mth60-Fimbrien von *Methanothermobacter thermoautotrophicus*. Doctoral thesis, University of Regensburg.
Sarmiento, F., J. A. Leigh and W. B. Whitman (2011). "Genetic systems for hydrogenotrophic methanogens." Methods Enzymol **494**: 43-73.
Schiebahn, S., T. Grube, M. Robinius, V. Tietze, B. Kumar and D. Stolten (2015). "Power to gas: Technological overview, systems analysis and economic assessment for a case study in Germany." Int J Hydrog Energy **40**(12): 4285-4294.
Schill, N. and U. von Stockar (1995). "Thermodynamic analysis of *Methanobacterium thermoautotrophicum*." Thermochim Acta **251**: 71-77.
Schill, N. A., J. S. Liu and U. v. Stockar (1999). "Thermodynamic analysis of growth of *Methanobacterium thermoautotrophicum*." Biotechnol Bioeng **64**(1): 74-81.
Schofield, L. R., A. K. Beattie, C. M. Tootill, D. Dey and R. S. Ronimus (2015). "Biochemical characterisation of phage pseudomurein endoisopeptidases PeiW and PeiP using synthetic peptides." Archaea **2015**: 828693.
Seifert, A. H., S. Rittmann and C. Herwig (2014). "Analysis of process related factors to increase volumetric productivity and quality of biomethane with *Methanothermobacter marburgensis*." Appl Energy **132**: 155-162.
Shaw, A. J., D. A. Hogsett and L. R. Lynd (2010). "Natural competence in *Thermoanaerobacter* and *Thermoanaerobacterium* species." Appl Environ Microbiol **76**(14): 4713-4719.
Sheehan, R., A. C. McCarver, C. E. Isom, E. A. Karr and D. J. Lessner (2015). "The *Methanosarcina acetivorans* thioredoxin system activates DNA binding of the redox-sensitive transcriptional regulator MsvR." J Ind Microbiol Biotechnol **42**(6): 965-969.
Shinzato, N., M. Enoki, H. Sato, K. Nakamura, T. Matsui and Y. Kamagata (2008). "Specific DNA binding of a potential transcriptional regulator, inosine 5'-monophosphate dehydrogenase-related protein VII, to the promoter region of a methyl coenzyme M reductase I-encoding operon retrieved from *Methanothermobacter thermautotrophicus* strain ΔH." Appl Environ Microbiol **74**(20): 6239-6247.
Simon, R., M. O'connell, M. Labes and A. Pühler (1986). "Plasmid vectors for the genetic analysis and manipulation of *Rhizobia* and other gram-negative bacteria." Meth Enzymol **118**: 640-659.
Šmigáň, P., P. Polák, A. Majerník and M. Greksák (1997). "Isolation and characterization of a neomycin-resistant mutant of *Methanobacterium thermoautotrophicum* with a lesion in Na+-translocating ATPase (synthase)." FEBS letters **420**(1): 93-96.
Smith, D. R., L. Doucette-Stamm, C. Deloughery, H. Lee, J. Dubois, T. Aldredge, R. Bashirzadeh, D. Blakely, R. Cook and K. Gilbert (1997). "Complete genome sequence of *Methanobacterium thermoautotrophicum* ΔH: Functional analysis and comparative genomics." J Bacteriol **179**(22): 7135-7155.
Smith, G. R. (1988). "Homologous recombination in procaryotes." Microbiol. Rev. **52**(1): 1.

Smith, M. D. and W. R. Guild (1980). "Improved method for conjugative transfer by filter mating of *Streptococcus pneumoniae*." J Bacteriol **144**(1): 457-459.
Spang, A., E. F. Caceres and T. J. G. Ettema (2017). "Genomic exploration of the diversity, ecology, and evolution of the archaeal domain of life." Science **357**(6351).
Stettler, R., P. Pfister and T. Leisinger (1995). "Characterization of a plasmid carried by *Methanobacterium thermoautotrophicum* ZH3, a methanogen closely related to *Methanobacterium thermoautotrophicum* Marburg." Syst Appl Microbiol **17**(4): 484-491.
Susanti, D., M. C. Frazier and B. Mukhopadhyay (2019). "A genetic system for *Methanocaldococcus jannaschii:* An evolutionary deeply rooted hyperthermophilic methanarchaeon." Front Microbiol **10**: 1256.
Tabassum, R., K. Sandman and J. Reeve (1992). "HMt, a histone-related protein from *Methanobacterium thermoautotrophicum* ΔH." J Bacteriol **174**(24): 7890-7895.
Tanaka, T., S. Yamamoto, T. Moriya, M. Taniguchi, H. Hayashi, H. Kagamiyama and S. Oi (1994). "Aspartate aminotransferase from a thermophilic formate-utilizing methanogen, *Methanobacterium thermoformicicum* strain SF-4: Relation to serine and phosphoserine aminotransferases, but not to the aspartate aminotransferase family." J Biol Chem **115**(2): 309-317.
Teal, R. and D. P. Nagle (1986). "Effects of 5-fluorouracil on growth and methanogenesis in *Methanobacterium thermoautotrophicum* (Marburg)." Curr Microbiol **14**(4): 227-230.
Thauer, R. K. (1998). "Biochemistry of methanogenesis: A tribute to Marjory Stephenson: 1998 Marjory Stephenson prize lecture." Microbiology **144**(9): 2377-2406.
Thauer, R. K. (2015). "My lifelong passion for biochemistry and anaerobic microorganisms." Annu Rev Microbiol **69**: 1-30.
Thauer, R. K. (2019). "Methyl (alkyl)-coenzyme M reductases: Nickel F-430-containing enzymes involved in anaerobic methane formation and in anaerobic oxidation of methane or of short chain alkanes." Biochemistry **58**(52): 5198-5220.
Thauer, R. K., A. K. Kaster, H. Seedorf, W. Buckel and R. Hedderich (2008). "Methanogenic archaea: Ecologically relevant differences in energy conservation." Nat Rev Microbiol **6**(8): 579-591.
Thema, M., T. Weidlich, M. Hörl, A. Bellack, F. Mörs, F. Hackl, M. Kohlmayer, J. Gleich, C. Stabenau, T. Trabold, M. Neubert, F. Ortloff, R. Brotsack, D. Schmack, H. Huber, D. Hafenbradl, J. Karl and M. Sterner (2019). "Biological CO_2-methanation: An approach to standardization." Energies **12**(9): 1670.
Thema, M., T. Weidlich, A. Kaul, A. Böllmann, H. Huber, A. Bellack, J. Karl and M. Sterner (2021). "Optimized biological CO_2-methanation with a pure culture of thermophilic methanogenic archaea in a trickle-bed reactor." Bioresour Technol **333**: 125135.
Thoma, C., M. Frank, R. Rachel, S. Schmid, D. Näther, G. Wanner and R. Wirth (2008). "The Mth60 fimbriae of *Methanothermobacter thermoautotrophicus* are functional adhesins." Environ Microbiol **10**(10): 2785-2795.
Tominaga, Y., T. Ohshiro and H. Suzuki (2016). "Conjugative plasmid transfer from *Escherichia coli* is a versatile approach for genetic transformation of thermophilic *Bacillus* and *Geobacillus* species." Extremophiles **20**(3): 375-381.
Touzel, J. P., E. C. De Macario, J. Nölling, W. M. De Vos, T. Zhilina and A. Lysenko (1992). "DNA relatedness among some thermophilic members of the genus *Methanobacterium*: emendation of the species *Methanobacterium thermoautotrophicum* and rejection of *Methanobacterium thermoformicicum* as a synonym of *Methanobacterium thermoautotrophicum*." Int J Syst Evol Microbiol **42**(3): 408-411.
Tumbula, D. L., T. L. Bowen and W. B. Whitman (1997). "Characterization of pURB500 from the archaeon *Methanococcus maripaludis* and construction of a shuttle vector." J Bacteriol **179**(9): 2976-2986.
Turk, S. C., W. P. Kloosterman, D. K. Ninaber, K. P. Kolen, J. Knutova, E. Suir, M. Schurmann, P. C. Raemakers-Franken, M. Muller, S. M. de Wildeman, L. M. Raamsdonk, R. van der Pol, L. Wu, M. F. Temudo, R. A. van der Hoeven, M. Akeroyd, R. E. van der Stoel, H. J. Noorman, R. A. Bovenberg and A. C. Trefzer (2016). "Metabolic engineering toward sustainable production of Nylon-6." ACS Synth Biol **5**(1): 65-73.

Valgepea, K., K. Q. Loi, J. B. Behrendorff, R. de SP Lemgruber, M. Plan, M. P. Hodson, M. Köpke, L. K. Nielsen and E. Marcellin (2017). "Arginine deiminase pathway provides ATP and boosts growth of the gas-fermenting acetogen *Clostridium autoethanogenum*." Metab Eng **41**: 202-211.
Verbeke, J., A. Beopoulos and J.-M. Nicaud (2013). "Efficient homologous recombination with short length flanking fragments in Ku70 deficient *Yarrowia lipolytica* strains." Biotechnol Lett **35**(4): 571-576.
Visweswaran, G. R., B. W. Dijkstra and J. Kok (2010). "Two major archaeal pseudomurein endoisopeptidases: PeiW *P*and PeiP." Archaea **2010**: 480492.
Waege, I., G. Schmid, S. Thumann, M. Thomm and W. Hausner (2010). "Shuttle vector-based transformation system for *Pyrococcus furiosus*." Appl Environ Microbiol **76**(10): 3308-3313.
Wagner, M., M. van Wolferen, A. Wagner, K. Lassak, B. H. Meyer, J. Reimann and S. V. Albers (2012). "Versatile genetic tool box for the crenarchaeote *Sulfolobus acidocaldarius*." Front Microbiol **3**: 214.
Walters, A. D., S. E. Smith and J. P. Chong (2011). "Shuttle vector system for *Methanococcus maripaludis* with improved transformation efficiency." Appl Environ Microbiol **77**(7): 2549-2551.
Wang, H., N. Peng, S. A. Shah, L. Huang and Q. She (2015). "Archaeal extrachromosomal genetic elements." Microbiol Mol Biol Rev **79**(1): 117-152.
Wasserfallen, A., J. Nölling, P. Pfister, J. Reeve and E. C. De Macario (2000). "Phylogenetic analysis of 18 thermophilic *Methanobacterium* isolates supports the proposals to create a new genus, *Methanothermobacter* gen. nov., and to reclassify several isolates in three species, *Methanothermobacter thermautotrophicus* comb. nov., *Methanothermobacter wolfeii* comb. nov., and *Methanothermobacter marburgensis* sp. nov." Int J Syst Evol Microbiol **50**(1): 43-53.
Weiss, M. C., F. L. Sousa, N. Mrnjavac, S. Neukirchen, M. Roettger, S. Nelson-Sathi and W. F. Martin (2016). "The physiology and habitat of the last universal common ancestor." Nat Microbiol **1**(9): 16116.
Woese, C. R. and G. E. Fox (1977). "Phylogenetic structure of the prokaryotic domain: The primary kingdoms." Proc Natl Acad Sci U S A **74**(11): 5088-5090.
Woese, C. R., O. Kandler and M. L. Wheelis (1990). "Towards a natural system of organisms: Proposal for the domains archaea, bacteria, and eucarya." Proc Natl Acad Sci U S A **87**(12): 4576-4579.
Worrell, V. E., D. P. Nagle, D. McCarthy and A. Eisenbraun (1988). "Genetic transformation system in the archaebacterium *Methanobacterium thermoautotrophicum* Marburg." J Bacteriol **170**(2): 653-656.
Xie, Y. and J. N. Reeve (2005). "Regulation of tryptophan operon expression in the archaeon *Methanothermobacter thermautotrophicus*." J Bacteriol **187**(18): 6419-6429.
Yamamoto, K., A. Tachibana, G. Dhavises, T. Tanaka, M. Taniguchi and S. Oi (1989). "Characterization of a thermophilic formate-utilizing methanogen, *Methanobacterium thermoformicicum* strain SF-4." Agric Biol Chem **53**(2): 533-534.
Yanisch-Perron, C., J. Vieira and J. Messing (1985). "Improved M13 phage cloning vectors and host strains: Nucleotide sequences of the M13mpl8 and pUC19 vectors." Gene **33**(1): 103-119.
Young, C. L., Z. T. Britton and A. S. Robinson (2012). "Recombinant protein expression and purification: A comprehensive review of affinity tags and microbial applications." Biotechnol J **7**(5): 620-634.
Zeikus, J. and R. Wolfe (1972). "*Methanobacterium thermoautotrophicus* sp. n., an anaerobic, autotrophic, extreme thermophile." J Bacteriol **109**(2): 707-713.
Zhang, G., W. Wang, A. Deng, Z. Sun, Y. Zhang, Y. Liang, Y. Che and T. Wen (2012). "A mimicking-of-DNA-methylation-patterns pipeline for overcoming the restriction barrier of bacteria." PLoS Genet **8**(9): e1002987.

Zhang, G., F. Zhang, G. Ding, J. Li, X. Guo, J. Zhu, L. Zhou, S. Cai, X. Liu, Y. Luo, G. Zhang, W. Shi and X. Dong (2012). "Acyl homoserine lactone-based quorum sensing in a methanogenic archaeon." ISME J **6**(7): 1336-1344.

IX. List of abbreviations

DNA	deoxyribonucleic acid
5-FOA	5-fluor orotic acid
5-FU	5-fluor uracil
6-AU	8-Aza-uracil
8-ADP	8-Aza-2,4 diaminopurine
A	absorbance
ADI	adenosin deiminase pathway
Amp	ampicillin
ATP	adenosin triphosphase
bgaB	thermostable beta-galactosidase *Geobacillus stearothermophilus*
bp	basepair
BRE	transcription factor B recognition element
Cam	chloramphenicol
CIP	calf intestine phosphatase
CRISPR	clustered regularly interspaced short palindromic repeats
DMSO	Dimethyl sulfoxide
e.g.	*exempli gratia*
EDTA	Ethylenediaminetetraacetic acid
exp	exponential
$fdh_{Z\text{-}245}$	formate dehydrogenase cassette *M. thermautotrophicus* Z-245
hpt	hypoxanthine phosphoribosyl transferase gene
i.e.	*it est*
IF	inserted fragment
Kann	kanamycin
kb	kilo basepairs
LB	lysogeny broth
LUCA	Last universal common ancester
M.t.	*Methanothermobacter thermautotrophicus*
M.v.	*Methanococcus voltae*
mcr	methyl-coenzyme M reductase gene
MCS	multiple cloning site
MMEJ	micro-homology-mediated-end-joining
MS	Sea salt
n.t.	not tested
NEB	New England Biolabs

Neo	neomycin
NHEJ	non-homologous end joining
OD	optical density
ONPG	o-Nitrophenyl-β-D-galactopyranosid
ORF	open reading frame
ori	origin of replication
P	promoter
pac	puromycin acetyl transferase gene
PCR	polymerase chain reaction
PEG	polyethylen glycol
PeiP	pseudomurein endo-isopeptidase P
PeiW	pseudomurein endo-isopeptidase W
PhD	doctor of philosophy
pMVS	plasmid Methanothermobacter vector system
PNPG	4-Nitrophenyl β-D-glucopyranoside
Pol	polymerase
Pur	puromycin
pyrF	Orotidine 5'-phosphate decarboxylase gene
R/r	resistance
RNA	Ribonucleic acid
rpm	rounds per minute
RT	room temperature
SAM	S-adenosyl methionin
SAP	shrimp-alkaline phosphatase
SDS	sodium dodecyl sulfate
S-Gal	3,4-Cyclohexenoesculetin-β-D-galactopyranosid
sgRNA	single guide RNA
SOC	super optimal broth
spp.	species
stat	stationary
Synth	synthetic
T	terminator
T.k.	*Thermococcus kodakarensis*
TAE	Tris-acetate-EDTA
Tet	tetracyclin
TRIS	Tris(hydroxymethyl)aminomethan

wt	wild-type
X-Gal	5-Brom-4-chlor-3-indoxyl-β-D-galactopyranosid
X-Gluc	5-Bromo-4-chloro-1H-indol-3-yl β-D-glucopyranosiduronic acid

X. Acknowledgements

First of all, I want to thank **Prof. Dr. Largus T. Angenent** for the opportunity to make my PhD in his Environmental Biotechnology Group at the University of Tübingen. With all the effort to set-up the laboratory in the beginning, you provided all the excellent conditions to perform great research, thank you! Additionally, I want to thank you and especially **Dr. Bastian Molitor**, that you never stopped believing in me and the project during all the hard time of false positive and negative results. Your support and calmness were necessary to test all the different conditions and parameters to reach the final goal. Furthermore, I would like to thank you both for the help, the edits, and the helpful discussion about my papers and the dissertation. Without you I would not have had the possibility to improve my English writing skills as they are now. Also, a big thank you for implementing so many different nationalities and cultures in the Environmental Biotechnology Group. It is a pleasure to get so many new impressions from all around the world, different styles of work, and experience to work in an international scientific group.

Second, I want to thank **Dr. Sebastian Beblawy, Dr. Pengfei Xia** and **Christian Klask** for their very helpful Tips and Tricks with cloning strategies, genetic modification, and all the other small problems occurring from day to day in the lab. It was and is an absolute pleasure to work with you behind and left of me!

Third, a huge thanks to **Akanksha Mishra**, **Dr. Tianran Sun**, **Dr. Ramiro Blasco**, **Andrés Ortiz Ardila**, **Dr. Byoung Seung Jeon** and **Nils Rohbohm** to always build me up during hard times, but also for the celebrations at the good times after the breakthrough.

Fourth, I want to thank all my **HiWis** who helped a lot with the establishment of the genetic system (Caroline Schlaiß, Michael Buchner, Mark-Andreas Enkerlin and Sylvia Lemke). Without your hard work, the fast progress in the project would not have been possible!

Fifth, I want to thank the entire **Environmental Biotechnology Group** with all the members through the time I have been here. It was and is such a great environment to perform research. One can find help in all different endeavors of studies and everyone is willing to help wherever one can. That is awesome! I want to put a special emphasis on the **Methanogen Subgroup**, who helped me with the first set of results for the paper with putting back their own research project. This is not as if it was the most natural thing in the world and I did not take that for granted. Thank you for the help and the nice familiar atmosphere in the lab!

And last but not least, I want to thank all my **Family and Friends** who forgave me all the times, when I was not available and on the other hand supported me with great love. I am so glad to have you all in my life!